Title

Synthesis, Structure, and Reactivity of High Oxidation State Silver Fluorides and Related Compounds

Author

Lucier, G.M.

Publication Date

1995-05-09

Thesis/dissertation

LBL-37334
UC-401

Lawrence Berkeley Laboratory
UNIVERSITY OF CALIFORNIA

CHEMICAL SCIENCES DIVISION

Synthesis, Structure, and Reactivity of High Oxidation State Silver Fluorides and Related Compounds

G.M. Lucier
(Ph.D. Thesis)

May 1995

Prepared for the U.S. Department of Energy under Contract Number DE-AC03-76SF00098

DISCLAIMER

LBL-37334
UC-401

Synthesis, Structure, and Reactivity of High Oxidation State Silver Fluorides and Related Compounds

George Michael Lucier
Ph.D. Thesis

Department of Chemistry
University of California, Berkeley

and

Chemical Sciences Division
Lawrence Berkeley Laboratory
University of California
Berkeley, CA 94720

May 1995

This work was supported by the Director, Office of Energy Research, Office of Basic Energy Sciences, Materials Sciences Division, of the U.S. Department of Energy under Contract No. DE-AC03-76SF00098.

Synthesis, Structure, and Reactivity of High Oxidation State Silver Fluorides and Related Compounds

by

George Michael Lucier

B.S. (Stanford University) 1990

A dissertation submitted in partial satisfaction of the

requirements for the degree of

Doctor of Philosophy

in

Chemistry

in the

GRADUATE DIVISION

of the

UNIVERSITY of CALIFORNIA at BERKELEY

Committee in charge:

Professor Neil Bartlett, Chair
Professor Angelica Stacy
Professor Alex Zettl

1995

Abstract

Synthesis, Structure, and Reactivity of

High Oxidation State Silver Fluorides and Related Compounds

by

George Michael Lucier

Doctor of Philosophy in Chemistry

University of California at Berkeley

Professor Neil Bartlett, Chair

The research described in this thesis has been largely concerned with defining the oxidizing power of Ag(III) and Ag(II) species in anhydrous hydrogen fluoride (aHF) solution. Emphasis has been placed on the study of cationic species, since in a cation the electronegativity of a given oxidation state is greater than in the neutral or anionic relatives. Cationic Ag^{III}_{solv} has a short half life at ordinary temperatures, oxidizing the solvent to elemental fluorine with formation of Ag(II). Salts of such a cation have not yet been preparable, but solutions which must contain such a species have proved to be effective and powerful oxidizers. In the presence of PtF_6^-, RuF_6^-, or RhF_6^-, Ag^{III}_{solv} effectively oxidizes the anions to release the neutral hexafluorides. Such reactivity ranks cationic Ag(III) as the most powerfully oxidizing chemical agent known so far.

Unlike its trivalent relative, Ag^{II}_{solv} is thermodynamically stable in acid aHF. Nevertheless, it has been observed to oxidize IrF_6^- to IrF_6 at room temperature, placing its

oxidizing potential not more than 2 eV below that of cationic Ag(III). The range of $Ag^{2+}(MF_6^-)_2$ salts attainable in aHF has been explored. An anion must be stable with respect to loss of its electron to Ag^{2+}. The anion must also be a poor F^- donor; otherwise, either AgF^+ salts or AgF_2 are generated.

A general method for the synthesis of $AgF^+MF_6^-$ salts has been found in which $Ag^+MF_6^-$ salts are fluorinated in aHF. $AgFIrF_6$ is preparable, but $AgFOsF_6$ is not, placing the oxidizing potential of the polymeric fluorine-bridged $(AgF)_n^{n+}$ cation ~1 eV lower than that of Ag^{II}_{solv}. The $AgF^+MF_6^-$ salts have been found to adopt at least three different structure types, ranging from monoclinic to tetragonal symmetry. The structures of $AgF^+BF_4^-$ and $AgF^+IrF_6^-$ reveal a polymeric chain cation of formula $(AgF)_n^{n+}$ in which the Ag(II) is linearly coordinated. A second $AgF^+MF_6^-$ structure type occurs in $AgF^+RuF_6^-$, which exhibits square coordination of the cation, generating a one-dimensional ribbon. The $AgF^+MF_6^-$ (M = Sb, Bi) represent yet another structure type (based on X-ray powder data), but the atomic arrangement is not yet known. All AgF^+ salts examined exhibit a small temperature-independent paramagnetism indicative of a metallic band structure (*i.e.* Pauli paramagnetism). Polarized light transmission experiments on single crystals of $AgFBF_4$ support the hypothesis that these salts are one-dimensional metals, but no direct evidence for electronic conductivity has been found.

Synthesis, Structure, and Reactivity of

High Oxidation State Silver Fluorides and Related Compounds

Table of Contents

List of Figures

List of Tables

Acknowledgments

I would like to thank Professor Neil Bartlett for his infectious enthusiasm and for giving me the responsibility to determine the details of my research projects. His direction and guidance are greatly appreciated, as is his readiness to share his knowledge and wisdom.

Bill Casteel deserves the recognition and the blame for training me in the fundamental techniques of fluorine chemistry - thanks, Bill, for your patience and especially for your courage. I am ingratiated to Byron Shen for our many enlightening discussions, and for hosting many parties during his time here. I should express my thanks to the Bartlett Group postdocs, including Horst Borrmann, Rika Hagiwara, Jörg Münzenberg, Philippe Botkovitz, Scott Elder, and Marc Whalen - I learned directly from all of them, and indirectly by sharing my experience with the later ones. Another very special colleague was Professor Boris Žemva, whose diligence and friendly demeanor helped me to get through the tedious and frustrating parts of my work. And thanks to Lisa Chacón for sharing her creativity and vitality. Finally, my friends Carrie, Harry, Dave, Rick, and most of the Stacy Group have brought me many good times and carried me through the difficult times.

This work was supported by the U.S. Department of Energy under contract No. DE-AC03-76SF00098 and supplemented for the first two years by fellowship money provided by the Department of Education.

Chapter 1

Introduction and Experimental Considerations

1.1. General Introduction

In 1989, a synthetic route to thermally unstable fluorides such as NiF_4, NiF_3, and AgF_3 was discovered.[1] Because of their instability, attempts to generate these materials with standard high-pressure fluorination reactions had all failed. Dissolution of AgF_3 in anhydrous hydrogen fluoride (aHF) solution by acidification with arsenic pentafluoride, in an attempt to prepare a cationic Ag(III) salt was found, in these laboratories, to generate $AgFAsF_6$ with slow release of elemental fluorine.[2] Frlec *et al.*[3] had first made this AgF^+ salt by the interaction of the same acidic solution on the divalent silver compound AgF_2. In their search for evidence for a cationic Ag(III) intermediate in the AgF_3 reduction in acidified aHF, Bartlett and Žemva and their coworkers[2] discovered the unexpectedly high electron-withdrawing potential of cationic Ag(II), which was demonstrated in its oxidation of xenon gas to Xe(II), and, later, in its oxidation[4] of

oxygen gas to O_2^+. These results indicated that cationic Ag(II) rivaled even platinum hexafluoride in electron affinity. It was soon recognized that such remarkable oxidizing power available in the divalent Ag(II) solution species presaged potentially unmatched oxidizing power in the (as yet unobserved) trivalent solution species, Ag^{III}_{solv}. Experiments were devised to investigate the possibility of generating and utilizing the Ag^{III}_{solv} species in acidic aHF solution before its decomposition into Ag^{II}_{solv} and fluorine gas. Reactions of this design revealed Ag^{III}_{solv} to be a truly remarkable oxidizer even at temperatures below 0 °C.

However, the reactivity of these silver materials was only one of their novel features. Because Ag(II) is a d^9 species, distortion from octahedral symmetry is often found, as explained by Crystal Field Theory, as a consequence of the Jahn-Teller effect. Gantar *et al.*[5] had solved the crystal structure of $AgFAsF_6$ in 1987, and this had revealed a one-dimensional cation of formula $(AgF)^{n+}_n$, in which the silver was essentially linearly coordinated with two nearly identical Ag-F bond lengths, five anion F ligands at long interatomic distances (~ 2.4 Å) completing the coordination. This approximately $D_{\infty h}$ symmetry (with the Ag-F-Ag axis designated *z*) requires that the antibonding sigma orbital, d_{z^2}, be the singly occupied orbital (SOMO). It was in work performed in these laboratories, however, that the magnetic characteristic exhibited by all AgF^+ salts was discovered: a small temperature-independent paramagnetism evident over a very broad temperature range. Such magnetic behavior can indicate an electronically conductive

system, which, if present, would likely be one-dimensional in nature, owing to the structure of AgF^+ salts. By analogy with the high oxidation state copper oxide systems, the strong oxidizing properties of AgF^+ raised the possibility of superconductivity. Additionally, the structures of other $(AgF)_n^{n+}$ salts with different anions remained to be explored. In many Cu(II) systems, a Jahn-Teller distortion results in elongation along one axis of the octahedron, yielding a square-coordinated metal center. Such a structural feature seemed probable in AgF_2^+ systems, if they could be prepared, and possible in the Ag(II) system as well. More likely than the latter were mixed oxidation state Ag(III)Ag(II) materials containing $(AgF_2)_n^+$ sheets with a two-dimensional network more closely related to those observed in Cu(II), so-called pseudo-perovskite materials.

1.2. Electron Affinities of Third Row Transition Metal Hexafluorides

For a more quantitative investigation of the oxidizing power of silver salts, it was desirable to have a scale against which potentials could be quantitatively measured. Due to the extremely reactive nature of the systems under investigation and their recent discovery, electrochemical techniques have yet to be devised. However, the values of the electron affinities of third row transition metals (from tungsten to gold) span the observed redox range needed for these silver systems, and do so with an essentially linear dependence of affinity on the atomic number of the metal atom involved (see Figure 1.1). Thus, release of neutral hexafluoride from these third row metal hexafluoride-monoanions serves as a semi-quantitative measure of the oxidizing potential of the

species capable of releasing one of the MF_6 but not the next higher in the series. For example, a silver species which can liberate gaseous OsF_6 from the dissolved OsF_6^- but not the IrF_6 from IrF_6^- probably has an oxidizing potential of at least 130 kcal·mol^{-1}, but is unlikely to exceed 155 kcal·mol^{-1} in that potential.

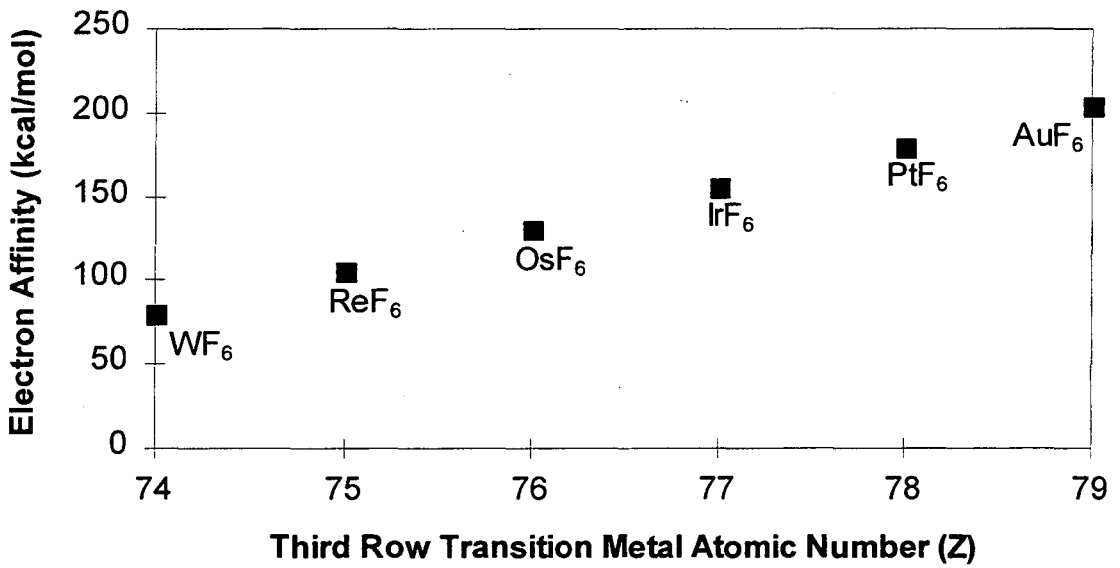

Figure 1.1. Electron Affinities of Third Row Transition Metal Hexafluorides. [6]

Table 1.1. Electron Affinities of Third Row Transition Metal Hexafluorides [6] (kcal·mol^{-1})

WF_6	ReF_6	OsF_6	IrF_6	PtF_6	AuF_6 [a]
81	102	133	155	184	205

[a] AuF_6 is as yet an unknown compound; the electron affinity is a calculated estimate.

1.3. Relative Fluoride Ion Affinities of Some Fluoro-acids

The work presented herein provides excellent examples of the importance of Lewis acid-base considerations in synthetic inorganic chemistry. In the aHF solvent system, a Lewis acid behaves as a fluoride ion acceptor and a Lewis base as a fluoride ion donor. In order to effectively predict the outcome of a reaction, it is critical to know the relative fluoride ion affinities (a.k.a., fluoro-acidities) of all species involved. This significance is illustrated well in the Ag(III) reactions of Chapter 4. Here, it is seen that $KAgF_4$ is stable in aHF solution,

$$KAgF_{4\,(s)} \overset{aHF}{\rightleftharpoons} K^+_{(solv)} + AgF^-_{4(solv)} \qquad (1)$$

thus indicating that AgF_3 is a stronger fluoro-acid than is HF itself. By contrast, such is probably not the case with CuF_3, as it appears that K_3CuF_6 generates CuF_3 immediately[7]

$$K_3CuF_{6\,(s)} \xrightarrow{aHF} 3\,K^+_{(solv)} + 3\,(HF)_nF^-_{(solv)} + CuF_{3\,(s)} \qquad (2)$$

upon exposure to liquid aHF. Addition of a very weak fluoro-acid (*e.g.* SiF_4) to the $KAgF_4$ solution results in no reaction:

$$KAgF_{4\,(s)} \overset{aHF}{\underset{SiF_4}{\rightleftharpoons}} K^+_{(solv)} + AgF^-_{4\,(solv)} \qquad (3)$$

Removal of solvent and acid merely recovers the $KAgF_4$ quantitatively. Introduction of the slightly stronger Lewis acid BF_3 strips the fluoride ion off the AgF_4^-, forming AgF_3 and BF_4^-:

$$KAgF_{4\,(s)} \xrightarrow[BF_3]{aHF} K^+_{(solv)} + BF^-_{4(solv)} + AgF_{3\,(s)} \qquad (4)$$

Excess BF_3 in this system produces no further reaction.

$$AgF_{3\,(s)} \xrightarrow[BF_3]{aHF} AgF_{3\,(s)} \qquad \text{(no reaction)} \qquad (5)$$

Now, by acidifying the aHF with a still stronger fluoride ion acceptor such as AsF_5, the reaction proceeds with the removal of at least one fluoride from the insoluble AgF_3, generating the soluble Ag^{III}_{solv} species.

$$AgF_{3\,(s)} \xrightarrow[AsF_5]{aHF} Ag^{III}_{(solv)} + x\,AsF^-_{6(solv)} \qquad (6)$$

Thus, selection of the proper fluoro-acid is the key to the preparation of pure $KAgF_4$, pure AgF_3, and the strongly oxidizing cationic Ag(III) system.

A classification of relative fluoride ion affinities in the aHF solvent system may be roughly determined through reaction chemistry. A series of acid-displacement reactions spanning a wide range of fluoro-acidities is useful for identification of appropriate reagents in synthetic fluorine chemistry. While factors such as lattice energy, solvation enthalpy, and change in entropy are not considered here, the hierarchical ranking obtained should have practical utility for the synthetic fluorine chemist.

1.3.1. Fluoro-acidity Ranking of Main Group Fluorides

Main group fluorides are frequently used as Lewis acid reagents and catalysts, many of them generating superacid[8] conditions in HF solution. HF itself autoionizes according to Equation (7).[8]

$$2\,HF \rightleftharpoons H_2F^+ + F^- \qquad K \sim 10^{-10} \qquad (7)$$

The Group I fluorides (LiF through CsF) are all very good fluoro-bases in this solvent. Group II fluorides are also basic but of low solubility in aHF. Boron and aluminum are the only Group III elements whose fluorides are commonly used for their ability to act as Lewis acids. Boron trifluoride has a high fluoride ion affinity; the molecule is planar in the gas phase and becomes tetrahedral upon formation of the conjugate base BF_4^-. Equations (1) and (4) above suggest that BF_3 has a significantly higher fluoride ion affinity than HF. In the solid AlF_3, the aluminum occupies octahedral-hole sites in the F ligand array. Because of its three-dimensional, energetically favorable structure, AlF_3 monomer (even aHF solvated) is not a significantly available species and AlF_3 is only a very weak fluoro-acid.

While four-coordinate carbon exhibits fluoro-neutrality as the tetrafluoride, the other Group IV elements may form five-coordinate MF_5^- and doubly-negative octahedral species. Silicon tetrafluoride is such a poor Lewis acid that, in dilute aHF solution, it does not form fluorosilicates with even the alkali fluoride bases. This failure arises because HF itself has a higher fluoride ion affinity than SiF_4, as can be observed in their reaction chemistry with the strong fluoro-base KF. K_2SiF_6 is not preparable in dilute aHF solution; KHF_2 is produced instead.

$$KF \xrightarrow[SiF_4]{aHF} KHF_2 \qquad (8)$$

(When the KF concentration is sufficiently high that F^- is available over and above that needed to make at least HF_2^-, then SiF_6^{2-} salt formation can occur.) K_2SiF_6 may be

prepared in water, however, by passing SiF_4 into a concentrated aqueous solution of KF. Material obtained in this manner gives an X-ray powder pattern (XRPP) indicative of pure K_2SiF_6 (cubic[9], a_o = 8.133 Å). Subsequent dissolution of this product in an abundance of aHF results in rapid evolution of SiF_4 and formation of solvated KF, which, upon removal of the solvent, crystallizes from solution as KHF_2.

$$K_2SiF_6 \xrightarrow{aHF} 2\,K^+_{(solv)} + 2\,F^-_{(solv)} + SiF_{4\,(g)} \qquad (9)$$

Mallouk *et al.*[10] have found that GeF_4 has only a slightly higher first fluoride ion affinity than that of BF_3 (however, the doubly negative ion provides for high lattice enthalpy or solvation enthalpy, which renders GeF_4 a rather strong flouro-acid in aHF).

All of the Group V elements except for nitrogen form pentafluorides which span a wide range of fluoride ion affinities. PF_5 is the weakest acid in the group, ranking slightly behind the trifluoride of boron. Similar to BF_3, PF_5 is seen to generate AgF_3 from a solution of $KAgF_4$. However, Žemva *et al.*[11] have observed that removal of the PF_5 overpressure causes the reaction to go in the reverse direction, thus reforming $KAgF_4$.

$$K^+_{(solv)} + AgF^-_{4(solv)} \underset{PF_5}{\overset{aHF}{\rightleftharpoons}} KPF_{6\,(s)} + AgF_{3\,(s)} \qquad (10)$$

This reversibility occurs despite the lower solubility of KPF_6 than KBF_4 in aHF. Gillespie and coworkers[12] studied the complete set of Group V pentafluorides and found their hierarchy of acidity to be as follows: $PF_5 < AsF_5 < BiF_5 < SbF_5$. These results are in good agreement with the observations made in this laboratory.

Overall, the hierarchy of the main group Lewis acids discussed above is as follows, in order of increasing fluoro-acidity:

$$SiF_4 < HF < PF_5 < BF_3 < GeF_4 < AsF_5 < BiF_5 < SbF_5 \quad (11)$$

1.4. Stabilization of High Oxidation State Cations Such as AgF_2^+

If cations such as AgF_2^+ are to be stabilized, it is clear that the counter anion must resist both electron transfer and fluoride ion transfer. Although the main group fluoro-anions are probably all of sufficiently high ionization potential to resist electron transfer, it is probable that only the poorest F^- donors, SbF_6^- and BiF_6^-, could resist fluoride transfer to such an electrophilic center as AgF_2^+. Perhaps the best choice of transition metal counter ion would be the Au(V) fluoro-anion AuF_6^-. It was observed in this laboratory that the interaction of XeF_5AuF_6 with excess SbF_5 in aHF does not result in the displacement of AuF_5. Although the product of this reaction is unidentified, it is believed that a complex anion $AuSbF_{11}^-$ results.

$$XeF_5AuF_6 + \text{xs } SbF_5 \xrightarrow[?]{\text{aHF}} XeF_5AuSbF_{11} \quad (12)$$

Such reactivity indicates that AuF_5 is comparable to SbF_5 in fluoro-acidity, so AuF_6^- is therefore unlikely to undergo fluoride transfer. And it is improbable that AuF_6^- would experience electron transfer since the neutral hexafluoride of gold has yet to be observed. These stability considerations apply not only to AgF_2^+, but to other high oxidation state cationic species at the limits of chemical oxidizability as well.

1.5. References

[1] B. Žemva, K. Lutar, A. Jesih, W. J. Casteel, Jr., and N. Bartlett, *J. Chem. Soc., Chem. Comm.*, (1989), p 346.

[2] B. Žemva, R. Hagiwara, W. J. Casteel, Jr., K. Lutar, A. Jesih, and N. Bartlett, *J. Am. Chem. Soc.*, **112** (1990), pp 4846-4849.

[3] B. Frlec, D. Gantar, and J. H. Holloway, *J. Fluorine Chem.*, **20** (1982), pp 385-396.

[4] W. J. Casteel, Jr., Ph. D. Thesis, (1992) Chapter 7, U.C. Berkeley.

[5] D. Gantar, B. Frlec, D. R. Russell, and J. H. Holloway, *Acta Cryst.*, **C43** (1987), pp 618-620.

[6] For WF_6: P. M. George and J. L. Beauchamp, *Chem. Phys.*, **36** (1979), p 345.

For ReF_6, OsF_6, and IrF_6: N. Bartlett, *Proc. Of the Robert A. Welch Foundation Conference on Chem. Res.*, Oct-Nov (1988), p 269.

For PtF_6 and AuF_6: M. I. Nikitin, L. N. Sodorov, and M. V. Korobov, *Int. J. Mass Spec. Ion Phys.*, **37** (1981), p 13.

[7] K_3CuF_6 generated in a high-temperature, high-pressure fluorine bomb reactor, when placed into aHF solution, immediately undergoes solvolysis to form the red CuF_3 precipitate; unpublished work in this group, J. Münzenberg, 1993.

[8] F. A. Cotton and G. Wilkinson, Advanced Inorganic Chemistry, 5th ed. (1988), New York: John Wiley and Sons.

---

[9] *Natl. Bur. Stand. (U.S.), Circ. 539*, **5** (1955), p 50.

[10] T. E. Mallouk, G. L. Rosenthal, G. Müller, R. Brusasco, and N. Bartlett, *Inorg. Chem.*, **23** (1984), pp 3167-3173.

[11] B. Žemva, K. Lutar, A. Jesih, W. J. Casteel, Jr., A. P. Wilkinson, D. E. Cox, R. B. Von Dreele, H. Borrmann, and N. Bartlett, *J. Am. Chem. Soc.*, **113** (1991), pp 4192-4198.

[12] R. J. Gillespie, K. Ouchi, G. P. Pez, *Inorg. Chem.*, **8** (1969), p 63.

Chapter 2

Experimental Methods

2.1. Apparatus

A stainless steel and monel vacuum line fitted with a Helicoid Instruments (Watertown, CT) pressure gauge (fluorine service, 1500 torr) and rotary vane mechanical pump was used for the handling of gases. Autoclave Engineers (Erie, PA) supplied the stainless steel and monel valves (series 30VM). A fluorine gas supply was connected to a high-pressure (500 psi, 3.8×10^5 torr) fluorine service Helicoid gauge and then to the vacuum line. Low pressure measurements were made with the use of a thermocouple gauge head (Varian Vacuum Products, Santa Clara, CA; model 0531) which was read by a millitorr gauge (Varian, model 801, 0 - 2 torr). For reactions involving the use of aHF, a section of vacuum line constructed from FEP tubing (Chemplast, Inc., Wayne, NJ) and Teflon valves, as described elsewhere[1], and unions (Oakland Valve and Fitting Co., Concord, CA) was attached to the metal line. Reactors for aHF solvent reactions were made from two FEP tubes (diameter 3/8" or 1/2", length ~20 cm) which had been sealed

at one end by heating over a Bunsen flame and then clamping shut with pliers. These two tubes were joined at right angles via Teflon Swagelok compression fittings to a Teflon T (Oakland Valve and Fitting Co.), the assembly being connected via FEP tubing to a Teflon valve (see Figure 2.1). Volatile fluoride compounds were destroyed by passing through a copper column (diameter 5 cm, length 30 cm) containing granular soda lime. Solid fluorides were handled inside a Vacuum Atmospheres (Hawthorne, CA) DRILAB containing a dry argon atmosphere.

2.2. Characterization Techniques

2.2.1. X-ray Powder Diffraction

When necessary, powder samples were ground in an agate mortar and pestle inside the DRILAB. Quartz capillaries (either 0.3 mm or 0.5 mm diameter) were prepared by heating to ~700 °C for more than 15 hours under high vacuum (ca. 10^{-8} torr). An Enraf Nonius FR 590 X-ray generator fitted with a copper target tube (energized to 40 kV and 20 mA), and a nickel filter provided the required radiation. Typical exposure time was 12 hours with a General Electric Debye-Scherrer cassette loaded with Kodak Industrex AA film (cut to size). X-ray powder patterns (XRPP's) were measured with the aid of a Norelco film-measuring light box. Microsoft Excel for Windows v. 4.0 and v. 5.0, U-fit v. 1.2, and Lazy Pulverix were used in the determination and refinement of unit cell dimensions.

2.2.2. Single Crystal X-ray Diffraction

Because of the highly reactive nature of the materials under study, neither oil nor glue mounts could be used to fix a single crystal. Instead, each crystal was loaded into a quartz capillary, which had been drawn down from 0.3 mm diameter (to provide a gradual taper) and dried as described above for powder samples. Crystals were gently tapped into the tapered end of the capillary, sometimes only tenuously holding their position. Data was collected on an Enraf Nonius Diffractis 585 diffractometer fitted with a graphite monochromator and a molybdenum target tube energized to 50 kV and 26 mA.

2.2.3. SQUID Magnetometry

A Quantum Design (San Diego, CA) SQUID magnetometer (model MPMS) was used to take magnetic measurements on powder samples. The sample container was constructed from two Kel-F cylindrical cups, one fitting inside the other to provide an internal volume 6.5 mm in diameter and 6.5 mm in length. A known quantity of powder material was loaded into the smaller cup and was capped by the larger, each having been passivated with 1500 torr F_2. A thin ring of halocarbon grease around the outside of the smaller cup ensured a gas-tight seal. The two cups were tied together with nylon line.

2.3. Anhydrous HF as an Oxidatively Inert Solvent

Traditionally, high oxidation state fluorine chemistry has required the use of high pressures of molecular fluorine heated to hundreds of degrees in a metal "bomb" reactor. While this preparative technique is still quite useful and even necessary at times, the use of a liquid solvent at or below room temperature is preferred for its safety with respect to

fires and explosions. Although there are many fluorinated solvents which can be used with highly oxidizing materials, none seems to offer the convenience of handling that anhydrous hydrofluoric acid (aHF) does. Although it is highly corrosive and toxic, special handling procedures have been developed which allow for the manipulation of aHF in FEP or Teflon apparatus (sealed from exposure to the air) in much the same way that water is handled in glass. At 19.5 °C, aHF has a vapor pressure[2] of 1 atm, so a reactor containing this solvent at room temperature poses no overpressure danger. A colorless liquid, its density is 1.0015 $g \cdot cc^{-1}$ at 0 °C, and its dielectric constant is very similar to that of water {ε (HF, 0 °C) = 83.6, ε (H_2O, 0 °C) = 87.7}. Despite the non-wetting properties of FEP and Teflon, aHF in reactors made of these materials flows much like water in glass; this is because aHF has a much lower surface tension than does water {σ (HF, 0 °C) = 10.1 $dyn \cdot cm^{-1}$, σ (H_2O, 18 °C) = 73.1 $dyn \cdot cm^{-1}$}[2,3].

Another feature of aHF that makes it a good solvent for the study of high oxidation state fluorides is its oxidative inertness. The systems under study and discussed here are among the most oxidizing known. Solvents which might traditionally be considered stable to oxidation, such as carbon tetrachloride or acetonitrile, will burn vigorously in contact with many of the materials under investigation. Unfortunately, because of the acidity of aHF, contact with metal vacuum line apparatus must be carefully avoided when a reaction is in progress in order to prevent contamination by hydrogen gas. Furthermore, glass apparatus must be protected from any contact with

aHF in order to prevent severe etching. Such etching is, in fact, a problem which arises with the X-ray capillary samples if the powder inside the quartz capillary has not been thoroughly dried or contains solvated HF. Although dry solid fluorides are usually kinetically stable in contact with quartz, chemical attack of the capillary wall by HF generates H_2O, which can then react with the fluoride sample to reform the HF in a catalytically destructive cycle.

2.4. Reaction Technique

Construction of a typical reactor for use with high-oxidation state chemistry in aHF solution is described above and is depicted in Figure 2.1. The Swagelok fittings which connect the FEP tubing to the Teflon tee permit the safe pressurization of the reactor to three atmospheres absolute pressure. All reactors are assembled outside the DRILAB, evacuated, then filled with 2 atm F_2 gas and left to sit for several hours. After removal of this fluorine to a soda lime scrubber under dynamic vacuum, the reactor is brought into the DRILAB where the Swagelok connections allow for removal of the reactor tubes so that they may be loaded with solid reagents.

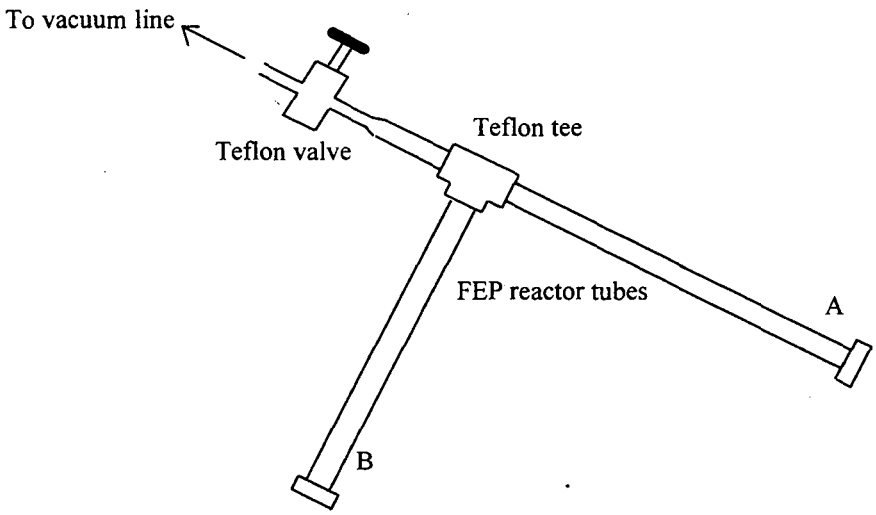

Figure 2.1. A typical reactor tube for use with anhydrous HF solution chemistry.

After removing the reactor from the DRILAB and connecting to the vacuum line, the Teflon valve is opened to the vacuum and the argon atmosphere is evacuated. Usually, the reactor tubes are loaded so that the reaction takes place in tube A. By cooling one or both of the FEP tubes in liquid nitrogen (LN_2), aHF is easily condensed in from a reservoir tube. Thermal control of the reaction is maintained by immersing the reaction tube in a cold-bath (reactions requiring temperatures above 25 °C have not been attempted because of the danger of reactor overpressurization). Gases are tensimetrically admitted through delicate control of the Teflon valve. Reaction mixing is performed with the aid of either a Teflon-coated magnetic stir bar placed inside the reactor tube, or by mechanical tapping of the tube from an external device. Separations based upon solubility in the aHF are accomplished by careful decantation of the solution from one arm of the reactor to the other. Following a decantation, the aHF can be condensed back

over using a cold-bath. The aHF solvent and any remaining gaseous reagents or undesired gaseous products are removed by slow evaporation under dynamic vacuum with continuous agitation in order to reduce violent boiling of the aHF.

2.5. References

[1] K. Lutar, A. Jesih, I. Leban, B. Žemva, and N. Bartlett, *Inorg. Chem.,* **28** (1989), p 3467.

[2] Matheson Gas Data Book, 4th edition (1966), New Jersey: The Matheson Company, Inc.

[3] R. C. Weast, ed., CRC Handbook of Chemistry and Physics, 70th edition (1989), Florida: CRC Press, Inc..

Chapter 3

Preparation of Reagent Materials

3.1. Introduction

Despite the existence of several commercial suppliers of good quality fluorine compounds, the study of high oxidation state fluorine chemistry requires the synthesis of many rudimentary materials that are not commercially available. This deficiency in availability is due, in part, to the very low demand of rarely used compounds which may also contain expensive transition metals, as well as to the great effort and expense required to maintain high oxidation state compounds in storage. Syntheses for main group binary fluorides and ternary alkali fluorides have generally been known for many years. However, older techniques frequently involve the use of high temperatures and high pressures of fluorine. With the advent of Teflon and translucent FEP, the easy manipulation of aHF in a non-corroding container has permitted the development of techniques which utilize this liquid as a solvent at room temperature and at pressures very close to atmospheric. Such reactions are inherently safer and usually lead to greater

yields and cleaner products. For this reason, synthetic procedures involving these newer aHF solvent techniques (which have become routine in this laboratory) to generate new, as well as previously-described, materials in a novel manner are described here.

3.2. Commercially Available Reagents

Anhydrous HF (aHF) (Matheson, Newark, CA) was condensed from the cylinder into a reservoir FEP tube containing K_2NiF_6 (Ozark-Mahoning Pennwalt, Tulsa, OK) in order to destroy trace quantities of water. Fluorine gas (Matheson) was used as received. BF_3, PF_5 (Matheson), and AsF_5 (Ozark-Mahoning) gases were checked by I.R. spectroscopy to ensure absence of major impurities, then used as supplied. Liquid SbF_5 (Ozark-Mahoning) was distilled from its cylinder into a reservoir FEP tube and stored in the DRILAB. Solid BiF_5 (Ozark-Mahoning) was recrystallized from aHF solution prior to use in an attempt to free it of any BiF_3 that might be present. AgF is light sensitive, thus necessitating its recrystallization from aHF. However, because AgF forms a fairly stable bifluoride, prolonged evacuation at room temperature was required in order to carefully remove all complexed HF in the recrystallization product. LiF, NaF, and KF were evacuated overnight to 10^{-8} torr prior to storage in the DRILAB. Transition metals were reduced with a flowing hydrogen atmosphere in a platinum crucible over a flame prior to storage in the DRILAB.

3.3. Preparation of IrF_5 and IrF_6

In the DRILAB, approximately 2.5 g (~ 13 mmol) reduced Ir metal was placed into a passivated monel reaction vessel having a Teflon gasket seal. After evacuating the

can reactor, F_2 gas (~ 13 mmol) was condensed in at -196 °C. A forced-air heat gun was used to heat the can for ca. 10 min, after which the can was cooled to room temperature and opened to the line. The pressure of fluorine that remained equated to about one-fourth the quantity that had been introduced. Again, the can was cooled to -196 °C and 13 mmol F_2 gas condensed in. This was heated again with the heat gun for 10 min, then cooled back down to -196 °C. Another 15 mmol F_2 gas was condensed into the reactor can, and it was heated to 225 °C overnight in a sand bath. The following day, another 20 mmol F_2 gas was introduced at -196 °C, after which the reactor was heated to 245 °C for ca. 4 h. Cooling the can once again to -196 °C permitted removal of the remaining F_2 under dynamic vacuum without evacuating the IrF_6 product.

IrF_6 was easily obtained in aliquots from this storage can by vacuum distillation. Once all the IrF_6 had been removed and used for reaction chemistry, the can was brought into the DRILAB. Removal of the screw-top lid revealed a copious quantity of bright yellow solid whose XRPP proved to be that of pure IrF_5 {monoclinic[1], a_o = 12.267(3), b_o = 9.982(4), c_o = 5.431(2) Å, β = 99.9(2)° }. This product was placed into a passivated FEP tube for storage.

3.4. Preparation of $SF_3^+OsF_6^-$ and $SF_3^+IrF_6^-$

Because of the volatility of OsF_6 and IrF_6 and their reactivity with Teflon and FEP over extended periods of time (evidence for reactivity of IrF_6 with FEP appears within a few hours), initial weights of these two reagents as obtained from their monel storage

cans are imprecise. Nonetheless, the interaction between the metal hexafluoride dissolved in aHF and SF_4 gas {see Equation (1)}appears to go to completion as the

$$3\ SF_{4\,(g)} + 2\ MF_{6\,(g)} \xrightarrow{aHF} 2\ SF_3MF_{6\,(solv)} + SF_{6\,(g)} \qquad (1)$$

desired product may be obtained with no volatile color remaining in the reactor (IrF_6 is a yellow gas and OsF_6 is colorless in the gas phase but turns yellow upon condensation). Details of this reaction for the iridium are provided here; all else being equal, osmium hexafluoride requires a greater reaction time than does iridium hexafluoride.

IrF_6 (240 mg, 0.783 mmol) was condensed at -196 °C from its monel storage can into a passivated FEP T-reactor. Approximately 2.5 mL aHF was condensed onto the yellow solid. Upon warming to room temperature, a yellow solution formed above undissolved yellow solid. Introduction of a large excess of SF_4 gas resulted in the disappearance of the yellow solid within a few minutes time while intermittently cooling the solution then rewarming it in order to encourage dissolution of the SF_4. After 1.5 h, the solution retained a slight yellow tint. The reactor was evacuated, slowly removing the aHF solvent. Because of the extreme solubility of SF_3IrF_6 in aHF, no solid precipitated from solution; rather, a light yellow powder crashed out of solution just as the last bit of liquid aHF was removed. An X-ray powder photograph of the product gives only the XRPP of SF_3IrF_6 (cubic[2], a_o = 5.581(4) Å). The weight of the powder (282 mg) suggests a 91% yield of the desired product based upon the imprecise weight of IrF_6 reagent.

3.5. Preparation of AMF_6 salts

3.5.1. Synthesis of $LiPtF_6$ and $KPtF_6$ from $O_2^+PtF_6^-$

In two separate reactions, passivated FEP T-reactors were loaded with alkali salt (LiF: 29 mg, 1.1 mmol; KF: 107 mg, 1.84 mmol) in one tube and O_2PtF_6 (343 mg, 1.01 mmol; 354 mg, 1.04 mmol, respectively) in the other. About 2 mL aHF was condensed into the reactor at -196 °C, divided equally between the two reagents. The alkali salt solution was poured onto the partially dissolved O_2PtF_6, resulting in immediate effervescence. Once the bubbling had slowed, the reactor was opened to release some of the pressure that had built up. Then it was closed again and agitated continuously until no bubbles were seen to form. The potassium salt was sufficiently insoluble in the aHF to permit decantation of the supernatant solution. However, the lithium salt was completely dissolved and could not be washed free of excess LiF. X-ray powder photography confirmed the presence and purity of the two alkali salts (for $LiPtF_6$, see Table 3.1; for $KPtF_6$, the unit cell is rhombohedral[3], $a_o = 4.96$ Å, $\alpha = 97.4$ °). The $LiPtF_6$ was deep orange in color while the $KPtF_6$ was orange-yellow. Yields were essentially quantitative ($LiPtF_6$: 324 mg, 102%; $KPtF_6$: 348 mg, 96%).

Table 3.1. X-ray powder data for $LiPtF_6$ with a rhombohedral unit cell.
$a_o = 5.386(5)$ Å; $\alpha = 55.56(1)$ °; V = 99.09 Å^3.

	$1/d^2 \times 10^4$						$1/d^2 \times 10^4$				
I/I_o	obsd.	calc.	h	k	l	I/I_o	obsd.	calc.	h	k	l
s	488	485	1	1	1	vwb	8283	8284	4	2	0
vs	586	583	1	0	0	vvw	8529	8513	3	-1	-1
vsb	749	744	1	1	0	vvw	8669	8674	2	2	-2
s	1400	1391	2	1	1	vwb	9108	9088	5	3	2
m	1595	1586	1	0	-1	vw	9363	9344	5	4	3
ms	1884	1876	2	2	1	vw	9346	9344	5	4	3
s	2076	2071	2	1	0	vw	10716	10708	5	3	1
mw	2181	2169	1	1	-1	vw	10713	10708	5	3	1
m	2339	2330	2	0	0	w	10924	10907	4	1	-1
ms	2986	2977	2	2	0	w	10920	10907	4	1	-1
w	3179	3169	3	2	2	w	11108	11099	5	1	1
vvw	3401					vw	11142	11099	5	1	1
w	3475	3462	3	1	1		11142	11102	3	-1	-2
s	3537	3526	3	2	1	vw	12276	12261	5	4	1
m	3767	3755	2	0	-1	w	12529	12516	6	3	3
m	3922	3916	2	1	-1	vw	12529	12516	6	3	3
w	3997	3977	3	3	2	vw	12682	12675	6	4	4
m	4576	4563	3	1	0	vvw	12680	12675	6	4	4
mb	4770	4755	3	3	1		12680	12685	5	2	0
	4770	4758	2	-1	-1	m	13051	13042	4	3	-1
mw	5058	5048	3	2	0	w	13055	13042	4	3	-1
mwb	5260	5243	3	0	0	w	13493	13493	5	3	0
wb	5584	5563	4	2	2	vw	13506	13493	5	3	0
mb	5953	5950	4	3	2	wb	14094	14079	3	3	-2
mb	6348	6341	4	2	1	vwb	14094	14079	3	3	-2
	6348	6344	2	0	-2	vwb	14270	14261	6	5	3
vwb	6729	6698	4	1	1		14270	14274	3	0	-3
wb	6844	6829	3	1	-1	vwb	14757	14759	4	1	-2
wb	6954	6927	2	1	-2	vvwb	14769	14759	4	1	-2
wb	7098	7088	3	0	-1	vw	15429	15433	6	3	1
wb	7139	7149	4	3	1	mw	15465	15466	6	2	1
vvw	7511	7502	4	4	2	vw	15462	15466	6	2	1
vwb	7756	7735	3	2	-1	vw	15665	15665	4	2	-2
	7756	7758	4	4	4	vvw	15662	15665	4	2	-2
vw	8224	8220	4	1	0						

3.5.2. Preparation of $LiRuF_6$

Ru powder (161 mg, 1.60 mmol) which had been previously reduced in a stream of H_2 gas was loaded into one tube of a passivated FEP T-reactor. Into the other tube was placed LiF (81 mg, 3.1 mg). After removing the argon from the reactor under vacuum, the two solids were combined. Anhydrous HF (~2.3 mL) was condensed onto the reagents at -196 °C and then warmed to room temperature. All of the LiF dissolved, but there was no apparent interaction with the Ru powder. The reactor was pressurized to 2 atm with F_2 gas and continuous agitation was begun. More F_2 was periodically introduced in order to replace that which was consumed in the reaction. After 16 h reaction time, the aHF solution appeared orange-brown with a burgundy-red precipitate present. The aHF solution was decanted from the burgundy-red solid. Removal of aHF under dynamic vacuum left a yellow-brown powder. X-ray powder photography of the burgundy material gave only the pattern of $LiRuF_6$ (rhombohedral[4], a_o = 5.39 Å, α = 56.0 °). No XRPP was taken of the yellow-brown soluble byproduct, which was assumed to be Li_2RuF_6. The yield of $LiRuF_6$ (176 mg) was 50%.

3.5.3. General Synthesis of AMF_6 from AF and MF_5

Combination of the alkali fluoride and the metal pentafluoride inside a passivated FEP T-reactor was accomplished with a range of alkali salts and pentafluorides. Table 3.2 gives representative reactions for each permutation. All reactions were carried out in

1.5 to 3 mL aHF. Separation of pure product from remaining reagents is as described in the final column of the table.

Table 3.2. Synthesis of AMF_6 from AF and MF_5

Alkali Fluoride Reagent	Metal Pentafluoride Reagent	Product and Yield	Solubility of AMF_6 @ ~20 °C	Purification Procedure
LiF 29 mg, 1.1 mmol	AsF_5 2 atm pressure	$LiAsF_6$ 215 mg, 99%	very high	Vacuum removal of excess AsF_5
CsF 153 mg, 1.01 mmol	AsF_5 900 torr pressure	$CsAsF_6$ 295 mg, 91%	low (~90 mmol/l)	Vacuum removal of excess AsF_5
KF 347 mg, 5.98 mmol	PF_5 2 atm pressure	KPF_6 1090 mg, 99%	low (~100 mmol/l)	Vacuum removal of excess PF_5
KF 57 mg, 0.98 mmol	BiF_5 271 mg, 0.89 mmol	$KBiF_6$ 310 mg, 96%	very high (>900 mmol/l)	Decantation of last drops of aHF soln. [a]
KF 91 mg, 1.56 mmol	RuF_5 214 mg, 1.09 mmol	$KRuF_6$ 239 mg, 86%	very low	Decantation and 3 washings in aHF
KF 23 mg, 0.39 mmol	RhF_5 68 mg, 0.34 mmol	$KRhF_6$ 89 mg, 101%	unknown (>160 mmol/l)	None performed
LiF 69 mg, 2.7 mmol	IrF_5 749 mg, 2.61 mmol	$LiIrF_6$ 369 mg, 45%	unknown	None performed (rxn incomplete)
KF 96 mg, 1.6 mmol	IrF_5 306 mg, 1.06 mmol	$KIrF_6$ 291 mg, 79%	very low	Decantation and 1 washing in aHF

[a] Even for a highly soluble salt such as $KBiF_6$ in aHF, the removal of KF contaminant could be achieved by removing most of the aHF under dynamic vacuum (the bulk of the $KBiF_6$ crystallizing), the last few drops of aHF containing the bulk of any KF impurity then being removed by decantation.

Table 3.3. X-ray powder data for $KRuF_6$ with a rhombohedral unit cell. $a_o = 4.970(1)$ Å, $\alpha = 97.42(1)$ °, $V = 119.4(5)$ Å^3.

	$1/d^2 \times 10^4$		rhombohedral			hexagonal		
I/I_o	obsd.	calc.	h	k	l	h	k	l
s	421	421	1	0	0	1	0	1
s	721	717	1	0	-1	1	1	0
s	974	967	1	1	0	0	1	2
mw	1142	1138	1	1	-1	0	2	1
mw	1695	1684	2	0	0	2	0	2
w	2161	2152	2	-1	-1	3	0	0
s	2413	2401	2	1	-1	1	2	2
m	2879	2869	2	0	-2	2	2	0
vw	3157	3150	2	1	1	1	0	4
w	3295	3290	2	1	-2	1	3	1
w	3811	3789	3	0	0	3	0	3
w	3870	3867	2	2	0	0	2	4
ms	4598	4584	3	1	0	2	1	4
w	4723	4724	3	0	-2	3	2	1
m	5024	5020	2	1	-3	1	4	0
m	5280	5270	3	1	-2	2	3	2
vvw	5525	5504	3	1	1	2	0	5
vw	6026	6019	3	2	-1	1	3	4
vvw	6473	6455	3	0	-3	3	3	0
vwb	6696	6704	4	-1	-1	5	0	2
vwb	7448	7421	4	0	-2	4	2	2
w	11592	11570	5	1	0	4	1	6
vw	11583	11570	5	1	0	4	1	6
w	12451	12442	5	0	-3	5	3	2
vw	12446	12442	5	0	-3	5	3	2
vw	13020	13004	5	2	-1	3	3	6
w	14633	14625	5	2	-3	3	5	4
vw	14628	14625	5	2	-3	3	5	4
vw	14755	14751	5	2	1	3	1	8
vvw	14751	14751	5	2	1	3	1	8
w	15873	15873	5	3	-2	2	5	6
vw	15870	15873	5	3	-2	2	5	6
w	16188	16186	5	3	0	2	3	8
vwb	16184	16186	5	3	0	2	3	8

Table 3.4. X-ray powder data for $KRhF_6$ with a rhombohedral unit cell.
$a_o = 4.958(2)$ Å, $\alpha = 97.71(2)$ °, V = 118 (1) Å^3.

	$1/d^2 \times 10^4$		rhombohedral			hexagonal		
I/I_o	obsd.	calc.	h	k	l	h	k	l
s	425	424	1	0	0	1	0	1
s	717	717	1	0	-1	1	1	0
w	865							
s	982	981	1	1	0	0	1	2
m	1138	1142	1	1	-1	0	2	1
w	1219							
m	1698	1698	2	0	0	2	0	2
vw	1862	1859	2	0	-1	2	1	1
w	2080							
w	2150	2152	2	-1	-1	3	0	0
vs	2419	2415	2	1	-1	1	2	2
mw	2875	2869	2	0	-2	2	2	0
w	3205	3205	2	1	1	1	0	4
mw	3292	3293	2	1	-2	1	3	1
vvw	3457							
mb	3838	3850	3	0	-1	3	1	2
w	3922	3922	2	2	0	0	2	4
w	4568	4567	2	2	-2	0	4	2
m	4641	4639	3	1	0	2	1	4
vw	4731	4728	3	0	-2	3	2	1
vvw	4852							
mw	5023	5021	3	-1	-2	4	1	0
w	5282	5284	3	1	-2	2	3	2

Table 3.5. X-ray powder data for $LiIrF_6$ with a rhombohedral unit cell.
$a_o = 5.395(5)$ Å; $\alpha = 55.88(1)°$; $V = 100.4$ Å^3.

	$1/d^2 \times 10^4$						$1/d^2 \times 10^4$				
I/I_o	obsd.	calc.	h	k	l	I/I_o	obsd.	calc.	h	k	l
sb	486	485	1	1	1	w	9325	9330	5	4	3
vsb	576	575	1	0	0	vw	9418	9419	4	3	0
vsb	740	737	1	1	0	vw	9951	9958	3	0	-2
sb	1388	1384	2	1	1	vw	10123	10120	3	1	-2
s	1547					vw	10169	10174	5	4	2
vw	1576	1564	1	0	-1	vw	10232	10228	5	2	1
mw	1713					w	10631	10623	5	3	1
m	1876	1869	2	2	1	vvw	10647	10623	5	3	1
sb	2055	2049	2	1	0	vw	10773	10767	4	1	-1
mw	2150	2139	1	1	-1	w	11275	11252	4	2	-1
mw	2307	2301	2	0	0	vw	11269	11252	4	2	-1
vvw	2399					w	11446	11432	3	2	-2
msb	2946	2948	2	2	0	vw	11449	11432	3	2	-2
mw	3174	3164	3	2	2	vw	11815	11792	4	4	0
w	3444	3433	3	1	1	w	12187	12169	5	4	1
ms	3516	3505	3	2	1	vw	12179	12169	5	4	1
m	3722	3703	2	0	-1	w	12468	12457	6	3	3
m	3888	3865	2	1	-1	w	12555	12547	5	2	0
w	3983	3973	3	3	2	vw	12778	12763	6	4	3
vw	4331		3	3	3	mw	12894	12888	4	3	-1
vw	4465					w	12899	12888	4	3	-1
mw	4538	4512	3	1	0	w	13313	13302	6	3	2
mwb	4721	4691	2	-1	-1	mw	13300	13302	6	3	2
mw	5013	4997	3	2	0	mw	13366	13356	5	3	0
mw	5186	5177	3	0	0	vw	13362	13356	5	3	0
w	5557	5537	4	2	2	vw	13711	13698	6	5	4
mb	5952	5932	4	3	2	vw	13906	13895	3	3	-2
wb	6307	6291	4	2	1	w	14224	14219	6	5	3
vvw	6512					w	14560	14560	4	1	-2
vvw	6644	6633	4	1	1	vw	14556	14560	4	1	-2
vw	6747	6741	3	1	-1	w	14804	14811	4	0	-2
vw	6851	6830	2	1	-2	w	14799	14811	4	0	-2
vw	7001	6992	3	0	-1	mb	15303	15297	6	3	1
vw	7110	7100	4	3	1	w	15311	15297	6	3	1
vvw	7494	7478	4	4	2	w	15456	15458	4	2	-2
vw	7651	7639	3	2	-1	vw	15459	15458	4	2	-2
vw	8125	8125	4	1	0	m	15883	15890	1	3	13
vw	8201	8197	4	2	0			15891	6	6	4
wb	9068	9060	5	2	2						

3.6. References

---

[1] P. R. Rao, R. Burbank, and N. Bartlett, (1968) unpublished data.

[2] N. K. Jha, Ph.D. Thesis, (1965) Chapter 2, U. British Columbia.

[3] N. Bartlett and D. H. Lohmann, *J. Chem. Soc.,* February (1964), pp 619-626.

[4] J. L. Boston, and D. W. A. Sharp, *J. Chem. Soc.,* (1960), p 907.

Chapter 4

The Oxidizing Chemistry of Solvated Ag^{III}

4.1. Introduction

Synthesis of the binary fluoride AgF_3 was first claimed by Bougon and Lance[1] in 1983. The red-brown material they described was generated by the oxidation of the metal or the mono- or difluoride of silver with KrF_2 in aHF at room temperature. The material was reported to be weakly paramagnetic, but the data could be fit to the Curie law. In 1988, Kiselev *et al.*[2] claimed that the interaction of AgF_2 with O_2F_2 in ClF_5 generated AgF_3. These two materials, however, were not the same. Furthermore, neither was isomorphous with AuF_3, which raised suspicion because of the structural similarity[3] of AgF_4^- and AuF_4^-. Both of these claims were shown to be incorrect when, in 1989, a novel synthetic route to thermodynamically unstable binary fluorides such as AgF_3 was found in these laboratories.[4] The AgF_3 prepared by this route was bright red and diamagnetic. Its XRPP closely resembled that of AuF_3. Furthermore, a neutron diffraction study performed in 1991 demonstrated[5] a close structural relationship of AgF_3 with that of

AuF_3. Other chemical and magnetic studies[5] established that the material reported by Bougon and Lance as the trifluoride was $Ag^{II}Ag^{III}_2F_8$ {probably $Ag^{2+}(AgF_4^-)_2$}, and the similarity of the Kiselev *et al.* X-ray powder diffraction data to that of the Bougon and Lance material indicates that they also had prepared Ag_3F_8 and not AgF_3.

The successful synthetic route to the trifluoride of silver involved the abstraction of a fluoride ion from AgF_4^- by the fluoroacid BF_3 in aHF at or below room temperature. This synthesis was successful, in part, because it could be performed at low temperature, where the decomposition of the thermally unstable AgF_3 was kinetically unfavorable. Genuine AgF_3 loses[5] elemental fluorine slowly in aHF to yield Ag_3F_8:

$$3\ AgF_3 \xrightarrow{aHF} Ag_3F_8 + \tfrac{1}{2}\ F_2 \qquad (1)$$

AgF_3 was found[5] to oxidize xenon gas spontaneously at room temperature according to the following equation:

$$2\ AgF_3 + Xe \rightarrow 2\ AgF_2 + XeF_2 \qquad (2)$$

Simple electrostatics predict that the electron affinity of neutral AgF_3 is likely to be significantly less than that of a cationic Ag(III) species in aHF solution {*e.g.* $AgF_2(HF)_n^+$, $AgF(HF)_n^{2+}$, or $Ag(HF)_n^{3+}$, where HF is assumed to coordinate to the Ag(III) via the electron-rich F ligand, n perhaps providing a total Ag(III) ligation of four}. Such cations were assumed to be generated by the action of a strong F^- acceptor. So an investigation was undertaken to determine the scope of the oxidizing capabilities of cationic Ag(III). No cationic Ag(III) fluoride is yet known to exist in the solid state. In fact, in 1989,

attempts in this laboratory[5] to synthesize $AgF_2^+AsF_6^-$ at low temperature led to the formation of $AgFAsF_6$ as illustrated in Equation (3),

$$AgF_3 \xrightarrow[AsF_5]{aHF} AgFAsF_6 + \tfrac{1}{2} F_2 \qquad (3)$$

and eventually to the discovery of the remarkable oxidizing powers of both Ag(II) and Ag(III). Although the AgF_2^+ salt was never isolated, the production of F_2 gas as a decomposition product suggested the ready liberation of elemental fluorine, which, in turn, suggested formidable oxidizing potential within the solution. Since the F_2 evolution was slow, it was suspected that a transient Ag^{III}_{solv} species could be generated *in situ* by the extraction of F^- ions from AgF_3 with the help of a strong fluoride ion acceptor. The work reported in this chapter provides clear evidence for long-lived cationic Ag(III) species in the aHF and their remarkable oxidizing capabilities. The strong acids AsF_5, SbF_5, and BiF_5 in aHF produce the potent cationic Ag(III) oxidizers from AgF_3, but the relatively weak acids BF_3 and PF_5 do not.

4.2. Experimental

4.2.1. Preparation of AMF_6

See Chapter 3 for the details of alkali hexafluorometallate(V) syntheses. XeF_5AuF_6 was provided through a continuing collaboration with the Institute Jozef Stefan, Ljubljana, Slovenia.

4.2.2. Preparation of $KAgF_4$

$KAgF_4$ was prepared according to the synthesis provided by Hoppe[6]. $AgNO_3$ (3325 mg, 19.57 mmol) and KNO_3 (1958 mg, 19.36 mmol) were ground together in a mortar and pestle. The mixture was then placed into a nickel insert made to fit into a monel, high-pressure fluorine reactor. The insert was heated to 150 °C for 15 min prior to being placed into the high-pressure reactor, which was sealed with a copper gasket and fitted with an Autoclave Engineers valve. After evacuating the reactor, it was cooled to -196 °C and ~38 mmol F_2 was admitted, thus bringing the internal pressure to ~27 atm at room temperature. A resistance heater placed in a sand bath was used to heat the reactor to ~300 °C for 15 h. After cooling down, all volatile species were removed from the reactor under dynamic vacuum. A liquid nitrogen bath was used to cool the reactor down once again to -196 °C and condense in ~22 mmol F_2 (16 atm, in the reactor, at room temperature). This mixture was heated to ~300 °C for 15 h, then cooled to room temperature. After removing the volatile products and unreacted F_2, the reactor was brought into the DRILAB to be opened.

Scraping the solid product out of the nickel insert provided a mixture of orange and brown powder. This powder was placed into a passivated T-shaped FEP reactor. After evacuating the argon, aHF was condensed onto the mixture. At room temperature, the $KAgF_4$ dissolved to give an orange solution, and a significant amount of brown solid remained undissolved. A single decantation was performed, after which all the aHF was

removed under dynamic vacuum and the yellow-orange solid dried for 3 h. 2000 mg of solid were obtained, which gave the XRPP of $KAgF_4$ (tetragonal[3], a_o = 5.90 Å, c_o = 11.15 Å) with some KHF_2 as impurity.

Because of the synthesis used for the production of AgF_3 (see below), in most cases it was not necessary to have $KAgF_4$ which was free of KHF_2. However, it was found that high purity $KAgF_4$ could be obtained by first generating a room-temperature aHF solution of the $KAgF_4/KHF_2$ mixture, into which PF_5 was slowly introduced with brisk agitation of the solution. At first sign of a persistent red precipitate, the PF_5 supply was shut off. The weak fluoroacid complexes with the KF present much more readily than it displaces AgF_3. And because KPF_6 is only sparingly soluble in aHF, decantation provides a very clean sample, having sacrificed only a small quantity of $KAgF_4$.

4.2.3. Preparation of AgF_3

A T-shaped FEP reactor tube was loaded with $KAgF_4$ (740 mg, 3.32 mmol pure) and evacuated on the vacuum line. About 3 mL aHF was condensed onto the orange solid and warmed to room temperature. A very small quantity of brown precipitate was seen to settle out of solution, so the solution was decanted from it to the other arm of the reactor. The reactor was pressurized to 2 atm with BF_3, leading to the immediate precipitation of red AgF_3 from the aHF solution. More BF_3 was introduced to replace that which was consumed in reaction. Once all the color had gone from the aHF solution, it was decanted. Over the next 3 h, approximately twenty washings of the red product were performed by back-condensing the aHF extracting the KBF_4 and decanting at

approximately 0 °C. The washed product was dried under dynamic vacuum for 3 h. An XRPP of the red product shows only the lines of AgF_3 {hexagonal[5], a_o = 5.0782(2) Å, c_o = 15.4524(8) Å}; yield 449 mg (~82% yield).

4.2.4. Oxidation of RuF_6^-

The following reagents were all loaded into one arm of a T-shaped FEP reactor: $LiRuF_6$ (141 mg, 0.633 mmol), AgF_3 (219 mg, 1.33 mmol), and BiF_5 (1187 mg, 3.903 mmol). Approximately 2.0 mL of anhydrous HF was condensed onto the solids at -196 °C, then allowed to warm to -25 °C. At this temperature, the solution was slightly yellow in color with a red solid resting at the bottom. No reaction was evident at this temperature. As the temperature was increased to room temperature, the HF quickly became deep red. For 12 min, the reaction mixture was intermittently agitated as the deeply-colored, volatile material, RuF_6, was evolved, coloring the liquid HF as well as the vapor in the reactor tubes. Then all volatile material was condensed into the other arm of the reactor at -196 °C, leaving behind a deep green powder. An excess of dry oxygen gas was introduced into the reactor at this point, then the frozen volatile material was thawed. As the aHF/RuF_6 mixture melted, it first gave a red solution, which very quickly gave an almost colorless solution as the gaseous oxygen dissolved and precipitated dark red solid out of solution. Any remaining volatile compounds were pumped away and the red powder product was dried under dynamic vacuum for 3 h at 0

°C. Powder X-ray diffraction confirmed the material to be O_2RuF_6 {cubic[7], a_o = 10.004(3) Å}; the yield (91 mg) was 58%.

4.2.5. Oxidation of RhF_6^-

In the DRILAB, $KRhF_6$ (87 mg, 0.34 mmol), $KAgF_4$ (140 mg, 0.626 mmol), and BiF_5 (828 mg, 2.73 mmol) were mixed as solids in one tube of a passivated FEP T-reactor. After removing the argon atmosphere under dynamic vacuum, about 2.2 mL aHF was condensed onto the solids and warmed to room temperature. Not until the reaction mixture had warmed almost completely to room temperature was there evidence of reaction. A small amount of bubbling occurred as the orange solution turned blood red. After ~15 min, all volatile species were condensed into the other arm of the reactor. Dry O_2 was introduced and consumed as the red RhF_6 warmed, forming O_2RhF_6. After removing the aHF under vacuum and drying the product for 2.5 h, a red-brown O_2RhF_6 (16 mg, 0.062 mmol, yield = 18%) was recovered, as confirmed by X-ray powder photography {cubic, a_o = 10.18(2) Å, see Table 4.1}.

Table 4.1. X-ray powder data for O_2RhF_6 with a cubic unit cell. a_o = 10.18(2) Å.

	$1/d^2 \times 10^4$				
I/I_o	observed	calculated	h	k	l
s	389	386	2	0	0
vs	782	772	2	2	0
vw	1150	1158	2	2	2
vvw	1539	1544	4	0	0
w	1943	1930	4	2	0
vvw	2129	2123	3	3	2
m	2335	2316	4	2	2
vw	3057	3088	4	4	0

4.2.6. Oxidation of PtF_6^-

4.2.6.1. Using $KPtF_6$ as a Reagent

In the DRILAB, $KPtF_6$ (112 mg, 0.321 mmol) and $KAgF_4$ (161 mg, 0.724 mmol) were loaded into the same tube of a passivated FEP T-reactor fitted with a Teflon valve. After the reactor was pumped down under dynamic vacuum, aHF (1.5 mL) was condensed onto the solid mixture. Upon warming to room temperature, the solution turned bright orange with some orange solid remaining undissolved. (Presumably, the highly-soluble $KAgF_4$ completely dissolved to give the colored solution while some of the less soluble $KPtF_6$ remained in the solid phase.) A small portion of aHF was condensed into the other arm of the reactor; no colored phase was condensed over with it, so it was poured back. The reactor was then pressurized to 1500 torr with BF_3, which immediately precipitated a deep red solid from the solution. Additional BF_3 was added until the reaction consumed no more and the reactor remained at 1500 torr. The resulting HF solution was light yellow in color, but there were no transferable colored volatile species. In order to increase the solubility of the BF_3 in the HF, the reactor was cooled down below 0 °C and agitated with no visible change. Again, performing the volatility test for colored material gave a negative result. So the majority of the BF_3 was removed from the reactor by evacuating the reactor down to 750 torr (at which point the HF boiled). Then enough AsF_5 was introduced into the reactor to bring its pressure up to 1500 torr. Formation of a blood-red solution in the aHF was immediately apparent.

After allowing this reaction to continue for 10 min, a volatility test yielded a deep red material in the side arm. So all volatile material was condensed into the side arm and frozen down to -196 °C. The reactor was opened to a pressure of O_2 gas and then closed again before being allowed to warm. As the deep-red mixture melted, it immediately reacted to give a yellow solution with some deep red precipitate. Upon removal of the HF and other volatile gases under dynamic vacuum at room temperature, the yield of dark red solid precipitate increased. This solid gave an XRPP, all lines of which matched that of O_2PtF_6 {cubic[8], a_o = 10.032(2) Å}. The overall yield of O_2PtF_6 was 19.4%.

4.2.6.2. Using $LiPtF_6$ as a Reagent

The previously-described reaction was repeated using $LiPtF_6$ instead of the less soluble $KPtF_6$. Reagent quantities were as follows: $LiPtF_6$ (100 mg, 0.316 mmol), AgF_3 (103 mg, 0.625 mmol), BiF_5 (791 mg, 2.60 mmol), aHF (2.1 mL). The reaction was agitated for about 12 min at room temperature. O_2PtF_6 (78 mg) was isolated in 72% yield, and the light-green byproduct {probably $Ag(BiF_6)_2$ and excess BiF_5, with perhaps some $Ag(BiF_6)(PtF_6)$, as well} remaining in the other arm of the reactor was measured to be 907 mg.

In a similar reaction, AsF_5 was first used to generate AgF_3 *in situ*, and then to activate the cationic silver(III) in order to affect the oxidation of PtF_6^-. For this reaction, $LiPtF_6$ (101 mg, 0.320 mmol) and $KAgF_4$ (135 mg, 0.608 mmol) were combined, as solids, in one arm of a passivated FEP T-reactor. About 1.6 mL aHF was condensed onto

the solids at -196 °C, generating an orange solution above a small amount of undissolved solid at room temperature. AsF_5 was slowly introduced into the reactor, first forming a red suspension. As more AsF_5 was added, the red PtF_6 gas was produced in copious amounts. After approximately 20 min reaction time, a liquid N_2 bath was used to condense all volatile compounds into the other arm of the reactor. Then ~1 mmol O_2 gas was introduced into the reactor, leading to the formation of a red precipitate in an orange solution upon melting of the aHF. The aHF was removed as the reactor was evacuated, leaving the deep red O_2PtF_6 (82 mg, 75% yield) in one arm and a dark green-blue solid ($KAsF_6$, $LiAsF_6$, and $AgFAsF_6$, with perhaps some $AgFPtF_6$) in the other arm.

4.2.7. Attempted Oxidation of AuF_6^-

The following three reagents were all loaded into the same arm of a passivated FEP T-reactor: XeF_5AuF_6 (256.6 mg, 0.4776 mmol), AgF_3 (153.7 mg, 0.9323 mg), and BiF_5 (785.1 mg, 2.583 mmol). Approximately 2.2 mL of aHF were condensed onto the mixed solids at -196 °C and then allowed to warm to -40 °C. The solution appeared faint yellow with a red solid at the bottom. Intermittent agitation was maintained for 25 min, during which time no sign of reaction was visible other than the occasional release of a bubble of colorless gas. Liquid nitrogen was used to test for the presence of a volatile, colored compound by condensing a very small amount of volatile material in the other arm of the reactor. This test came up negative, so the -40 °C bath was removed. As the reaction mixture warmed, it began to bubble vigorously, and the yellow solution began to

turn green. Another test for volatile, colored material came up negative. The reaction was left to go to completion at room temperature over the next 1.5 h. Then the HF was pumped away and the green solid product dried for 3 hours.

4.3. Results and Discussion

Experimental evidence which established that the electron affinity of Ag^{II}_{solv} is just a few kcal·mole^{-1} below that estimated for PtF_6 (see Chapter 7) suggests that the much more potent trivalent species Ag^{III}_{solv} has more than the requisite electron affinity to affect the oxidation of PtF_6^-. Indeed, the rapid and vigorous evolution of blood-red PtF_6 from an acidified solution of Ag^{III}_{solv} and PtF_6^- at ordinary temperatures confirms this prediction. A similar reaction was performed to demonstrate that RuF_6, whose electron affinity is estimated to be approximately equal to that of PtF_6, could also be liberated from its anion. The yield of PtF_6 (measured gravimetrically after combination with O_2 to form O_2PtF_6) was 75%, while that of RuF_6 was nearly 60%. For the platinum and ruthenium reactions, the conditions were fairly well matched; however, a greater yield of O_2PtF_6 was measured. This observation is in accord with published results indicating that O_2PtF_6 and PtF_6 are more stable than their ruthenium counterparts. Edwards *et al.*[7] found that, upon heating a sample of O_2RuF_6, decomposition began at approximately 60 °C; and yet O_2PtF_6 remained intact to at least 100 °C. Furthermore, ruthenium pentafluoride was observed as the thermal decomposition product of O_2RuF_6, indicating ready loss of fluorine from the RuF_6 molecule. O_2PtF_6 merely falls apart into molecular oxygen and

the hexafluoride of platinum, the two of which spontaneously recombine at lower temperatures. Therefore, it is possible that some of the RuF_6 which was generated in the aHF decomposed to RuF_5 and F_2 in solution[9] as O_2RuF_6. The overall reaction scheme for the oxidation of MF_6^- to MF_6 is as follows:

$$AgF_3 + LiMF_6 + 3\,BiF_5 \xrightarrow{aHF} Ag(BiF_6)_2 + LiBiF_6 + MF_6$$

$$MF_6 \xrightarrow{O_2} O_2MF_6$$

So the byproduct arm of the reactor should contain a mixture of $Ag(BiF_6)_2$, $LiBiF_6$, and excess BiF_5. Small quantities of metal pentafluoride, which are commonly poorly crystalline, should not be detected by XRPP in such a mixture of salts, and were not.

Observations in this laboratory have determined that lithium hexafluorometallate(V) salts are generally significantly more soluble than their potassium counterparts in aHF solution. In addition, $LiRuF_6$ has been qualitatively observed to be more soluble than $KPtF_6$. These solubility considerations may account for the relatively low yield obtained in the oxidation of $KPtF_6$ (~20 %) as compared to those obtained in the oxidations of $LiPtF_6$ (75%) and $LiRuF_6$ (58%). It follows, then, that an extended reaction time could have increased the extent of oxidation of the $KPtF_6$. However, the hexafluoride of platinum (as well of those of ruthenium, rhodium, and iridium) is seen to attack even well-passivated FEP and Teflon reactor parts within just a few minutes, so reaction time was kept to a minimum.

The interaction of AgF_3 and XeF_5AuF_6 in acidified aHF did not generate a colored, volatile species. At lower temperatures, in fact, there was no sign of reaction at all. This is unfortunate, since it is considered that the electron affinity of the Au center of the as yet unknown molecule AuF_6 is sufficiently high that facile loss of a fluorine atom is likely to occur, even with moderate vibrational energy. All efforts to prepare AuF_6 in hot reactions akin to those used for MF_6 (M = Pt, Ru, Rh) have failed. A low-temperature electron oxidation of AuF_6^- promised to be the best synthetic approach to AuF_6. As the reaction mixture was warmed toward room temperature, all indications are that the AgF_3 decomposed in the acid solution by the reaction expressed in Equation (4). The XeF_5AuF_6 merely provided XeF_5^+ and AuF_6^- spectator ions to the system,

$$AgF_3 \xrightarrow[BiF_5]{aHF} Ag(BiF_6)_2 + \tfrac{1}{2} F_2 \qquad (4)$$

the oxidation of AuF_6^- being out of reach of the cationic Ag^{III}_{solv}, the most powerfully-oxidizing silver system known. The green product recovered was probably a solid mixture of yellow XeF_5AuF_6 and blue-green $Ag(BiF_6)_2$, although XRPP showed a very faint pattern containing only those lines which belong to the silver salt.

It is pertinent that KrF^+ oxidizes[10] O_2 to O_2^+, and thus has an oxidizing potential comparable with MF_6 (M = Pt, Ru, Rh). However, because $KrFPtF_6$ has been reported by Gillespie and Schrobilgen[10] to decompose in solution with formation of PtF_5, it appears that in aHF solution KrF^+ does not capture the electron from PtF_6^-, but rather the F^- ion. This result indicates that in aHF solution the KrF^+ is unable to electron oxidize PtF_6^-, yet

cationic Ag^{III}_{solv} is able to do so. Evidently, cationic Ag^{III}_{solv} is a more powerful oxidizer than KrF^+ in that same solvent. Indeed, the cationic Ag^{III}_{solv}, present in the aHF solutions containing strong F^- acceptors such as AsF_5 or BiF_5, is the most potent chemical oxidizer so far discovered.

4.4. Conclusions

The red solid AgF_3 is of very low solubility in aHF solution, although suspensions in aHF slowly lose F_2. However, introduction of a strong fluoro-acid (*e.g.* AsF_5 or BiF_5) appears to capture fluoride from the Ag(III), permitting a cationic solution phase species, Ag^{III}_{solv}, to be formed. With no appropriate reducing agent present, this cationic silver species eventually captures an electron from F^- ion, or reductively eliminates fluorine, generating F_2 gas and Ag(II). The lifetime of the cationic Ag^{III}_{solv} is sufficiently long to provide for the production of PtF_6 from PtF_6^- in 75% yield, and the other platinum metal hexafluorides that are capable of oxidizing oxygen, RuF_6 and RhF_6, are also effectively liberated from their MF_6^- anions. This cationic Ag^{III}_{solv} species in aHF is a superior electron oxidizer to KrF^+ and therefore the most potent chemical oxidizer found so far. It does not liberate AuF_6 from AuF_6^-, however (see Chapter 1).

4.5. References

[1] R. Bougon and M. Lance, *C. R. Seances Acad. Sci., Ser. 2,* **297** (1983), p 117.

[2] Y. M. Kiselev, A. I. Popov, A. A. Timakov, K. V. Bukharin, and V. F. Sukhoverkhov, *Zh. Neorg. Khim.*, **33** (1988), p 1252.

[3] R. Hoppe and R. Homann, *Z. Anorg. Allg. Chem.*, **379** (1970), p 193.

[4] B. Žemva, K. Lutar, A. Jesih, W. J. Casteel, Jr., and N. Bartlett, *J. Chem. Soc., Chem. Comm.*, (1989), pp 346-347.

[5] B. Žemva, K. Lutar, A. Jesih, W. J. Casteel, Jr., A. P. Wilkinson, D. E. Cox, R. B. Von Dreele, H. Borrmann, and N. Bartlett, *J. Am. Chem. Soc.,* **113** (1991), pp 4192-4198.

[6] R. Hoppe, *Z. Anorg. Allg. Chem.,* **292** (1957), p 28.

[7] A. J. Edwards, W. E. Falconer, J. E. Griffiths, W. A. Sunder, and M. J. Vasile, *J. Chem. Soc., Dalton Trans.,* (1974), pp 1129-1133.

[8] N. Bartlett and D. H. Lohmann, *J. Chem. Soc.,* (1962), p 5253.

[9] In this laboratory, it has been observed that prolonged evacuation of O_2RuF_6 at room temperature generates a green solid which is very likely RuF_5.

[10] R. J. Gillespie and G. J. Schrobilgen, *J. Chem. Soc., Chem. Commun.,* (1974), p 90; and *Inorg. Chem.,* **15** (1976), p 22.

Chapter 5

Synthesis and Oxidizing Properties of AgF^+ Salts

5.1. Introduction

In 1982, Frlec *et al.*[1] reported the synthesis of $AgF^+AsF_6^-$, the first compound containing the silver(II) cation AgF^+. Several years later, experimentation in this lab[2] revealed that the interaction of AgF_3 and AsF_5 in aHF released elemental fluorine, leading to the formation of $AgFAsF_6$ by way of the following reaction:

$$AgF_3 + AsF_5 \rightarrow AgFAsF_6 + \tfrac{1}{2} F_2 \qquad (1)$$

An attempt to utilize the electron-withdrawing ability of the Ag(III) in this reaction to oxidize Xe, however, did not result in the formation of the Ag(II) salt, but rather the Ag(I) salt, $AgAsF_6$, and divalent Xe. Starting with AgF_2 instead of AgF_3, the following interaction was observed[3] to occur:

$$4\,AgF_2 + 5\,AsF_5 + 2\,Xe \rightarrow 4\,AgAsF_6 + Xe_2F_3AsF_6 \qquad (2)$$

Thus, it was concluded that, under acidic conditions in aHF at room temperature, Ag(II) was able to oxidize Xe(0) to Xe(II). A systematic search for other AgF^+ salts and an

investigation into the oxidizing properties of this cation were undertaken and soon led to the discovery[3] of the tetrafluoroborate analogue, and then the discovery[4] of the tetrafluoroaurate(III) and the hexafluoroaurate(V) analogues.

In his studies, Casteel[5] showed that the $(AgF)_n^{n+}$ salts were less oxidizing than the blue solutions in aHF obtained by supplying additional acid to them. Since $(AgF)_n^{n+}$ involves the addition of the electron-rich F^- to Ag^{2+}, the lower oxidizing potential of the complex cation relative to the Ag^{2+} is easily understood. It is less obvious that the solvated Ag^{2+} cation (Ag^{II}_{solv}) would also be more potent than $(AgF)_n^{n+}$, but experimental evidence shows it to be so.[6] However, the oxidizing power of the $(AgF)_n^{n+}$ itself remained to be better defined.

In this chapter, the general question of which AgF^+ salts can be prepared is explored. A large part of this study was directed to MF_6^- salts of third transition series elements because they provided a well-defined, nearly isodimensional set of anions, the oxidizability of which changes regularly across the series, and therefore responded to the question of the oxidizing power of $(AgF)_n^{n+}$. The synthetic work was accompanied always by X-ray powder diffraction studies supplemented wherever possible by single crystal investigations to discover the structures, or at least prove the purity, of the phases prepared. Magnetic measurements were also important in demonstrating that possible impurities such as $Ag(MF_6)_2$ salts (simple paramagnets[7]) or AgF_2 (a ferromagnet[9], T_c =

163 K) were absent from the preparations, the magnetic susceptibility of AgF^+ salts characteristically exhibiting temperature-independence (see Experimental and Chapter 6).

5.2. Experimental

5.2.1. Interaction of $LiOsF_6$ with F_2 in aHF

A passivated FEP T-reactor was loaded with $LiOsF_6$ (26 mg, 0.084 mmol) and placed on the vacuum line. Approximately 1.2 mL aHF was condensed onto the colorless solid at -196 °C, dissolving it completely upon warming to room temperature to give a colorless solution. The reactor was pressurized to 2 atm with F_2 gas, following which the solution was cooled to near freezing (in order to increase the solubility of the gas in the HF), then rewarmed with agitation. A liquid N_2 bath was used to condense a small quantity of the HF into the other arm of the reactor. Because OsF_6 is a volatile gas which appears bright yellow when condensed, the presence of any in the reactor would be made obvious by this test. In fact, no color was seen in the condensate. So the reaction mixture was agitated for 30 min and the test repeated. Again, a negative result indicated the absence of OsF_6. The reactor was warmed to room temperature and all volatile compounds removed under vacuum; the $LiOsF_6$ was recovered.

5.2.2. Preparation of AgF_2

A passivated FEP T-reactor was loaded with AgF (566 mg, 4.46 mmol) which had been recrystallized from aHF. 1.5 mL aHF was condensed onto the orange solid, dissolving it at room temperature to give a slightly orange-tinted solution with a small

quantity of brown solid left undissolved. This solution was decanted before F_2 was used to pressurize the reactor to 2 atm and continuous agitation was begun. Over the next few hours, more F_2 was intermittently added as it was consumed in the reaction to give the brown, insoluble AgF_2. After 6 h reaction time, the aHF was decanted and removed under vacuum. The brown powder was dried for more than 5 h. An X-ray powder photograph of material prepared in this manner exhibits the XRPP of AgF_2 {orthorhombic[8], $a_o = 5.568(1)$, $b_o = 5.831(1)$, $c_o = 5.101(1)$ Å} in a highly crystalline form (599 mg, 92% yield). AgF_2 displays a ferromagnetic susceptibility[9], with a transition temperature of 163 K (see Figure 5.1 and Discussion below). CaF_2 is used as a diamagnetic diluent in this sample because of the very large magnitude of the volume susceptibility of AgF_2 below its transition temperature.

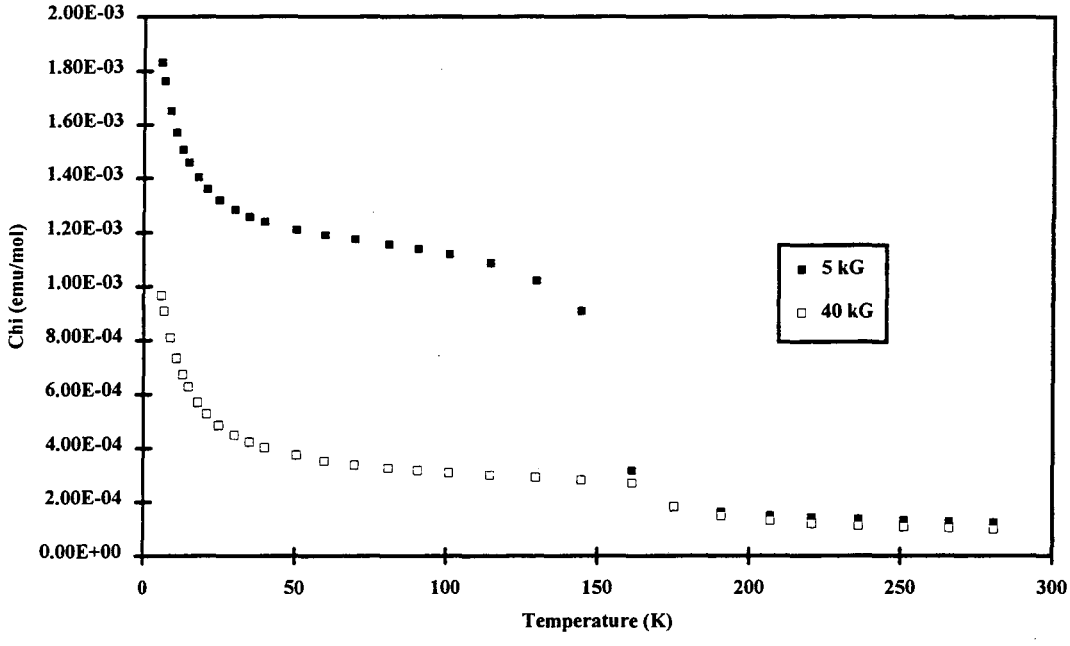

Figure 5.1. Magnetic data for mixture of 15% AgF_2, 85% CaF_2.

5.2.3. Preparation of $Ag(BiF_6)_2$

Recrystallized AgF (141 mg, 1.11 mmol) and BiF_5 (748 mg, 2.46 mmol) were loaded into separate tubes of a passivated FEP T-reactor inside the DRILAB. After evacuating the argon gas from the reactor, approximately 3 mL aHF was condensed onto the AgF, dissolving it completely after warming to room temperature. Fluorine gas was repeatedly introduced into the reactor as it was consumed in the production of AgF_2 (see AgF_2 synthesis above). After all signs of reaction had ceased, the reactor was evacuated to 1000 torr. Then the solid BiF_5 was shaken over into the reaction tube. Turquoise solid was seen to form immediately on the walls of the reactor tube. A small quantity of aHF was condensed over into the other tube and used to rinse over any remaining BiF_5. The

reaction mixture was agitated continuously for 15 h. The colorless aHF solution was then decanted from the turquoise solid and all volatile species were pumped away under dynamic vacuum. An X-ray powder photograph of the product (835 mg, 99.7% yield) gave the XRPP of $Ag(BiF_6)_2$, as shown in Table 5.1. A single crystal X-ray structure solution was later performed in this laboratory, permitting extensive indexing of the powder pattern observed. Magnetic susceptibility measurements performed on this material (see Figure 6.8) show Curie-Weiss behavior above ~50 K, with a magnetic moment of approximately 2.2 B.M. This value is in exact agreement with that calculated[10] for Cu^{2+} assuming free-ion values of spin-orbit coupling.

Table 5.1. X-ray powder data for $Ag(BiF_6)_2$ with a triclinic unit cell.
$a_o = 5.217(2)$ Å, $b_o = 5.583(3)$ Å, $c_o = 8.948(5)$ Å,
$\alpha = 76.01(3)°$, $\beta = 88.98(3)°$, $\gamma = 65.12(3)°$, $V = 228.4$ Å^3.

I/I_o		$1/d^2 \times 10^4$					
observed	calculated [a]	observed	corrected [b]	calculated [c]	h	k	l
m	55	425	420	418	0	1	0
m	19	456	452	451	1	0	0
vs	36	542	537	535	0	0	2
	40			538	1	0	-1
	37			554	1	1	1
vs	100	639	633	631	1	0	1
vs	90	718	712	705	1	1	-1
	87			709	0	1	2
vs	39	1216	1209	1197	0	1	-2
	11			1205	0	0	3
	41			1205	1	-1	-1
m	36	1321	1313	1313	1	2	1
m	16	1479	1471	1475	2	1	0
	20			1475	1	1	3
w	17	1526	1518	1515	1	0	-3
vvw	7	1727	1718	1718	0	2	2
w	17	1813	1804	1802	2	0	0

I/I_o		$1/d^2 \times 10^4$					
observed	calculated [a]	observed	corrected [b]	calculated [c]	h	k	l
vw	16	1927	1919	1926	1	1	-3
vw	18	1995	1986	1989	1	2	3
vvw	5	2072	2062	2067	2	1	-2
m	17	2161	2152	2150	2	0	-2
w	15	2224	2215	2217	2	2	2
vvw		2410	2400				
m	12	2534	2524	2525	2	0	2
vw	6	2606	2596	2594	2	1	3
vw	5	2730	2720	2729	1	2	4
w	13	2839	2829	2836	0	2	4
m	18	2977	2966	2965	2	-1	0
vvw	4	3066	3056	3069	-2	1	2
m	13	3208	3197	3198	-1	2	3
m	14	3347	3336	3327	2	3	0
	13			3339	1	3	3
w	8	3517	3506	3508	3	1	1
w	2	3594	3583	3570	2	0	-4
	5			3608	0	-2	3
m	7	3763	3752	3736	1	2	5
	6			3743	-1	1	5
vvw	2	3955	3944	3932	2	-1	2
w		4070	4059				
vw	2	4288	4277	4259	0	-3	1
w	8	4401	4390	4384	3	2	3
w	11	4530	4519	4505	3	1	-3
vvw	2	4692	4681	4681	2	0	-5
vw	4	4867	4855	4863	1	1	6
vw	5	5054	5042	5048	-1	3	1
vvw	1	5173	5161	5154	-2	2	3
vvw	5	5254	5242	5251	2	4	2
vw	5	5363	5351	5336	1	4	1
vvw	2	5450	5439	5434	2	-2	1
vvw	4	5610	5598	5617	2	0	5
vvw	3	5916	5904	5900	4	2	0
vvw	2	6073	6062	6060	2	0	-6
vvw	3	6209	6197	6172	1	-2	4
vvw	1	6384	6373	6380	0	3	6
w	2	6561	6550	6559	2	3	-4
	2			6559	0	0	7

I/I_o		$1/d^2 \times 10^4$					
observed	calculated [a]	observed	corrected [b]	calculated [c]	h	k	l
w	5	6699	6687	6683	0	4	0
	2			6689	1	-3	2
vw	1	6802	6791	6794	3	1	5
vvw	2	6923	6912	6934	4	2	3
vvw	2	7091	7079	7074	1	-1	6
vw	2	7212	7201	7209	4	0	0
w	2	7404	7393	7389	-1	2	7
vvw	1	7555	7544	7537	4	1	3
vvw	2	7836	7825	7814	4	2	4
vw	2	8292	8282	8270	4	2	-4
vw	2	8609	8598	8602	4	0	-4
vvw	2	8952	8941	8937	0	-3	5
vvw	2	9030	9020	9000	3	4	6
vvw	1	9349	9339	9353	0	-4	3
vvw	2	9391	9381	9384	-3	2	5
vvw	2	9699	9689	9702	5	3	-1
vvw	1	9795	9786	9787	3	1	-7
vvw	1	10463	10454	10445	5	2	-3
vvw	3	10853	10844	10851	-3	3	3

[a] Calculated intensities are based on cell parameters and atom positions provided in the single crystal structure solution.

[b] An absorption correction has been applied to the line positions.

[c] Calculated line positions are based on cell parameters and atom positions provided by a refinement on the powder data presented here.

5.2.4. Preparation of $AgBF_4$

A passivated FEP T-reactor was loaded with ~1 gm AgF as received. After condensing ~2 mL aHF onto the AgF, the solution was warmed to room temperature. Probably due to the light sensitivity of AgF, there is always some brown solid which slowly settles out of solution, but everything else dissolves to give a slightly orange-colored solution. After allowing several hours for the brown solid to settle, the HF

solution was decanted into the other arm of the reactor. BF_3 was then introduced into the reactor, immediately forming colorless needles. As the BF_3 was consumed, more was intermittently added until no more needles could be seen to form. Then the reactor was pressurized to 1500 torr with BF_3 and agitated continuously for over 2 h. The HF/BF_3 was then removed and the colorless product dried for approximately 3 h. X-ray powder photography was used to confirm the identity and purity of the $AgBF_4$ product (orthorhombic[11], $a_o = 8.157$, $b_o = 5.345$, $c_o = 6.792$ Å).

5.2.5. Preparation of $AgFBF_4$

5.2.5.1. Violet Colored $AgFBF_4$

A passivated FEP T-reactor was loaded with $AgBF_4$. Approximately 1 to 2 mL aHF was condensed onto the white solid, only partially dissolving it at room temperature. The reactor was pressurized to ~900 torr with BF_3 and then to 1500 torr with F_2 gas, and the solution was mechanically agitated or stirred. More F_2 gas was periodically introduced to replace that which was consumed in the reaction as the white solid slowly turned gray-blue. Mixing was continued for at least 12 h, until no more F_2 uptake was observed. Most of the F_2 was then removed from the reactor by slowly pumping on the reactor until its internal pressure dropped to 800 torr at room temperature. At this point, the reactor was pressurized to 2 atm with BF_3, which slightly darkened the blue tint of the solution. This mixture was left to sit for 15 min. Then the product was dried as fully as possible by decantation. All volatile species present were pumped away and the gray-blue product dried for over 3 h under dynamic vacuum. X-ray powder photography of

material prepared in this manner gives the XRPP expected of pure $AgFBF_4$ {tetragonal[4], $a_o = 6.7000(3)$, $c_o = 4.0113(2)$ Å}. Magnetic susceptibility data for this material were obtained (Figure 5.2), showing it to be essentially free of AgF_2, and to have a very small magnitude temperature-independent paramagnetism.

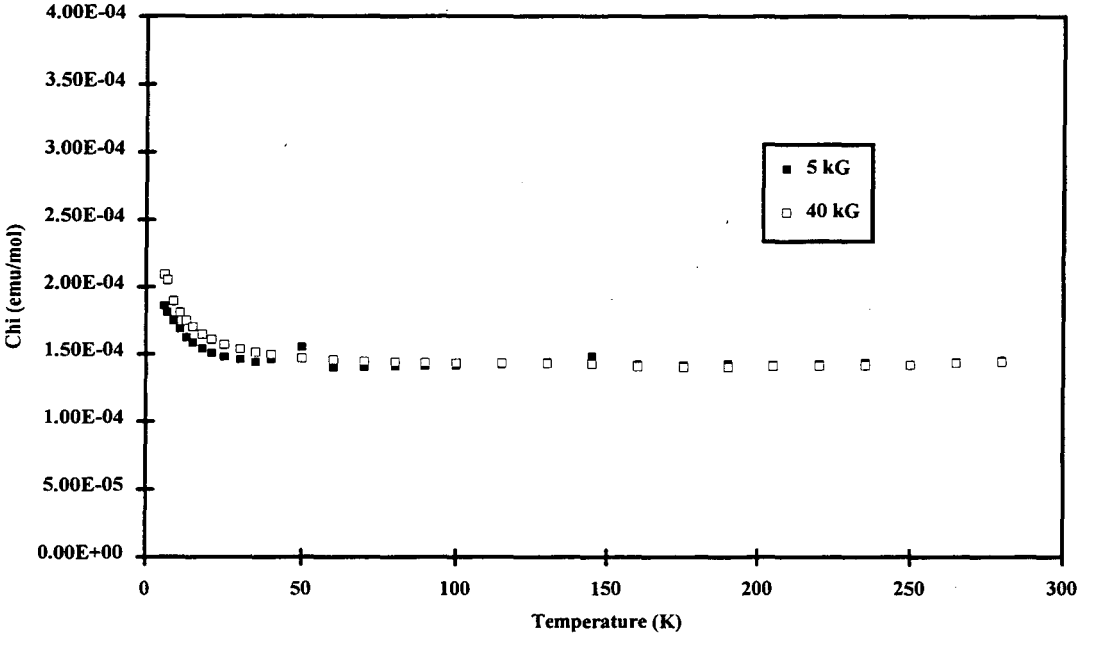

Figure 5.2. Magnetic data for $AgFBF_4$.

5.2.5.2. Bronze Colored $AgFBF_4$

Several different proportions for the two solid reagents were tried, the most successful of which is described. A passivated FEP T-reactor was loaded with $AgBF_4$ (149 mg, 0.765 mmol) and AgF (5 mg, 0.04 mmol) in the same arm. After evacuating the reactor, 1 mL aHF was condensed onto the solids. The reactor was pressurized to

1000 torr with F_2 and intermittently agitated. A bronze precipitate formed immediately and the HF turned very light blue. After just 15 min of intermittent agitation, the HF/F_2 was removed and the bronze crystalline material dried for 3 h. An X-ray photograph reveals only the patterns of $AgFBF_4$ and AgF_2. Macroscopic crystals of this bronze material were visible, one of which was selected for single crystal X-ray structure determination (see Chapter 6).

Similar results were obtained when AgF_2 was used in place of AgF, although the crystallinity was noticeably worse.

5.2.6. Preparation of $AgAsF_6$

A passivated FEP T-reactor was loaded with recrystallized AgF (385 mg, 3.04 mmol). 1.5 mL aHF was condensed onto the solid and warmed to room temperature. A very small quantity of undissolved, brown solid was visible in a slightly orange solution. After letting the brown solid settle, the solution was decanted into the other arm of the reactor. AsF_5 was introduced into the reactor and immediately formed a colorless powder precipitate. Over the next 2 h of intermittent agitation, the AsF_5 pressure was periodically restored to ~1500 torr as it was consumed in the reaction. The HF solution was decanted and the HF back-distilled onto the white solid. Two more such washings of the precipitate were performed prior to drying the $AgAsF_6$ product (861 mg, 96% yield) under dynamic vacuum for 3 hours. Material prepared in this manner gives an XRPP indicative of pure $AgAsF_6$ (cubic[12], a_o = 7.74 Å).

5.2.7. Preparation of $AgFAsF_6$

A passivated FEP T-reactor fitted with 1/2" tubes was loaded with $AgAsF_6$ (734 mg, 2.47 mmol). 3 mL aHF was condensed onto the white solid, dissolving very little of it. The reactor was pressurized to 1000 torr with AsF_5 and then to 1500 torr with F_2. Continuous mechanical agitation was begun, and as the reaction consumed F_2, more was intermittently added. After 15 h of reaction time, F_2 uptake had ceased; the solid was aqua blue and the solution a slightly deeper blue. After decanting the HF, the volatile species were pumped out and the $AgFAsF_6$ product (709 mg, 91% yield) dried for over 3 h. X-ray powder photography of material prepared in this manner shows only the XRPP of $AgFAsF_6$ {orthorhombic[13], a_o = 7.585(1), b_o = 6.997(6), c_o = 9.852(1) Å}. The magnetic susceptibility of this material is shown in Figure 5.3, in which the signal is essentially temperature-independent above ~100 K. A paramagnetic impurity may be responsible for the low-temperature rise in susceptibility.

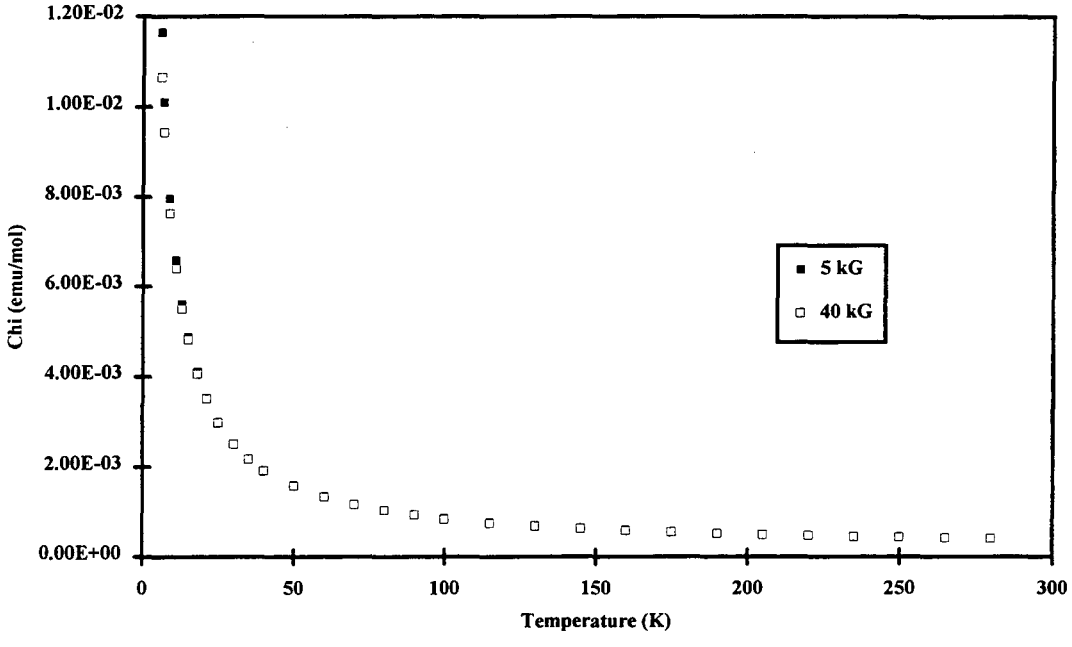

Figure 5.3. Magnetic data for $AgFAsF_6$.

5.2.8. Preparation of $AgBiF_6$

A passivated FEP T-reactor was loaded with $AgBF_4$ (206 mg, 1.06 mmol) in one tube and BiF_5 (347 mg, 1.14 mmol) in the other. Approximately 1.0 mL aHF was condensed onto each of the reagents, dissolving all of the BiF_5, but only a small portion of the $AgBF_4$. As the BiF_5 solution was slowly poured into the $AgBF_4$ solution, there was vigorous gas evolution and precipitation of a light yellow solid. The gas evolution quickly abated, so some of the BF_3 pressure was released into the vacuum line before continuous agitation of the reaction mixture was begun. After 30 min, the solution was cooled to 0 °C and decanted. The HF (containing some BF_3) was then condensed back

over at -196 °C, warmed to 0 °C, and then decanted again. The volatile species were pumped away and the light yellow product dried for 3 hours. An X-ray powder photograph of the product shows an XRPP (see Table 5.2) related to those of $AgRuF_6$, $AgOsF_6$, $AgIrF_6$, and $AgSbF_6$, which Kemmitt *et al.*[14] report as the $KNbF_6$ structure type. The indexing provided in Table 5.2 is based upon this tetragonal structure type and yields reasonable lattice cell parameters for the formulation $AgBiF_6$ (467 mg, 102% yield).

Table 5.2. X-ray powder pattern of $AgBiF_6$ with a tetragonal unit cell. $a_o = 5.073(1)$ Å, $c_o = 9.540(3)$ Å, $V = 245.5(2)$ Å^3.

	$1/d^2 \times 10^4$						$1/d^2 \times 10^4$				
I/I_o	obsd.	calc.	h	k	l	I/I_o	obsd.	calc.	h	k	l
s	390	389	1	0	0	m	5910	5898	2	1	6
m	438	439	0	0	2	w	6219	6217	4	0	0
vs	780	777	1	1	0	m	7049	7045	4	1	2
vs	831	828	1	0	2	vvw	7456	7453	3	0	6
vvw	957					vw	7794	7798	3	2	5
vvw	1028					vvw	7981	7975	4	0	4
vvw	1164					vvw	8579	8586	2	0	8
vw	1218	1217	1	1	2	vvw	8772	8761	4	2	3
s	1562	1554	2	0	0	vw	9000	9007	3	2	6
s	1772	1766	1	1	3	vw	9525	9530	4	2	4
vvw	1938	1943	2	1	0	w	10126	10103	5	1	0
vvw	1999	1994	2	0	2	vw	10548	10543	5	1	2
vvw	2149	2146	1	0	4	vvw	10920	10918	3	1	8
vvw	2236					vvw	11396	11379	5	2	1
vs	2390	2382	2	1	2	vw	11679	11708	5	2	2
s	2546	2543	2	0	3	vw	11835	11861	5	1	4
s	3120	3109	2	2	0	vvw	12931	12930	2	1	10
s	3323	3312	2	0	4	vvw	12946	12930	2	1	10
vvw	3569	3548	2	2	2	vvw	13195	13212	5	3	0
vvw	3704	3701	2	1	4	vvw	13207	13212	5	3	0
s	3891	3886	3	1	0	vw	13640	13638	4	1	8
s	3945	3937	3	0	2	vvw	13959	13951	3	2	9
m	4354	4344	1	0	6	vvw	14452	14429	6	0	2
vvw	4750	4732	1	1	6	vw	14802	14803	4	2	8
m	4872	4867	2	2	4	vw	14808	14803	4	2	8
vvw	5053	5052	3	2	0	vvw	14960	14970	5	3	4
vvw	5275	5255	3	0	4	vvw	14981	14970	5	3	4
m	5499	5491	3	2	2	vvw	15176	15181	4	4	5
m	5654	5644	3	1	4						

5.2.9. Preparation of $AgFBiF_6$

This material was synthesized in a multitude of ways: by oxidation of $AgBiF_6$ with F_2, by metathesis between $AgFBF_4$ and $KBiF_6$, by an attempted oxidation of

$AgFBF_4$ using O_2BiF_6 as the oxidizer, and by an acid displacement reaction with $AgFBF_4$. The acid displacement preparation yielded the most crystalline material, and so is described here. A passivated FEP T-reactor was loaded with $AgFBF_4$ (97 mg, 0.45 mmol) in one arm and BiF_5 (128 mg, 0.42 mmol) in the other. ~2 mL aHF was condensed onto the BiF_5 at -196 °C and then warmed to room temperature. All of the BiF_5 dissolved to give a colorless solution, which was then poured over onto the dry $AgFBF_4$. There was immediate effervescence as a dark blue-gray solid precipitated from the solution. After 30 min of agitation, the HF solution was decanted and removed, leaving behind a yellow-brown solid. A photograph of the blue-gray material (180 mg yield) showed an unidentified, complex pattern very similar to one generated here previously[15] by the interaction of F_2 on $AgSbF_6$ in aHF. Magnetic measurements on this material reveal the same temperature-independent paramagnetism associated with all of the other AgF^+ salts (see Figure 5.4). Taking the product to be $AgFBiF_6$, the yield was 97%.

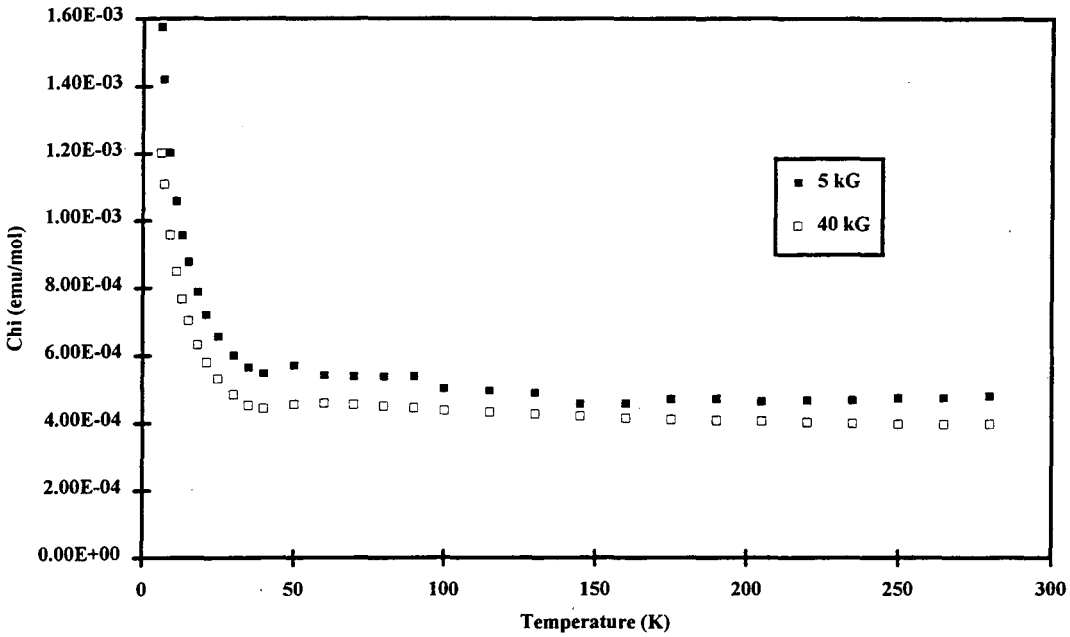

Figure 5.4. Magnetic data for $AgFBiF_6$.
The field-dependence is likely an artifact of the instrumentation or due to a trace of a ferromagnetic impurity.

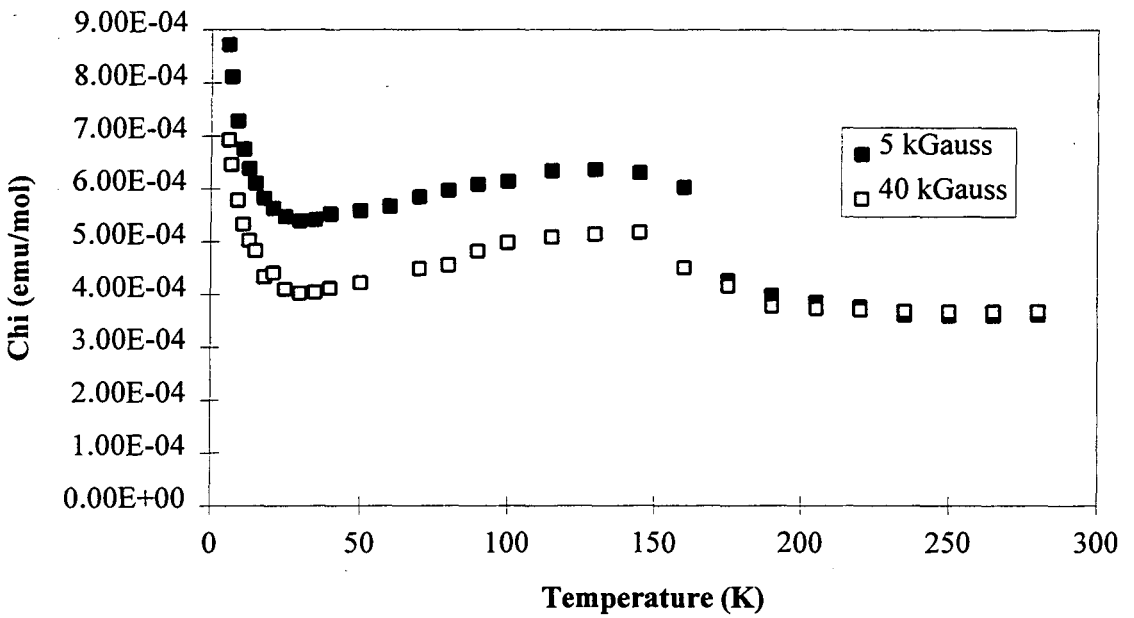

Figure 5.5. Magnetic data for $AgFSbF_6$.
The field-dependence below 160 K is due to a small quantity of AgF_2 present as impurity.

5.2.10. Preparation of $AgRuF_6$

A passivated FEP T-reactor was loaded with AgF (311 mg, 2.45 mmol) in one arm and RuF_5 (409 mg, 2.08 mmol) in the other. Approximately 1.5 mL aHF was condensed onto the AgF, dissolving it completely at room temperature. This solution was poured onto the dry RuF_5. Reaction was immediately evident as the green RuF_5 was replaced by an orange solid in less than a minute. Agitation of the reaction mixture was maintained for 5 h, during which the product became a homogeneous orange solid. The solid was washed by decantation of the aHF solution, the aHF being back-distilled.

Three more such washings were performed prior to removal of the HF. The orange product (650 mg, 97% yield $AgRuF_6$) was dried for 3 h. An X-ray photograph of material prepared in this manner confirmed the identity of the product (tetragonal[14], a_o = 4.85, c_o = 9.54 Å). The temperature dependence of the magnetic susceptibility of the orange solid is that of a simple paramagnet (see Figure 5.6). Because $AgRuF_6$ has shown signs of photosensitivity, FEP storage tubes containing the solid were wrapped in aluminum foil.

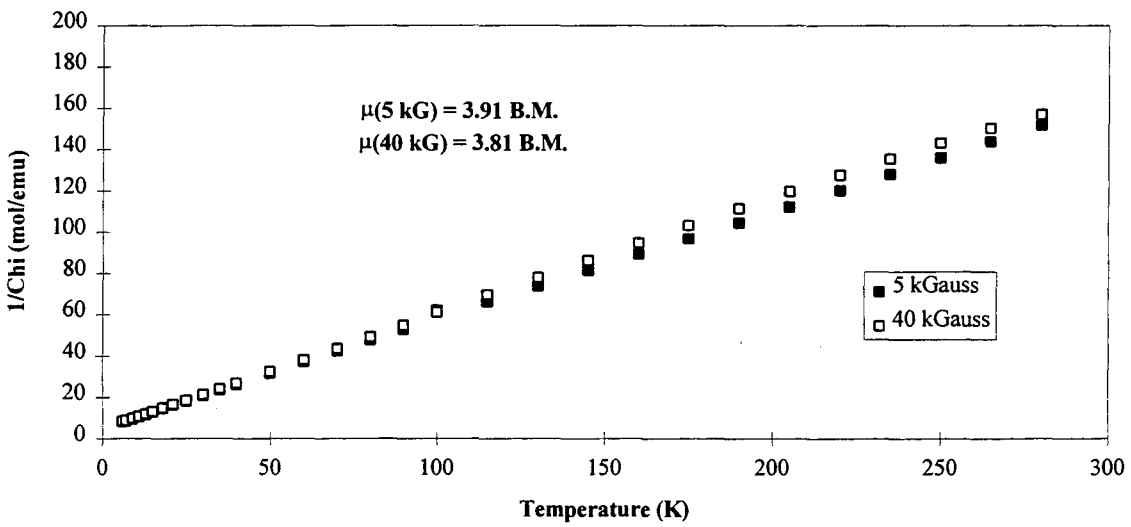

Figure 5.6. Magnetic data for $AgRuF_6$, indicating a simple three-electron paramagnet.

5.2.11. Preparation of $AgFRuF_6$

A passivated FEP T-reactor was loaded with $AgRuF_6$ (247 mg, 0.765 mmol). After condensing 1.5 mL aHF onto the orange solid, the HF was warmed to room

temperature. No color was visible in the solution as all the orange solid appeared to remain undissolved. The reactor was pressurized to 1500 torr with F_2. Aluminum foil was used to wrap the arm of the reactor because of the suspected light sensitivity of $AgRuF_6$. Continuous mechanical agitation was maintained for 19 h, after which most of the F_2 was removed by pumping the reactor down to 800 torr at room temperature. BF_3 was then used to pressurize the reactor to 1400 torr. After less than a minute of agitation, the solution above the black product became very slightly blue. This solution was decanted and the product dried for 3 h under dynamic vacuum. An X-ray photo of the black product showed an XRPP unlike any other AgF^+ salt and indicated the presence of no known impurity. Gravimetry suggested that the material may be $AgFRuF_6$ (257 mg, 98% yield). The magnetic susceptibility of the product is shown in Figure 5.7 in a Curie-Weiss plot. Considering the susceptibility data from 50 K up to 280 K, magnetic moments of 3.98 B.M. at 5 kGauss and 3.87 B.M. at 40 kGauss are calculated, corresponding very well with the spin-only value of 3.87 B.M. for a 3-electron paramagnet. These values are in good agreement with the Ag(I) salt $AgRuF_6$, whose magnetic susceptibility data are shown in Figure 5.6. This result suggests that the d^3 Ru(V) anion dominates the magnetic signal, and the d^9 Ag(II) lends an insignificant contribution to the overall susceptibility.

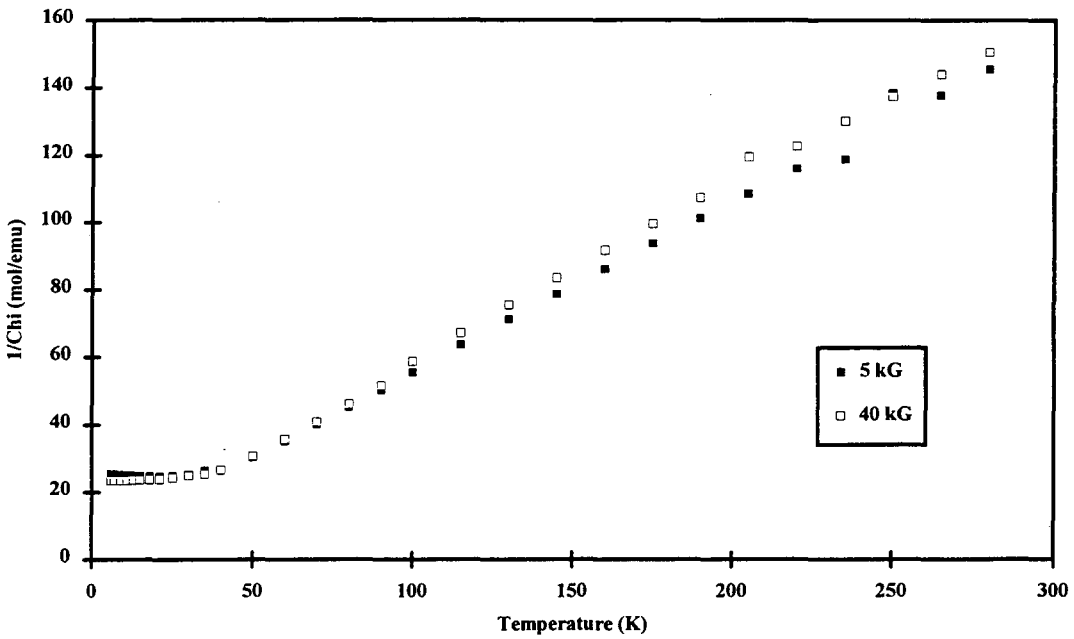

Figure 5.7. Magnetic data for $AgFRuF_6$.

5.2.12. Preparation of $AgOsF_6$

See the synthesis of $AgIrF_6$ below in which reaction details are identical, the only exception being that $AgOsF_6$ is a white solid. Representative weights are as follows: recrystallized AgF reagent (104 mg, 0.820 mmol), SF_3OsF_6 prepared as described in Chapter 3 (264 mg, 0.671 mmol), $AgOsF_6$ product (265 mg, 96% yield). The tetragonal unit cell (a_o = 4.92, c_o = 9.58 Å) is described by Kemmitt *et al.*[14]

5.2.13. Attempted Preparation of $AgFOsF_6$

Two synthetic routes were investigated for the production of $AgFOsF_6$; the first was an oxidation reaction, and the second a metathetical attempt.

A passivated FEP T-reactor containing $AgOsF_6$ (118 mg, 0.286 mmol) and about 2 mL aHF in one tube was pressurized with 2 atm F_2 gas. Formation of the colorless gas OsF_6 was not evident at room temperature. However, upon cooling the other arm of the reactor to -196 °C, the OsF_6 condensed over as a yellow solid. SF_4 was introduced and slowly reacted to form SF_3OsF_6 by the reaction express in Equation (1). In this

$$3\ SF_{4\,(g)} + 2\ OsF_{6\,(g)} \xrightarrow{aHF} 2\ SF_3OsF_{6\,(solv)} + SF_{6\,(g)} \qquad (1)$$

experiment, the yield (70 mg SF_3OsF_6) based on Os metal was 62% and the formation of AgF_2 as a byproduct was confirmed with X-ray powder photography. Unreacted $AgOsF_6$ also showed up as a minor component in the photograph.

The two powders $AgFBF_4$ (110 mg, 0.513 mmol) and $KOsF_6$ (89 mg, 0.26 mmol) were placed into the same tube of a passivated FEP T-reactor inside the DRILAB. After evacuation of the argon from the reactor, approximately 1.2 mL aHF was condensed onto the solid mixture at -196 °C and left to warm to room temperature. Reaction was evident even below room temperature as the blue $AgFBF_4$ solid diminished in quantity, giving way to a brown precipitate. After 10 min of intermittent agitation at room temperature, no blue solid remained, so the volatile species were condensed into the other arm of the reactor at -196 °C. Upon condensation, a deep yellow color was observed, indicative of OsF_6. Approximately 1.5 mmol SF_4 was condensed onto the frozen volatile species and then warmed to ca. 0 °C. Repeated thermal cycling of this mixture, followed by 1h 10 min at room temperature consumed all the OsF_6 {see Equation (1)}, as revealed by the

absence of yellow color upon freezing. The reactor was then evacuated, removing the aHF and any gases present, which resulted in the precipitation of a lavender solid. X-ray powder photography confirmed the identity of the product to be SF_3OsF_6 {cubic[16], a_o = 11.162(4) Å}, and the yield was 65 mg, 64%.

5.2.14. Preparation of $AgIrF_6$

AgF (118 mg, 0.931 mmol) which had been recrystallized from anhydrous HF was loaded into one tube of a passivated FEP T-reactor inside the DRILAB. SF_3IrF_6 (241 mg, 0.610 mmol), prepared as described in Chapter 3, was placed into the other tube of the reactor. After removing the argon from the reactor, about 3/4 mL aHF was condensed onto each of the reagents. Upon warming to room temperature, both of the powders dissolved completely to give colorless solutions. As the AgF solution was slowly poured onto the SF_3IrF_6 solution, the reaction mixture bubbled and an orange solid precipitated out of solution. The product was washed in the aHF three times then dried under dynamic vacuum for 3 h. The XRPP of material prepared in this manner indicates the presence of pure $AgIrF_6$ (tetragonal[14], a_o = 4.85, c_o = 9.70 Å). The yield is essentially quantitative (248 mg, 98% yield).

5.2.15. Preparation of $AgFIrF_6$

A passivated FEP T-reactor was loaded with $AgIrF_6$ (244.1 mg, 0.5895 mmol) inside the DRILAB. After removing the argon under dynamic vacuum, approximately 1 mL aHF was condensed onto the reagent. There were no signs of dissolution of the $AgIrF_6$ as the HF melted and warmed to room temperature. The reactor was then

pressurized to 1500 torr with F_2 gas and continuous agitation of the reaction mixture was begun. Within a few minutes, there was a noticeable darkening of the bright orange solid. After 3 h of continuous agitation, no orange solid remained; instead, there was a black powder beneath a slightly yellow HF solution. Agitation was continued for another 3 h before liquid nitrogen was used to freeze the reaction mixture solid at -196 °C. Any remaining F_2, having a vapor pressure of about 300 torr at this temperature, was then pumped away under dynamic vacuum. Once again, the HF was melted and warmed up to room temperature. Then the reactor was pressurized to 1500 torr with BF_3 gas. This turned the HF solution from pale yellow to pale green, presumably due to the formation of the slightly soluble species $AgFBF_4$. After washing the black product six times in the HF, the solution still appeared green, so the HF was decanted and pumped away, leaving a brown residue in the other arm of the reactor. Temperature- and field-dependent magnetic susceptibility measurements of this sample reveal the presence of only a minute AgF_2 impurity (see Figure 5.8). X-ray powder photographs of material prepared in this manner show only the XRPP of $AgFIrF_6$ {orthorhombic[17], $a_o = 7.627(2)$, $b_o = 7.068(2)$, $c_o = 10.253(4)$ Å}.

A plot of the magnetic susceptibility is provided in Figure 5.8. Once again, temperature-independence is observed, except in the low-temperature realm. In this case, a dip in the susceptibility, which has been observed in other AgF^+ samples, appears to be the result of impurity. In many other AgF^+ compounds, this dip was apparent in some of

the magnetic measurements, but not reproducible from one sample preparation to the next. In this case, careful attention to the purity of the product was not successful in eliminating the dip below ~65 K from these data, only minimizing it.

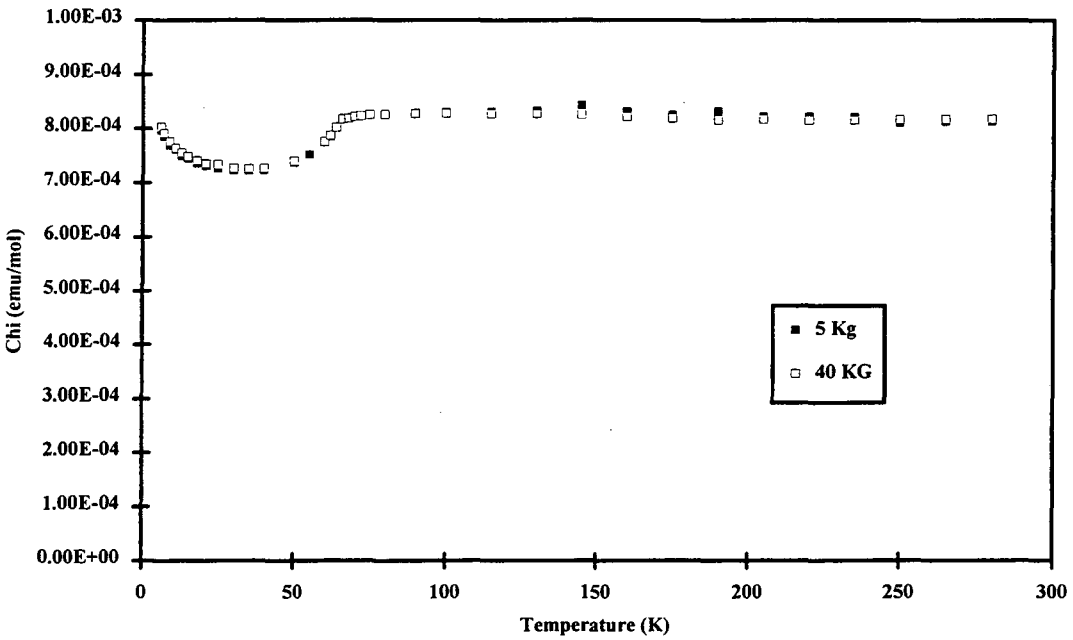

Figure 5.8. Magnetic data for $AgFIrF_6$.

5.3. Results and Discussion

The early work on AgF^+ salts in these laboratories[15] had included preparation of $AgF^+BF_4^-$ and $AgF^+SbF_6^-$ by fluorination of the Ag(I) salts in aHF. These syntheses were so clean that they immediately invited extension of the approach to the general class. An additional advantage that this approach provided to the fluorination of the Ag(I) salt was the slowness of the oxidation since neither $Ag^+A_LF^-$ salts (where A_L is a Lewis acid) nor

F_2 are very soluble in aHF. This proved to be fruitful in the production of highly crystalline AgF^+ salts.

To check on the chemical purity of the preparations, it was routine to fingerprint the material by its X-ray powder diffraction pattern, and these patterns were indexed by single crystal data wherever possible. In addition, the preparations were characterized by their magnetic properties, which, as revealed in the Experimental section above and discussed in Chapter 6, were highly characteristic for all AgF^+ salts. In all cases, the magnetic susceptibility of the cation exhibited temperature-independent paramagnetism at least above 50 K. When field-dependent paramagnetism was observed, this was invariably associated with AgF_2 impurity (ferromagnetic[9] T_c = 163 K). Except in the case of $AgFRuF_6$, whose anion is a simple paramagnetic, simple paramagnetism would have indicated $Ag(MF_6)_2$ salts (see Chapter 6), but such impurities were not present in the preparations involving the fluorination of $Ag^+A_LF^-$ salts.

The experimental findings indicate that there are two important limitations to the existence of $Ag^+A_LF^-$ salts. One is due to the high fluoro-acidity of the cation, which can abstract F^- from less strong acids, A_L. And the other (which is observed particularly with certain transition-element A_L) arises from the high electron affinity of AgF^+, which can bring about electron oxidation of the anion.

The weak fluoro-acidity of PF_5 is responsible for the failure to prepare $AgFPF_6$ by fluorination of $AgPF_6$, this reaction proceeding[17] as follows:

$$AgPF_6 + \tfrac{1}{2} F_2 \xrightarrow{aHF} AgF_2 + PF_5 \quad (3)$$

Here, PF_6^- is seen to be an effective F^- donor even to AgF^+. Although the F^- affinity of $BF_{3\,(g)}$ is approximately 10 kcal·mol^{-1} less than that of $PF_{5\,(g)}$, the greater lattice energy of small-cation BF_4^- salts more than compensates for that deficiency. This probably accounts for the existence of $AgFBF_4$ and the failure to prepare $AgFPF_6$.

Some of the acids (*e.g.* AsF_5) whose conjugate bases make up the anions (*e.g.* AsF_6^-) of the AgF^+ salts have a considerable HF-affinity, as gauged by their solubility in it. The affinity of A_L for aHF, working in concert with the high F^- affinity of the AgF^+ cation, probably explains the solvolysis of certain $AgF^+A_LF^-$ salts when they are immersed in a large quantity of aHF. Then the reaction is essentially as expressed in Equation (4):

$$AgF^+A_LF^- \overset{aHF}{\rightleftharpoons} AgF_2 + A_L(HF)_n \quad (4)$$

This solvolysis is not observed when A_L has only a weak HF-affinity, as in the case of $AgFIrF_6$, for which A_L (*i.e.* IrF_5) is insoluble in aHF. Because Equation (4) represents an equilibrium, additional acid may be introduced to avoid AgF_2 formation and ensure pure $AgFA_LF$ product. However, in such preparations, Ag(II) is always sacrificed to $Ag(A_LF)_2$ formation (at least in solution) by the following equilibrium:

$$AgF^+A_LF^- + A_L \overset{aHF}{\rightleftharpoons} Ag^{II}_{solv} + 2\,A_LF^-_{solv} \quad (5)$$

Attempts to synthesize $AgFOsF_6$ from the Ag(I) salt and molecular fluorine all met with failure, generating OsF_6 instead. Treatment of $KOsF_6$ or $LiOsF_6$ in aHF with

fluorine gas does not liberate OsF_6. Consequently, it may be surmised that the mechanism which leads to the release of OsF_6 from its anion involves the initial generation of a Ag(II) species, perhaps proceeding as follows:

$$Ag^+ + F\text{–}F \xrightarrow{aHF} AgF^+ + F^\bullet \quad (6)$$

$$AgF^+ + OsF_6^- \xrightarrow{aHF} AgF + OsF_6 \quad (7)$$

The AgF generated in this scenario is subsequently oxidized to AgF_2 by the fluorine gas present, and the fluorine radical may oxidize yet another Ag(I). There is, however, another possible mechanism in which the silver only indirectly assists in the oxidation of the osmium(V):

$$Ag^+ + F\text{–}F \xrightarrow{aHF} AgF^+ + F^\bullet \quad (8)$$

$$F^\bullet + OsF_6^- \xrightarrow{aHF} (HF)_nF^- + OsF_6 \quad (9)$$

In this scenario, the solvated AgF^+ and F^- quickly combine to form AgF_2. Reaction via this pathway does not suggest that polymeric $(AgF)_n^{n+}$ has sufficient electron affinity to affect the oxidation of OsF_6^-. Indeed, the only way to truly test such a hypothesis is to avoid the use of molecular fluorine altogether. For this reason, the metathetical synthetic approach was attempted, and produced essentially the same results:

$$KOsF_6 + AgFBF_4 \rightarrow KBF_4 + AgF + OsF_6 \quad (10)$$

thus confirming that the $(AgF)_n^{n+}$ cation does indeed have the electron-withdrawing potential required to generate OsF_6 from its monoanion.

In contrast to the osmium reaction, $AgFIrF_6$ was readily prepared by the oxidation of $AgIrF_6$ with molecular F_2 in aHF.

$$AgIrF_6 + \tfrac{1}{2} F_2 \xrightarrow{aHF} AgFIrF_6 \qquad (11)$$

This synthesis is particularly interesting because although the $(AgF)_n^{n+}$ cation forms a stable complex with the hexafluoroiridate(V) anion, evidence is provided in Chapter 7 for the oxidation of this anion by solvated Ag(II). Indeed, it is interesting to note that $AgFIrF_6$ can exist only in a narrow pH range in the aHF. Acidification of the solution with an appropriately strong Lewis acid (A_L) removes the fluoride from the AgF^+ unit, freeing the Ag(II) into solution and permitting oxidation of IrF_6^- to IrF_6.

$$AgFIrF_6 + A_L \xrightarrow{aHF} Ag^{II}_{(solv)} + IrF_6^- + A_LF^- \xrightarrow{aHF} AgA_LF_{(s)} + IrF_{6\,(g)} \qquad (12)$$

Furthermore, addition of a fluoro-base to the aHF results in the formation of AgF_2 and the dissolution of the IrF_6^- counterion.

$$AgFIrF_6 + F^- \xrightarrow{aHF} AgF_{2\,(s)} + IrF_{6(solv)}^- \qquad (13)$$

While any concentration of base in the aHF is sufficient to cause the decomposition of $AgFIrF_6$, it was observed that a weak fluoro-acid such as BF_3 does not have the fluoride ion affinity required to abstract the fluoride from AgF^+ to a significant extent. Consequently, it was possible to obtain $AgFIrF_6$ essentially free of AgF_2 by "washing" it in a solution of aHF/BF_3. This washing procedure first converts any AgF_2 to $AgFBF_4$ and then dissolves it, generating a slightly blue-tinted solution, probably $Ag^{2+}(BF_4^-)_2$ as

fully solvated ions. Since the BF_3 does not promote significant dissolution of $AgFIrF_6$, the absence of AgF_2 was manifest in a colorless solution above the black product.

5.4. Conclusions

Fluorination of Ag(I) salts in aHF has been found to be an appropriate method for the preparation of AgF^+ salts, in some cases yielding single crystals of sufficient quality for X-ray diffraction studies. Two considerations have been found to be important for the stability of a given $AgFA_LF$ salt: the fluoride affinity of A_L and, for transition-element acids, the electron affinity of neutral A_LF. $AgFPF_6$ is not preparable because of the weak F^- affinity of PF_5. And yet, this compound must be very close to thermodynamic stability because $AgFBF_4$ is preparable.

Oxidation of OsF_6^- is easily achieved at room temperature by $(AgF)_n^{n+}$ because the electron affinity of A_LF in this case (*i.e.* OsF_6) is not high enough to take the electron from Ag(I). This has been demonstrated by oxidative fluorination reactions of $AgOsF_6$, as well as by metathetical combination of an alkali OsF_6^- salt with another AgF^+ salt in aHF solution. $AgFIrF_6$, however, is readily prepared in high purity in aHF solution. Therefore, on the graded scale provided by the electron affinities of the third transition series metal hexafluorides, $(AgF)_n^{n+}$ lies somewhere between OsF_6 and IrF_6 in oxidizing potential.

5.5. References

[1] B. Frlec, D. Gantar, and J. H. Holloway, *J. Fluorine Chem.*, **20** (1982), pp 385-396.

[2] B. Žemva, K. Lutar, A. Jesih, W. J. Casteel, Jr., A. P. Wilkinson, D. E. Cox, R. B. Von Dreele, H. Borrmann, and N. Bartlett, *J. Am. Chem. Soc.*, **113** (1991), pp 4192-4198.

[3] B. Žemva, R. Hagiwara, W. J. Casteel, Jr., K. Lutar, A. Jesih, and N. Bartlett, *J. Am. Chem. Soc.*, **112** (1990), pp 4846-4849.

[4] W. J. Casteel, Jr., G. Lucier, R. Hagiwara, H. Borrmann, and N. Bartlett, *J. Solid State Chem.*, **96** (1992), pp 84-96.

[5] W. J. Casteel, Jr., Ph. D. Thesis, (1992) Chapter 7, U.C. Berkeley.

[6] G. Lucier, C. Shen, W. J. Casteel, Jr., L. Chacón, and N. Bartlett, *J. Fluorine Chem.*, (1995) in press.

[7] B. G. Müller, *Angew. Chem.*, **99** (1987), p 685.

[8] A. Jesih, K. Lutar, B. Žemva, *Z. Anorg. Allg. Chem.*, **588** (1990), pp 77-83.

[9] E. Gruner and W. Klemm, *Naturwissenschaften,* **25** (1937), p 59; and P. Charpin, A. J. Dianoux, H. Marquet-Ellis, and Nguyen-Nghi, *C. R. Acad. Sci. Paris,* **264** (1967), p 1108.

[10] B. N. Figgis, Introduction to Ligand Fields, (1966) New York: Interscience.

[11] J. Clark, Z. Pistorius, *Phys. Chem. Neue Folge. (Weisbaden),* **88** (1974), p 242.

[12] D. E. Cox, *J. Chem. Soc.*, (1956), p 876.

---

[13] D. Gantar, B. Frlec, D. R. Russell, and J. H. Holloway, *Acta Cryst.*, **C43** (1987), pp 618-620.

[14] R. D. W. Kemmitt, D. R. Russell, and D. W. A. Sharp, *J. Chem. Soc.*, **844** (1963), pp 4408-4413.

[15] W. J. Casteel, Jr., Ph. D. Thesis, (1992) Chapter 6, U.C. Berkeley.

[16] N. K. Jha, Ph.D. Thesis, (1965) Chapter 2, U. British Columbia.

[17] G. Lucier, J. Munzenberg, W. J. Casteel, Jr., and N. Bartlett, *Inorg. Chem.*, (1995) in press.

Chapter 6

Structure and Physical Properties of AgF^+ Salts

6.1. Introduction

In 1987, Gantar *et al.*[1] published the structure of $AgFAsF_6$. Their single-crystal X-ray study revealed that this AgF^+ salt contains a one-dimensional chain cation of formula $(AgF)_n^{n+}$ which is surrounded by nearly-octahedral AsF_6^- species. Although this chain is kinked at the fluorine bridges, it is straight at the silver links, and the two Ag-F bond lengths are not significantly different. The tetrafluoroborate, which was first made in these laboratories[2], was the next AgF^+ salt to be prepared. Its synthesis and X-ray powder diffraction data were reported[2] in 1990. Analysis of the unit cell data suggested that, again, the $(AgF)_n^{n+}$ chain cation was present, this time constrained by the symmetry of the structure to be perfectly linear. A technique for the growth of single crystals of the AgF^+ salts was soon developed as part of the work described in this chapter. Single crystal X-ray data for $AgFBF_4$ were collected, the resulting structure solution confirming[3] the suspected structure. In this same publication, X-ray powder diffraction data for the

tetrafluoroaurate(III) and hexafluoroaurate(V) salts were reported. $AgFAuF_4$ was found to be isomorphous[4] with $CuFAuF_4$, and $AgFAuF_6$ was seen to be isomorphous with $AgFAsF_6$, both structures containing $(AgF)_n^{n+}$ chains kinked at the F bridge of the cation. With the size of the class of AgF^+ salts having increased to include four compounds of three distinct structures, it was interesting to note that all of these materials contained the chain cation with intrachain Ag-F bond lengths always very nearly 2.0 Å. This work has since expanded the AgF^+ class of compounds to include the hexafluoroiridate(V) and hexafluororuthenate(V), whose structures have been solved and are discussed below, and the hexafluoroantimonate(V) and hexafluorobismuthate(V), single crystals of which have proven to be difficult to preserve.

It was recognized from the start of our investigations into the AgF^+ salts that the magnetic susceptibility data (provided in Chapter 5) are consistent with that to be expected of a metallic system. In fact, every known AgF^+ salt has exhibited the same temperature-independent, weak paramagnetism. Furthermore, polarized light transmission experiments performed on $AgFBF_4$ are indicative of a one-dimensional electronic conductor. So it is reasonable to postulate that a partially-filled conduction band arises for the $(AgF)_n^{n+}$ chain cation, for which one-dimensional electronic conductivity is anticipated. Unfortunately, no electrical conductivity has been directly measured, perhaps owing to the extreme reactivity of the materials under investigation.

6.2. Structure of $AgFBF_4$

The preparation of bronze $AgFBF_4$ almost unavoidably produced macroscopic crystals (see Experimental section of Chapter 5), one of which was selected for single crystal X-ray structure determination. Crystals of violet $AgFBF_4$ were obtained by first placing a small amount (~30-40 mg) of $AgBF_4$ in a passivated FEP T-reactor constructed with 3/8" tubing. About 1 mL aHF was condensed onto the powder and then warmed to room temperature. The reactor was pressurized to ~1000 torr with F_2 gas and left to sit undisturbed. After 20 h, there was no evidence of remaining $AgBF_4$, and violet-blue crystals, mostly needles, were seen to exist in contact with a light blue solution. The aHF solution was decanted off and the aHF removed under dynamic vacuum prior to vacuum-drying the crystals for 3 h.

Single crystal structure determinations of bronze and violet $AgFBF_4$ showed no significant differences[3], other than that the violet crystal provided a slightly higher precision. Details of the structure solution for the violet material are provided in Table 6.1. The structure was successfully refined in space group P 4/n. The earlier supposition[2] of a linear $(AgF)_n^{n+}$ chain, based on the tetragonal unit cell and tentative space group assignment, was confirmed.

Table 6.1. Crystal Data and Details of the Structure Refinement of $AgFBF_4$

Formula, mol wt	$AgBF_5$, 213.67 amu
Temperature	293 K
a_o	6.7000(3) Å
c_o	4.0113(2) Å
V	180.07(1) $Å^3$
Z	2
Space group	P 4/n (No. 85)
d_{calc}	3.940 $g \cdot cm^{-3}$
Crystal size	0.08 x 0.13 x 0.35 mm
Wavelength (Mo Kα)	0.71073 Å
μ	55.33 cm^{-1}
Diffractometer	Enraf-Nonius CAD4, graphite monochromator
Scan range	$3 < 2\Theta < 76°$; $\pm h, \pm k, l$
Scan angle	$1.1° + 0.35 \tan \Theta$; ω/Θ-scan
Scan speed	variable, t_{max} = 80 sec
Data collected	2166
Independent	494; $R_{int} = 0.026$
Absorption correction	Empirical Ψ-scans, $\Delta\Psi = 10°$, 8 *hkl*
Structure solution	Based on packing considerations from powder data
Refinement	Full matrix least squares, 17 parameters
Weighting scheme	$1/\sigma^2$
Extinction correction	$F_{corr} = F_{obs} \cdot (1 + g \cdot I)$, $g = 1.60 \times 10^{-5}$
R	0.0193
wR	0.0250
Goodness-of-fit	1.104

The extended structure of $AgFBF_4$ is illustrated in Figure 6.1. Four columns of linearly close-packed BF_4^- are seen to surround each linear $(AgF)_n^{n+}$ chain, and *vice versa*. Each Ag(II) atom is square-coordinated by four ligands of the anions, each from one of the four surrounding BF_4^-, and is almost in the same plane as these four F ligands. Interaction of the almost-ideally tetrahedral BF_4^- with four nearest-neighbor Ag(II)

species, via the F ligands, results in an alternation of the Ag(II) *z* parameters in the four surrounding $(AgF)_n^{n+}$ columns, these *z* parameters being in step with those of the F ligands of an anion. As illustrated in Table 6.4, the Ag--F interatomic distance between cation and each of the four nearest anion ligands is 2.330(2) Å. These are consistent with interionic contacts. The Ag--F distances within the chain, on the other hand, are short and must represent appreciable overlap of the valence-shell orbitals of the Ag(II) (*e.g.* $4d_{z^2}$) and the F (*e.g.* $2p_z$). Evidently the antibonding influence of the Ag(II) d^9 configuration is minimal in the cationic chain; therefore, the unique, half-filled *d* orbital is designated d_{z^2}. The crystal orbitals for the cationic chain must be dominated by the contributions from $4d_{z^2}$ of Ag(II) and $2p_z$ of F. Since this signifies a half-filled conduction band, a Peierls distortion is anticipated. In this room-temperature structure, however, no such distortion is manifest. Indeed, each Ag(II) is in a highly polar electric field, since all four nearest boron atoms of each Ag(II) are either above or below it with respect to the chain direction. Nevertheless, the two intrachain Ag--F distances are remarkably close at 2.002(3) and 2.009(3) Å. (The difference can be readily reconciled by the way in which the anion packing dictates that the four additional anion F ligands directed toward each Ag(II) are not in exactly the same plane as it.)

The Peierls distortion to be expected for the $(AgF)_n^{n+}$ chain is an alternation of linear, symmetrical $(F—Ag^{III}—F)^+$ species and Ag^+, interatomic distances in the chain becoming short about the Ag(III) and long about the Ag(I). But the polar field about each Ag(II) in the chain (see Figure 6.2) works against a centrosymmetric F ligand

arrangement at each Ag atom. The F ligands of the cation do not experience such a polar field. It is perhaps for these reasons that the magnetic susceptibility data show no evidence of a Peierls transition between 6 and 280 K.

Table 6.2. Positional Parameters for $AgFBF_4$ at 293 K

	x	*y*	*z*
Ag	0.25	0.25	0.19212(7)
B	0.25	0.75	0
F1	0.25	0.25	0.6930(7)
F2	0.3136(3)	0.5919(2)	0.1988(5)

Table 6.3. Thermal Parameters for $AgFBF_4$ at 293 K

	U(1,1)	*U*(2,2)	*U*(3,3)	*U*(1,2)	*U*(1,3)	*U*(2,3)
Ag	0.01496(6)	U(1,1)	0.00654(9)	0	0	0
B	0.021(1)	U(1,1)	0.017(2)	0	0	0
F1	0.0341(9)	U(1,1)	0.009(1)	0	0	0
F2	0.047(1)	0.0206(6)	0.0315(8)	0.0031(7)	-0.0065(8)	0.0013(7)

Table 6.4. Interatomic Distances (Å) and Angles (°) for $AgFBF_4$

Distances		Angles			
Ag-F1	2.002(3)	F1-Ag-F1'	180	2x F2-Ag-F2	178.68(9)
Ag-F1'	2.009(3)	4x F1-Ag-F2	90.66(5)	4x F2-B-F2	109.14(8)
Ag-F2	2.330(2)	4x F1'-Ag-F2	89.34(5)	2x F2-B-F2	110.1(2)
B-F2	1.393(2)	4x F2-Ag-F2	89.992(1)		

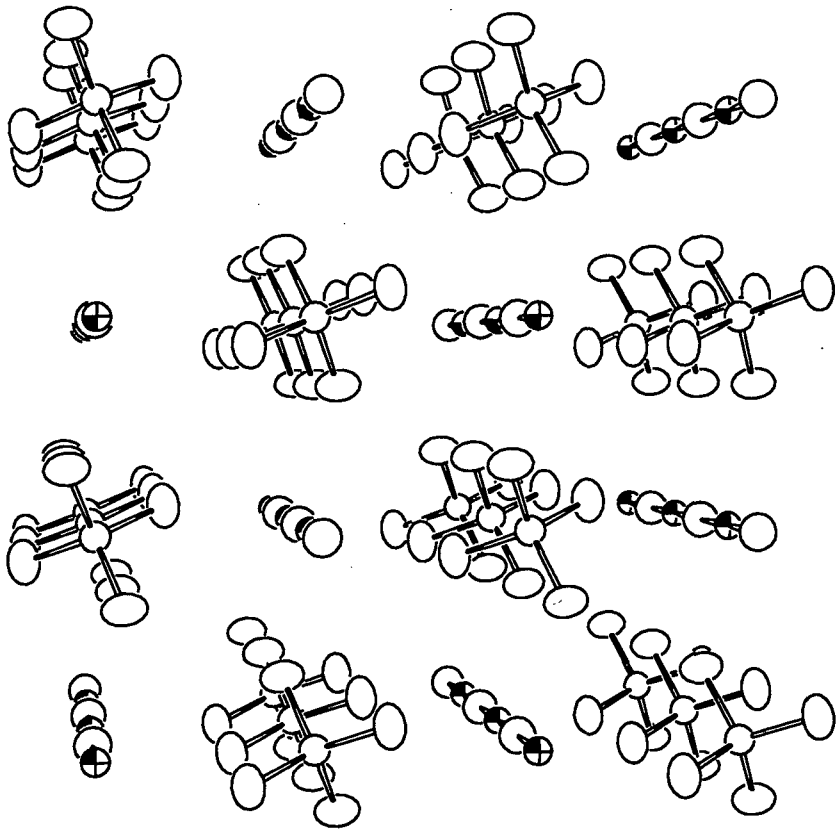

Figure 6.1. The extended structure of $AgFBF_4$.
Chains of Ag-F-Ag-F are surrounded by columns of BF_4^-.

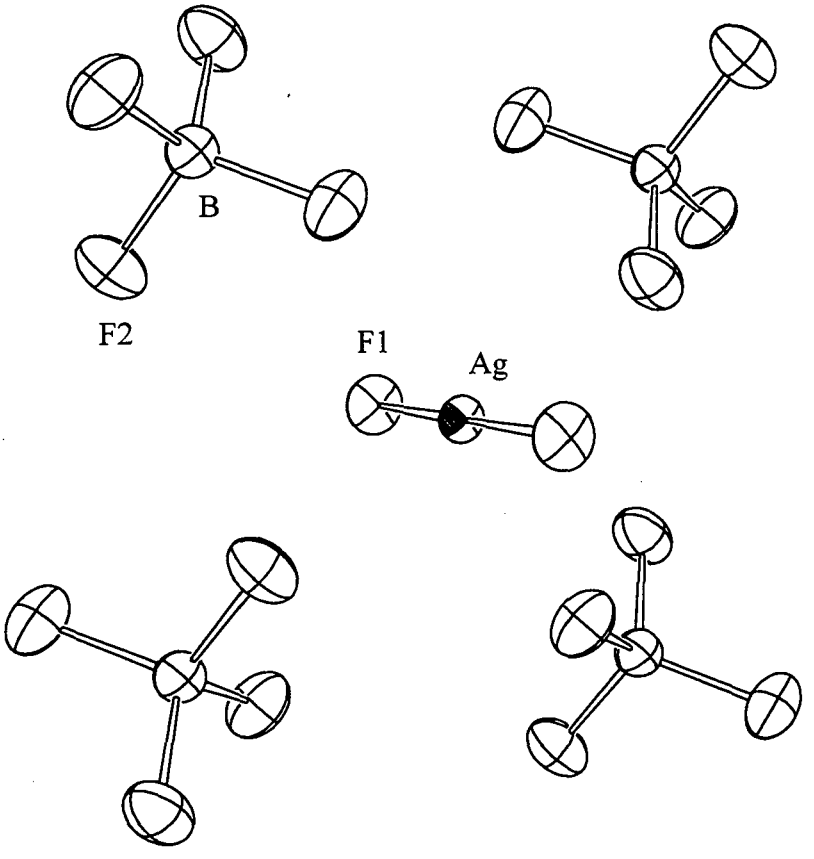

Figure 6.2. The tetragonally-distorted octahedral environment about the Ag(II) in $AgFBF_4$.

6.3. Structure of $AgFMF_6$

6.3.1. M = As, Ir, Au

X-ray powder diffraction data indicated that $AgFAuF_6$ and $AgFIrF_6$ would be isostructural with the previously determined[1] $AgFAsF_6$. Although no attempt was made to grow crystals of the gold material, crystals of $AgFIrF_6$ were grown from aHF solution in the same manner as that described for $AgFBF_4$, the black material exhibiting a needle

crystal habit. Details of the single crystal X-ray structure determination are given in Table 6.5.

Table 6.5. Crystal Data and Details of the Structure Refinement of $AgFIrF_6$

Formula, mol wt	$AgIrF_7$, 433.08 a.u.
Temperature	298 K
a_o	7.627(2) Å
b_o	7.068(2) Å
c_o	10.253(4) Å
V	552.7(3) $Å^3$
Z	4
Space group	P nma (No. 62)
d_{calc}	5.23 $g \cdot cm^{-3}$
Crystal size	0.16 x 0.26 x 0.23 mm
Wavelength (Mo Kα)	0.71073 Å
μ	275.5 cm^{-1}
Diffractometer	Enraf-Nonius CAD4, graphite monochromator
Scan range	$3 < 2\Theta < 50°$; -h, +k, -l
Scan angle	$0.65° + 0.35 \tan \Theta$
Scan speed	5.49 °/min
Data collected	608
Independent	531; 451 with $I > 3 \cdot \sigma(I)$
Absorption correction	Analytical, 10x16x14Gaussian Grid, $T_{max} = 0.079$, $T_{min} = 0.027$
Structure solution	Based on known $AgFAsF_6$ structure
Refinement	Full matrix least squares, 50 parameters
Weighting scheme	$1/\sigma^2$
Extinction correction	$F_{corr} = F_{obs} \cdot (1 + g \cdot I)$, $g = 2.2 \times 10^{-7}$
R, R'	0.026, 0.033
wR	0.030
Goodness-of-fit	1.235

Table 6.6. Positional Parameters for $AgFIrF_6$ at 298 K

	x	*y*	*z*
Ag	0.1368(1)	0.25	0.2431(1)
Ir	0.29858(8)	0.25	0.55958(1)
F1	0.387(1)	0.25	0.1931(9)
F2	0.523(1)	0.25	0.4821(9)
F3	0.082(1)	0.25	0.632(1)
F4	0.2256(9)	0.433(1)	0.4364(6)
F5	0.3766(9)	0.063(1)	0.6776(6)

Table 6.7. Thermal Parameters for $AgFIrF_6$ at 298 K

	U(1,1)	*U*(2,2)	*U*(3,3)	*U*(1,2)	*U*(1,3)	*U*(2,3)
Ag	0.0103(4)	0.0213(5)	0.0164(5)	0	-0.0026(4)	0
Ir	0.0207(3)	0.0225(3)	0.0135(2)	0	0.0004(3)	0
F1	0.019(4)	0.048(6)	0.028(5)	0	-0.003(4)	0
F2	0.027(5)	0.060(6)	0.028(5)	0	0.010(4)	0
F3	0.031(5)	0.082(8)	0.047(6)	0	0.023(5)	0
F4	0.048(3)	0.035(4)	0.027(3)	0.009(3)	-0.015(3)	0.003(3)
F5	0.057(4)	0.029(3)	0.028(3)	-0.001(3)	-0.007(3)	0.006(3)

Table 6.8. Interatomic Distances (Å) and Angles (°) for $AgFIrF_6$ at 298 K.
Roman numeral designations refer to those provided[1] for $AgFAsF_6$.

Distances		Angles			
Ag-F1	1.977(9)	F1-Ag-F1^{i}	176.1(4)	Ag-F1-Ag^{v}	146.0(5)
Ag-F1^{i}	2.014(9)	F1-Ag-F2^{i}	95.6(4)	F1^{i}-Ag-F2^{i}	88.4(4)
Ag-F2^{i}	2.467(10)	F1-Ag-F4	86.7(3)	F1^{i}-Ag-F4^{iv}	89.9(3)
Ag-F4	2.461(7)	F1-Ag-F5^{ii}	88.1(2)	F1^{i}-Ag-F5^{ii}	93.0(2)
Ag-F5^{ii}	2.311(7)	F2-Ag-F4^{iv}	148.3(2)	F2^{i}-Ag-F5^{ii}	73.3(2)
Ir-F2	1.886(9)	F4-Ag-F5^{iv}	138.4(2)	F4^{iv}-Ag-F5^{ii}	75.2(2)
Ir-F3	1.812(10)	F4-Ag-F4	63.3(2)	F5^{iii}-Ag-F5^{ii}	145.8(2)
Ir-F4	1.890(7)	F4-Ir-F5	92.4(3)	F4^{iv}-Ir-F5	177.8(3)
Ir-F5	1.891(7)	F4-Ir-F4	86.2(3)	F5-Ir-F5^{iv}	89.0(3)
		F2-Ir-F3	179.3(5)	F3-Ir-F4	90.3(3)
		F2-Ir-F4	89.2(3)	F3-Ir-F5	91.4(3)
		F2-Ir-F5	89.1(3)	Ag^{v}-F2-Ir	135.5(5)
		Ag-F4-Ir	105.1(3)	Ag^{ii}-F5-Ir	147.4(4)

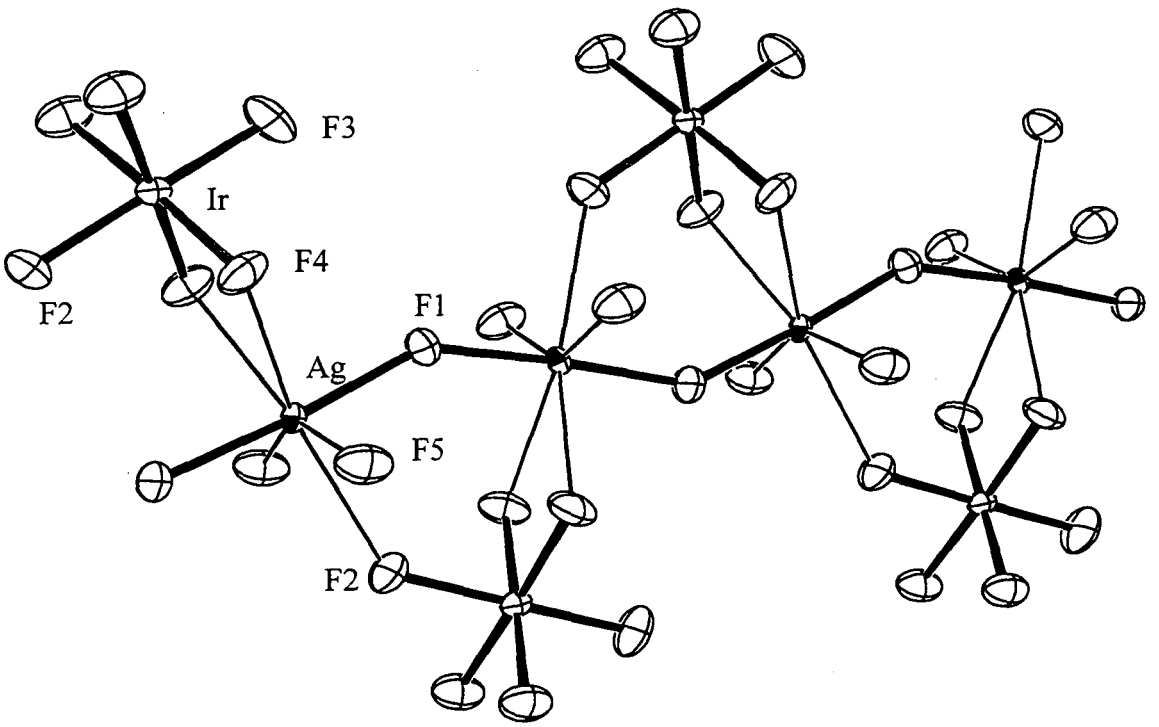

Figure 6.3. The Ag-F-Ag-F chain and its environment in $AgFIrF_6$.

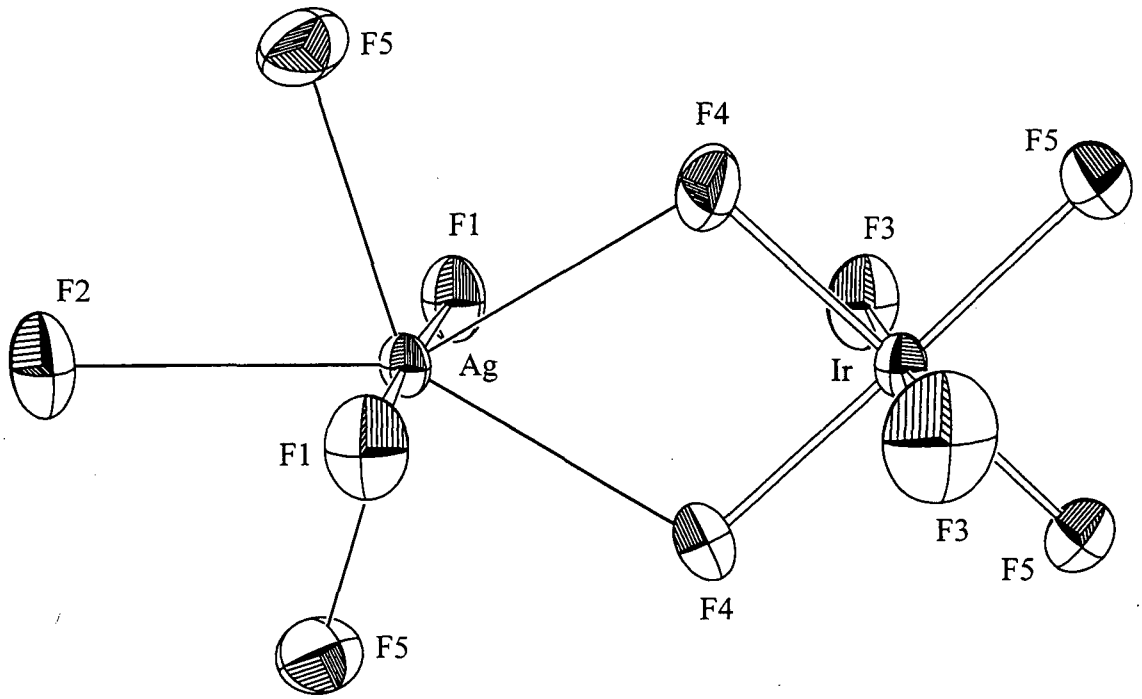

Figure 6.4. The Ag(II) and Ir(V) structural environments in $AgFIrF_6$.

6.3.2. M = Sb, Bi

Several synthetic routes to $AgFBiF_6$ have been investigated. The X-ray powder photographs of these products show an XRPP very similar to that obtained by Casteel[5] upon fluorination of $AgSbF_6$ in an attempt to generate $AgFSbF_6$. In the aHF, these solids appear blue and highly crystalline. However, all attempts to remove the solvent led to the crumbling of macroscopic crystals into a gray-blue powder. The XRPP of the gray-blue powder is highly complex, indicative of material whose symmetry is at least as low as

monoclinic and possibly triclinic. No attempt to assign Miller indices to the lines of the patterns has been attempted due to their poor quality (presumably resulting from poorly crystalline material due to rapid removal of HF from the solvated crystals). Consequently, very little is known of the structures of $AgFSbF_6$ and $AgFBiF_6$, although the magnetic data (provided in Chapter 5) indicate that polymeric $(AgF)_n^{n+}$ cations are present in these salts also.

6.3.3. M = Ru

The X-ray powder diffraction data of $AgFRuF_6$ exhibits a much more complicated pattern than that for the other known structures of AgF^+ salts. For this reason, there was great interest in obtaining a single crystal structure solution. Starting with $AgRuF_6$ powder, crystals of $AgFRuF_6$ were grown from aHF solution using the same technique as that used for $AgFBF_4$. This black material exhibited a very thin rectangular plate crystal habit. Details of the structure solution are provided in Table 6.9.

Table 6.9. Crystal Data and Details of the Structure Refinement of $AgFRuF_6$

Formula, mol wt	$AgRuF_7$, 341.93 amu
Temperature	293 K
a_o	8.3432(13) Å
b_o	5.4933(8) Å
c_o	11.9286(22) Å
β	108.36(1) °
V	518.9(3) $Å^3$
Z	4
Space group	P 2_1/n (No. 14)
d_{calc}	4.38 $g \cdot cm^{-3}$
Crystal size	0.05 x 0.13 x 0.18 mm
Wavelength (Mo Kα)	0.71073 Å
μ	66.7 cm^{-1}
Diffractometer	Enraf-Nonius CAD4, graphite monochromator
Scan range	$3 < 2\Theta < 60°$; $h, \pm k, \pm l$
Scan angle	0.70° + 0.35 tan Θ
Scan speed	5.49 °/min
Data collected	3216
Independent	1511, 1112 with $I > 3 \cdot \sigma(I)$
Absorption correction	Empirical Ψ-scans, $T_{max} = 1.21$, $T_{min} = 0.85$
Structure solution	Ag and Ru atoms with Patterson map
Refinement	Full matrix least squares, 83 parameters
Weighting scheme	$1/\sigma^2$
Extinction correction	$F_{corr} = F_{obs} \cdot (1 + g \cdot I)$, $g = 9.737 \times 10^{-7}$
R, R'	0.027, 0.039
wR	0.028
Goodness-of-fit	0.972

Despite the fact that RuF_6^- is only ~0.3$Å^3$ smaller[6] that IrF_6^-, the indication of the XRPP that $AgFRuF_6$ was of a different symmetry class was confirmed by the single crystal data. As may be seen in Figure 6.6 and Table 6.12, the Ag(II) species in this salt is approximately square-coordinated by 4 F ligands. Neighboring Ag(II) are brought into

close proximity with one another by two *cis*-related bridging F ligands, each nearly equidistant from two Ag(II). The nearly square F ligand array involves another two ligands, one from each of two RuF_6^-. Each RuF_6^- bridges two Ag(II), and as can be seen from Figure 6.5, all connected Ag(II) with their four near-neighbor F ligands lie in a common plane. The $(AgF)_n^{n+}$ cation is, therefore, in this case a one-dimensional ribbon.

Table 6.10. Positional Parameters for $AgFRuF_6$ at 298 K

	x	*y*	*z*
Ag	0.07248(1)	0.21192(7)	0.22002(1)
Ru	0.22722(1)	0.28784(7)	-0.06154(1)
F1	0.0755(3)	0.4622(5)	-0.1900(2)
F2	0.1559(3)	-0.0026(5)	-0.1487(2)
F3	0.0544(3)	0.2482(6)	0.0034(2)
F4	0.3904(3)	0.3208(6)	-0.1335(2)
F5	0.2867(3)	0.5730(6)	0.0181(2)
F6	0.3696(3)	0.1148(7)	0.0581(2)
F7	0.2124(3)	-0.0913(5)	0.2374(2)

Table 6.11. Thermal Parameters for $AgFRuF_6$ at 298 K

	U(1,1)	*U*(2,2)	*U*(3,3)	*U*(1,2)	*U*(1,3)	*U*(2,3)
Ag	0.0175(1)	0.0167(1)	0.0210(1)	0.0004(1)	0.00669(9)	0.0009(1)
Ru	0.0171(1)	0.0174(1)	0.0151(1)	-0.0002(1)	0.00541(9)	-0.0004(1)
F1	0.028(1)	0.025(1)	0.021(1)	0.006(1)	0.0067(9)	0.004(1)
F2	0.025(1)	0.020(1)	0.034(1)	-0.003(1)	0.0103(9)	-0.009(1)
F3	0.030(1)	0.036(1)	0.028(1)	-0.001(1)	0.0171(8)	0.000(1)
F4	0.0224(9)	0.047(1)	0.031(1)	-0.002(1)	0.0153(8)	0.003(1)
F5	0.036(1)	0.028(1)	0.036(1)	-0.008(1)	0.006(1)	-0.014(1)
F6	0.037(1)	0.042(1)	0.024(1)	0.013(1)	0.003(1)	0.011(1)
F7	0.024(1)	0.022(1)	0.041(1)	0.006(1)	0.0085(9)	0.004(1)

Table 6.12. Interatomic Distances (Å) and Angles (°) for $AgFRuF_6$ at 298 K

Distances		Angles			
Ag-F7	2.007(3)	F7-Ag-F7	88.64(3)	F1-Ru-F3	89.31(12)
Ag-F7	2.018(2)	F7-Ag-F1	176.21(11)	F1-Ru-F4	88.71(12)
Ag-F1	2.140(3)	F7-Ag-F1	90.82(11)	F1-Ru-F5	89.41(13)
Ag-F2	2.158(3)	F7-Ag-F2	90.65(11)	F1-Ru-F6	178.45(15)
Ag-F3	2.548(3)	F7-Ag-F2	171.68(12)	F2-Ru-F3	88.81(12)
Ag-F4	2.659(3)	F1-Ag-F2	89.34(11)	F2-Ru-F4	88.71(13)
Ag-F5	3.068(3)	F3-Ag-F1	85.29(10)	F2-Ru-F5	177.39(13)
Ru-F1	1.909(3)	F3-Ag-F2	83.04(10)	F2-Ru-F6	90.28(14)
Ru-F2	1.895(3)	F3-Ag-F7	90.95(11)	F3-Ru-F4	176.87(13)
Ru-F3	1.853(3)	F3-Ag-F7	88.68(11)	F3-Ru-F5	90.18(13)
Ru-F4	1.832(3)	F3-Ag-F4	143.93(9)	F3-Ru-F6	90.71(13)
Ru-F5	1.818(3)	F3-Ag-F5	158.98(8)	F4-Ru-F5	92.22(14)
Ru-F6	1.812(3)	F5-Ag-F7	70.39(10)	F4-Ru-F6	91.21(13)
		F5-Ag-F7	81.50(10)	F5-Ru-F6	92.14(15)
		F4-Ag-F1	75.39(10)	Ru-F1-Ag	139.11(14)
		F4-Ag-F2	66.84(10)	Ru-F2-Ag	138.65(14)
		F4-Ag-F5	55.15(8)	Ru-F3-Ag	128.92(13)
		Ag-F7-Ag	155.90(16)	Ru-F4-Ag	164.54(16)
		F1-Ru-F2	88.17(13)	Ru-F5-Ag	134.45(15)

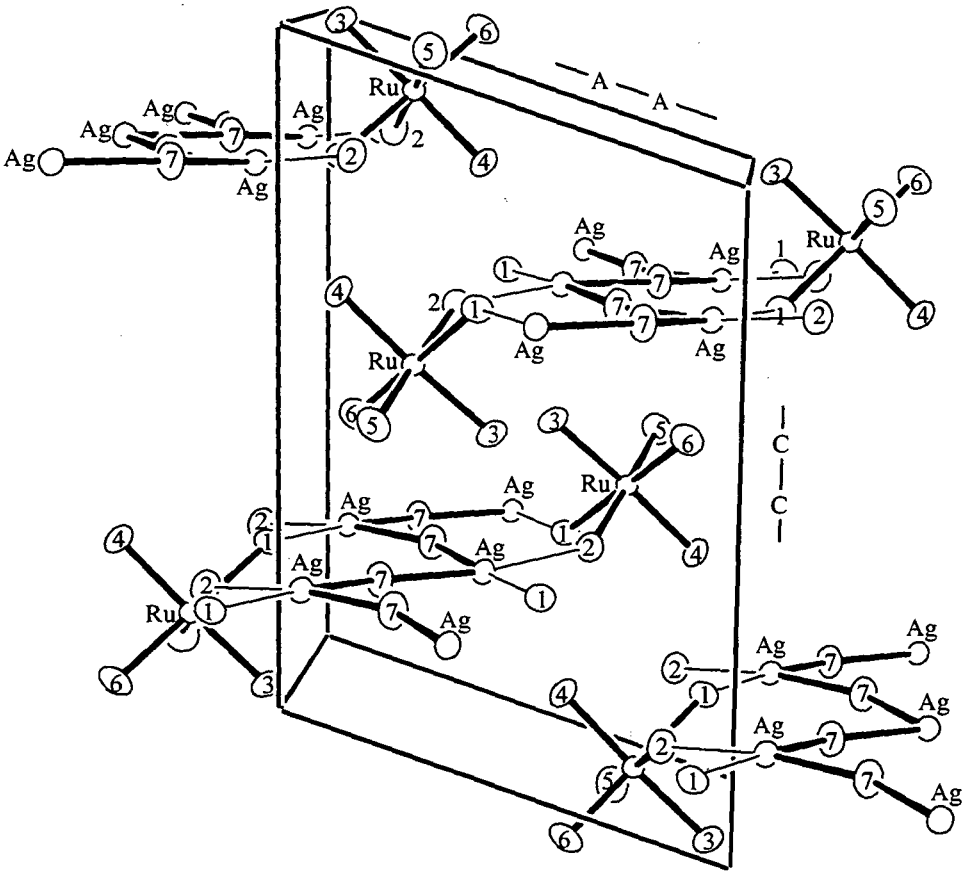

Figure 6.5. The structure of $AgFRuF_6$, showing the one-dimensional ribbon cationic chains.

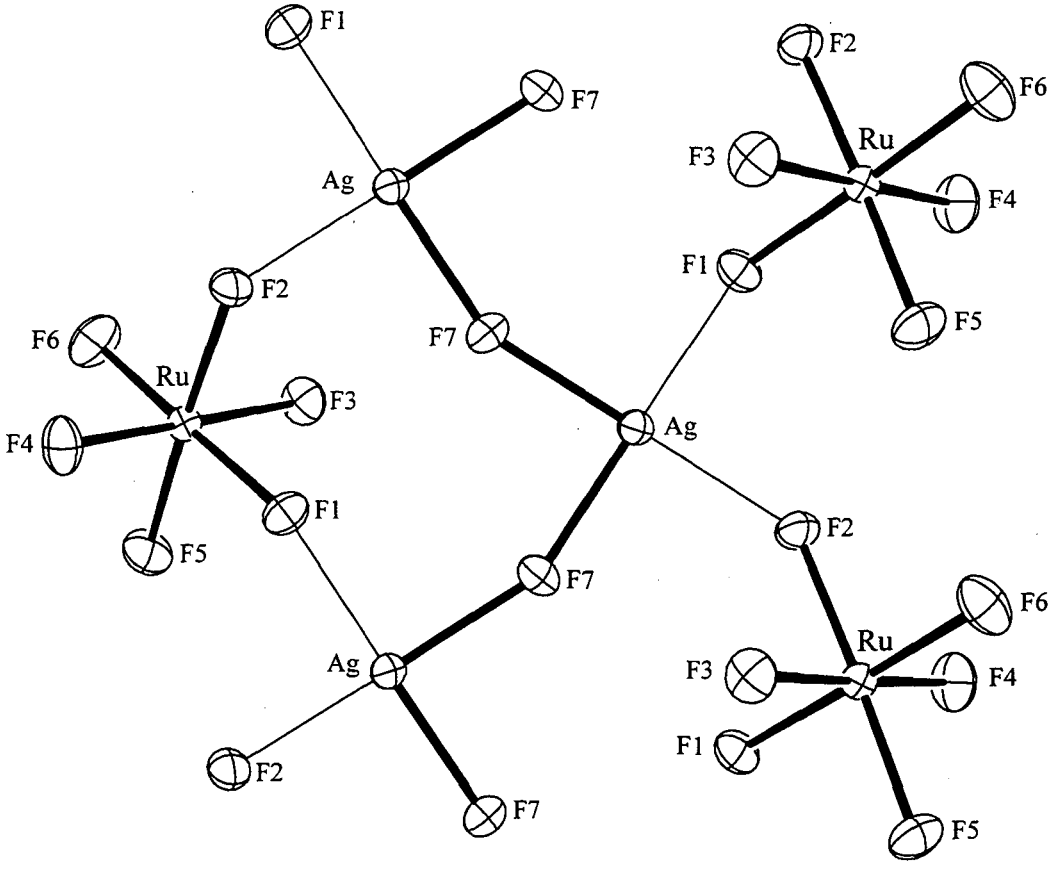

Figure 6.6. An ORTEP displaying the square-planar bonding to silver in $AgFRuF_6$.

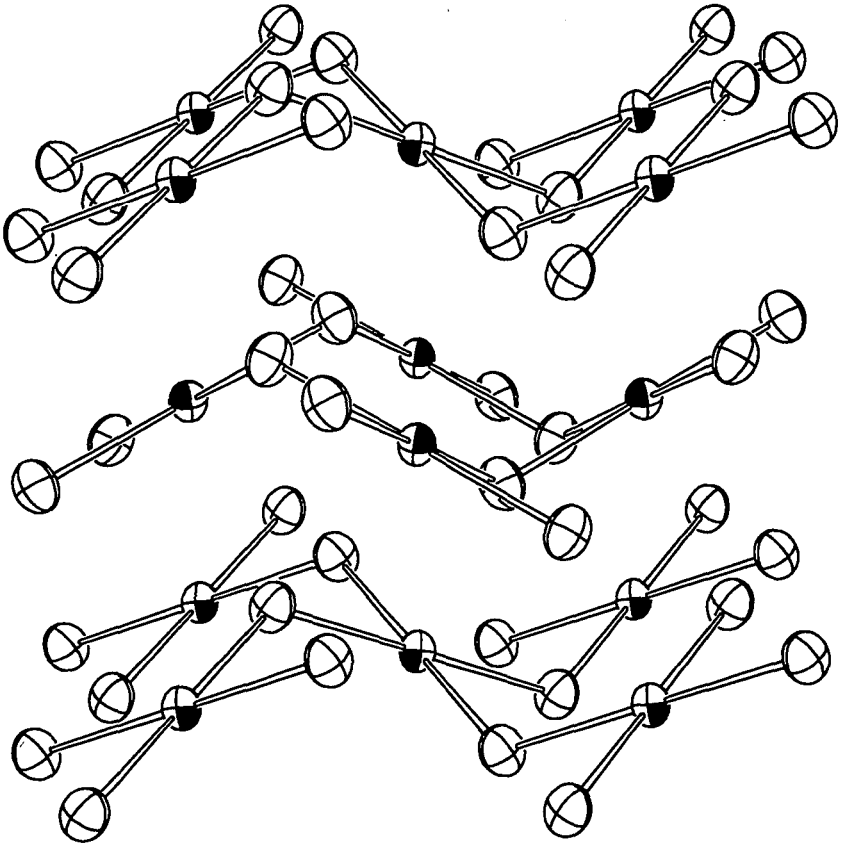

Figure 6.7. An ORTEP depicting the puckered planes of AgF_2.
Figure reconstructed from data provided by Jesih *et al.*[7]

6.4. Optical Anisotropy in $AgFBF_4$

A needle of the violet $AgFBF_4$, measuring ~2.0 mm in length and ~0.1 mm across, was mounted inside a carefully dried quartz capillary. The crystal was observed by transmitted light under a light microscope which was fitted with a plane polarizer in its stage. A crystal structure determination of this compound had established that its crystal habit is such that the $(AgF)_n^{n+}$ chain direction is coincident with the needle axis. With the axis of the needle in the plane of polarization of the light, the crystal extinguished visible

light, appearing black through the microscope. With the plane of polarization perpendicular to the axis of the needle, the crystal transmitted the visible light, appearing violet-blue when viewed through the microscope.

6.5. Results and Discussion

Three general crystal symmetries have been determined to exist in the AgF^+ salts that are currently known, with a fourth symmetry indicated by X-ray powder diffraction data, but not yet confirmed by single-crystal studies. The highest symmetry observed is that of the tetragonal material $AgFBF_4$. In this compound, the Ag(II) are linearly coordinated to two F atoms along the $(AgF)_n^{n+}$ chain direction, four long bonds to F atoms of BF_4^- ligands completing the pseudo-octahedral environment about the silver. The BF_4^- anions are of such a size that packing them in a strait column provides a repeat length along *z* that, with very little distortion of the tetrahedral ions, exactly matches the repeat length of the $(AgF)_n^{n+}$ chain.

By contrast, the larger anions present in $AgFAsF_6$, $AgFAuF_6$, and $AgFIrF_6$ are accommodated in the structure by an entirely different packing arrangement. The greater volume requirements for these anions forces the $(AgF)_n^{n+}$ chain to become kinked in order maintain the proper stoichiometry and still minimize repulsive electrostatic interactions, thus imposing a lower, orthorhombic symmetry upon the structure. Nevertheless, the kinks in the chain occur at the F ligand bridges while the Ag(II) still sits in a nearly linearly-coordinated F environment {$\angle$(F1-Ag-F1) = 176.1(4)° for $AgFIrF_6$} with five

long-bonded fluorine atoms (see Figure 6.4) once again contributed by the anions, creating a compressed pseudo-pentagonal bipyramid of F ligands about the Ag(II).

Even though the formula unit volume of $AgFAsF_6$ is 7.5 $Å^3$ less than that of its iridium relative, the structures are the same. Therefore, since RuF_6^- is 0.3 $Å^3$ smaller than IrF_6^-, it was anticipated that $AgF^+RuF_6^-$ would adopt the same structure. It does not. Perhaps the most interesting feature of the monoclinic structure that is observed is that, while the $(AgF)_n^{n+}$ chain is still observed to exist, and the chain is bent at the F links {∠(Ag-F1-Ag) = 146.0(5)° for Ir, ∠(Ag-F1-Ag) = 155.9(2)° for Ru}, we now also see a bending of the chain at the silver links. In fact, this angle {88.6(3)°} provides for the Ag(II) to exist in a square-coordinated F environment. The other two F ligands (each from a different anion) which lie in the plane defined by the ribbon chain are relatively short-bonded at 2.140(3) and 2.158(3) Å, while the remaining two F atoms of the pseudo-octahedral environment are at 2.548(3) and 2.659(3) Å (see Table 6.12 and Figure 6.5).

Such nearly square coordination of the Ag(II) is similar to that seen in the simple binary fluoride AgF_2. In this compound, each Ag(II) is square-coordinated by F ligands at 2.086(5) Å, which are equidistant from the two linked Ag(II), with ∠(F-Ag-F) = 129.6(1)°. The resulting structure (see Figure 6.7) contains puckered sheets which can only be weakly linked to one another since the closest intersheet Ag-F distance (two per silver atom, normal to the AgF_4 unit) is 2.588(6) Å. This intersheet distance is similar to the long-bonded contact that the Ag(II) in $AgFRuF_6$ makes to the anions, with Ag···F3 =

2.548(3) and Ag···F4 = 2.659(3) Å. The zig-zag-Ag-F-Ag-F chain in this salt has a shorter bridging fluorine distance than in AgF_2 {Ag-F7 = 2.007(3) and 2.018(2) Å, Ag-F7-Ag = 155.9(2)°}, but the form of the chain is very like a section of the puckered AgF_2 sheet, defined by tracing adjacent Ag(II) through *cis* F at each Ag. The short Ag-F distances between Ag(II) and the bridging RuF_6^- of $AgFRuF_6$ {2.158(3) and 2.140(3) Å} complete the square coordination; the Ag-F distances therefore average to 2.081 Å, a value similar to that in AgF_2. Evidently the Ru(V) centers attract F ligands more strongly than Ag(II). Withdrawal of 2 *cis* F ligands of the AgF_4 unit, by two Ru(V), shortens the trans Ag-F linkages, which are more cationic than in AgF_2 itself.

For a d^9 configuration, a Jahn-Teller distortion from octahedral symmetry results in the singly-occupied orbital being the highest in energy. In $AgFRuF_6$, the primary distortion from octahedral symmetry about the silver atom consists of an increase in interatomic distances along the *z*-direction; in the other AgF^+ salts, there is a shortening of the distances in the *z*-direction. Thus, in $AgFRuF_6$ the Jahn-Teller distortion is manifest in a lowering of the d_{z^2} orbital energy with single occupation of the higher energy $d_{x^2-y^2}$ orbital, the occupation being reversed for the other salts of known structure.

The explanation for the four-coordination of Ag(II) in $AgFRuF_6$ and for the two-coordination in the other known AgF^+ salts is uncertain. As discussed above, it does not appear likely that differing anion sizes are responsible for the appearance of two distinct geometric arrangements about the Ag(II) ion. Rather, it is more likely that the reason lies

in the fluoro-basicity of the complexing anion. RuF_6^- is a superior base to IrF_6^- (*i.e.* RuF_5 is a weaker F^- acceptor than IrF_5), so the former anion will tend to donate F^- more than the latter (note the short Ag-F interatomic distances involving RuF_6^- ligands). Because PF_5 is a relatively weak fluoro-acid and its fluoro-anion is octahedral, if $AgFPF_6$ could ever be made, it seems likely that it would adopt the $AgFRuF_6$ structure type. However, attempts in this laboratory by J. Münzenberg[8] to synthesize $AgFPF_6$ have failed, the reaction proceeding as depicted in Equation (1).

$$AgPF_6 \xrightarrow[F_2]{aHF} AgF_2 + PF_5 \qquad (1)$$

In each of the three known structure types, there exists a one-dimensional chain cation in which adjacent Ag(II) centers are bridged by F ligands bound only to the silver atoms. The Ag-F-Ag angles vary from linear to nearly 90°, but the two Ag-F interatomic distances are always close to 2.0 Å and not significantly different from one another. Furthermore, each of the chains is isolated from its nearest neighbor chain cations by the assembly of anions. This feature is most easily seen in $AgFBF_4$ (see Figure 6.1), where the cation chains are linear and each one is surrounded on four sides by columns of BF_4^- anions. For such an $(AgF)_n^{n+}$ chain, the crystal orbitals will be constructed from the highest energy valence *p* orbital of the fluorine atom in the chain (p_z in the case of $AgFBF_4$) and from the highest energy, singly-occupied valence *d* orbital of the Ag atom (d_{z^2} in the case of $AgFBF_4$). Such a construction gives a half-filled conduction band. Magnetic susceptibility measurements have been made on many of the AgF^+ materials

over a range of temperatures and fields. The data for $AgFBF_4$ (see Chapter 5) most strikingly illustrates a trait which is shared by all of the compounds containing diamagnetic anions: an essential temperature- and field- independence over a very large temperature range. This temperature-independence is in contrast to the 1/T Curie law behavior observed for localized unpaired electrons; however, it is predicted by Fermi-Dirac statistics for partially filled bands.[9] Other Ag(II) materials {*e.g.* $Ag(SbF_6)_2$ and $Ag(BiF_6)_2$}, whose structural data indicate electronically isolated silver atoms[10, 11], exhibit one-electron paramagnetism (see Figure 6.8 and Figure 6.9), consistent with weakly interacting d^9 Ag(II) cations.

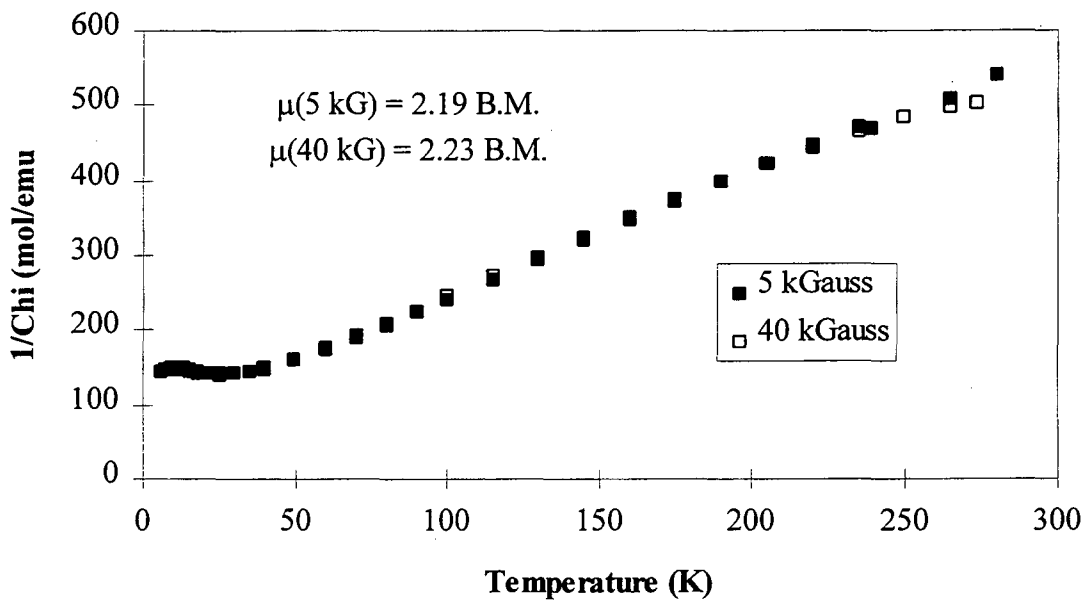

Figure 6.8. Magnetic data for $Ag(BiF_6)_2$.

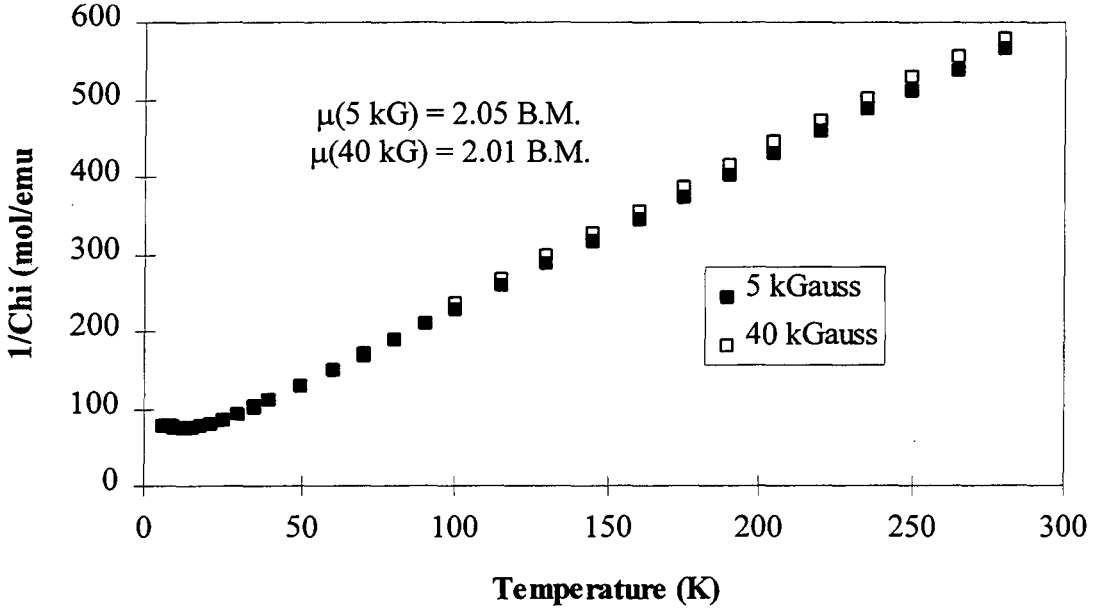

Figure 6.9. Magnetic data for $Ag(SbF_6)_2$.

Polarized light transmission is commonly used to identify one-dimensional electronic conductors. With the plane of polarization (*i.e.* the plane defined by the electric field vector and the direction of propagation vector) aligned perpendicular to the direction of conduction in a one-dimensional metal, the conduction electrons do not interact with the electro-magnetic field; the oscillating electric field is orthogonal to the direction in which the electrons can move. Consequently, the polychromatic light is both scattered and absorbed as it passes through the material and colored light may exit the

other side of the crystal. However, with the plane of polarization aligned parallel to the direction of conduction, the oscillating electric field interacts strongly with the free electrons of the conductor, resulting in efficient reflection of visible wavelengths of light. Thus, the crystal, in this case, appears opaque. Precisely these results were obtained in a study performed with a crystal of $AgFBF_4$. Unfortunately, attempts to directly measure a finite electrical resistance in packed powder samples of AgF^+ materials and along the chain direction of single crystals have all met with failure. These negative results do not preclude the existence of the delocalized electron feature, because the reactivity of the AgF^+ salts has prevented a conventional study of conductivity in which electrodes are painted onto the crystalline faces. However, the failure to detect a metallic conductance by this pressure contact with a gold or platinum wire does point to the possibility of these salts being sizable band gap materials, since other strong oxidizers known to be metallic are seen to be conductive in this kind of test.

Stoichiometric and structural information on the material referred to as $AgFBiF_6$ are lacking, making a definite assignment of this formula to the material obtained impossible. Casteel synthesized an analogous material[5] in a similar manner using $AgSbF_6$ as a starting reagent. X-ray powder diffraction data obtained by him show an XRPP almost identical to that seen for the suspected $AgFBiF_6$. More compelling evidence for the assignment of this formula, however, is the temperature-independent magnetic susceptibility (see Chapter 5) observed for the bismuth compound, which has

been found to be characteristic of AgF^+ materials. No other silver(II) system is known to produce such magnetic results.

Slow fluorination of each of $AgSbF_6$ and $AgBiF_6$ was found to produce lilac crystals of sufficient size for single crystal diffractometry. However, within several hours of removal of the aHF solvent, the crystals were always seen to crumble. The resulting powder gave the same poorly-crystalline, complex XRPP as that seen for the $AgFBiF_6$ which was used for the acquisition of magnetic susceptibility data. It is highly probable that $AgFSbF_6$ and $AgFBiF_6$ crystallize with one or more solvent molecules (HF) incorporated into the lattice. When cooled to -20 °C, the suspected $AgFMF_6 \cdot xHF$ crystals show signs of persistence upon removal of the aHF, but the dried product then crumbles within hours under vacuum or in an inert atmosphere at room temperature. The distinctive XRPP of these salts could be a consequence of some HF involvement in the coordination of the Ag(II) species, but the magnetic susceptibility data hint that the cation is still a F-ligand bridged polymer.

6.6. Conclusions

Three different structure types have been unequivocally identified for the AgF^+ class of materials. A fourth structure type is suggested by X-ray powder diffraction data. The three known types range in crystal symmetry from tetragonal to monoclinic, and all share the common feature of a one-dimensional, cationic $(AgF)_n^{n+}$ chain isolated from neighboring chains by counterions. All materials studied also exhibit temperature-

independent magnetic susceptibility of the cation over a range from 280 K down to at least as low as 70 K. These structural and magnetic features suggest the delocalization of electrons along the cationic chain, resulting in one-dimensional electronic conductivity. Polarized light transmission experiments performed on $AgFBF_4$ support this hypothesis. Despite efforts to measure resistance in powders and single crystals, no direct evidence for such conductivity has been obtained.

$AgFSbF_6$ and $AgFBiF_6$ appear to be preparable and isostructural, however there is some uncertainty as to whether or not they contain aHF of crystallization. Lilac single crystals grown under aHF fell to a powder on removal of the aHF.

6.7. References

[1] D. Gantar, B. Frlec, D. R. Russell, and J. H. Holloway, *Acta Cryst.*, **C43** (1987), pp 618-620.

[2] B. Žemva, R. Hagiwara, W. J. Casteel, Jr., K. Lutar, A. Jesih, and N. Bartlett, *J. Am. Chem. Soc.*, **112** (1990), p 4846.

[3] W. J. Casteel, Jr., G. Lucier, R. Hagiwara, H. Borrmann, and N. Bartlett, *J. Solid State Chem.* **96** (1992), pp 84-96.

[4] B. G. Müller, *Angew. Chem. Int. Ed. Engl.*, **26** (1987), p 688.

[5] W. J. Casteel, Jr., Ph. D. Thesis, (1992) Chapter 6, U.C. Berkeley.

[6] In $LiRuF_6$, $R\bar{3}$, a_o = 5.369(1) Å, α = 56.34(1) °, V/Z = 100.2 $Å^3$, and $LiIrF_6$, $R\bar{3}$, a_o = 5.397(1) Å, α = 55.88(1) °, V/Z = 100.5 $Å^3$, (P. Botkovitz and G. Lucier, unpublished data) the Li^+ is in an octahedral hole site and the formula unit volume must closely represent the anion size in these $A^+MF_6^-$ salts.

[7] A. Jesih, K. Lutar, B. Žemva, B. Bachmann, St. Becker, B. G. Müller, and R. Hoppe, *Z. Anorg. Allg. Chem.*, **588** (1990), pp 77-83.

[8] J. Münzenberg, unpublished results, (1993), U.C. Berkeley

[9] P. A. Cox, The Electronic Structure and Chemistry of Solids, (1987), Oxford: Oxford University Press, pp 66-69.

[10] D. Gantar, I. Leban, and B. Frlec, *J. Chem. Soc. Dalton Trans.*, (1987), pp 2379-2383.

---

[11] G. Lucier, J. Münzenberg, W. J. Casteel, Jr., and N. Bartlett, *Inorg. Chem.,* (1995) in press.

Chapter 7

The Oxidizing Chemistry of Solvated Ag^{II}

7.1. Introduction

Earlier work in these laboratories[1] had already shown that complete dissolution of $AgFAsF_6$ in aHF occurred when one equivalent of AsF_5 was added to yield a deep blue solution:

$$AgFAsF_6 + AsF_5 \xrightarrow{aHF} Ag^{II}_{solv} + 2\,AsF_6^- \qquad (2)$$

With the stronger fluoro-acids, SbF_5 and BiF_5, two equivalents of acid will bring one equivalent of AgF_2 into solution, and in those cases, the $Ag(MF_6)_2$ salts are recovered on removal of aHF. Therefore, Ag^{II}_{solv} can be easily and reproducibly generated. The work described in this chapter has focused on the oxidizing power of Ag^{II}_{solv}.

Casteel and Shen had already shown[2] that Ag^{II}_{solv} was able, at lower temperatures (< -60 °C), to oxidize O_2 to O_2^+, but it remained to be demonstrated how much superior to AgF^+ and how much inferior to Ag^{III}_{solv} these oxidizing capabilities were. Again, to this

end, the hexafluoro-anions of the third transition series (see Chapter 1) provided a convenient graded set of species to be oxidized.

7.2. Experimental

7.2.1. Preparation of AMF_6

See Chapter 3 for details of the syntheses of alkali hexafluorometallate(V) salts.

7.2.2. Interaction of $KIrF_6$ with F_2 in Acidic aHF

One tube of an FEP T-reactor was loaded with $KIrF_6$ (82 mg, 0.24 mmol). Cooling the reactor tube to -196 °C, ~2 mL aHF was condensed onto the solid, and then it was warmed to room temperature. The reactor was pressurized to ~1000 torr with BF_3, whereupon no sign of reaction was visible. So the reactor was further pressurized to ~1500 torr with F_2 and continuous agitation was begun. Although the solution became slightly yellow in color, this color failed a test for volatility (it did not condense in the other tube of the reactor upon cooling in a liquid N_2 bath). After 1.5 days with no evidence of IrF_6 generation, the $KIrF_6$ was recovered.

7.2.3. Oxidation of IrF_6^- with $AgFAsF_6$ in acidic aHF

$KIrF_6$ (234 mg, 0.679 mmol) was loaded into one tube of a passivated FEP T-reactor, and $AgFAsF_6$ (257 mg, 0.813 mmol) was loaded into the other. Approximately 1 mL aHF was condensed onto each of the solids at -196 °C and then warmed to room temperature. AsF_5 (~ 1.3 mmol) was introduced into the reactor, resulting in the dissolution of the $AgFAsF_6$ to give a blue solution. This was poured into the other arm of

the reactor (where most of the $KIrF_6$ remained as undissolved solid). There was some effervescence as a yellow precipitate was formed and the solution turned blue-green. A small aliquot of aHF was back-condensed and then poured over to flush any remaining $AgFAsF_6$ solution from the walls of the tube; this back-distillation was repeated once more. All volatile compounds were condensed over into the clean tube of the reactor, this condensate appearing bright yellow in color. An abundance of SF_4 was let into the reactor at -196 °C and yielded a colorless solution as the mixture melted, the surplus AsF_5 combining with the SF_4 in a simple acid base reaction {see Equation (3)} and the yellow IrF_6 combining in a redox reaction as shown in Equation (4).

$$SF_{4\,(g)} + AsF_{5\,(g)} \xrightarrow{aHF} SF_3AsF_{6\,(solv)} \qquad (3)$$

$$3\ SF_{4\,(g)} + 2\ IrF_{6\,(g)} \xrightarrow{aHF} 2\ SF_3IrF_{6\,(solv)} + SF_{6\,(g)} \qquad (4)$$

An off-white powder was obtained upon removal of the volatile gases and aHF under dynamic vacuum. Because an imprecisely measured quantity of AsF_5 had been introduced into the reactor, no yield could be computed by gravimetry. However, the XRPP of the off-white powder showed patterns belonging to both SF_3AsF_6 and SF_3IrF_6. The XRPP of the reaction byproduct showed patterns belonging to $AgIrF_6$ and $KAsF_6$.

7.2.4. Oxidation of IrF_6^- with $Ag(SbF_6)_2$

One tube of an FEP T-reactor was loaded with $LiIrF_6$ (104 mg, 0.332 mmol) and $Ag(SbF_6)_2$ (332 mg, 0.574 mmol), and aHF (~2.0 mL) was condensed onto the mixed solids. On warming to ~20 °C, the solution first became royal blue and then dark green

as a yellow solid precipitated out of solution. The aHF and the volatile, yellow IrF_6 were condensed into the other arm of the reactor. SF_4 was introduced into the reactor and produced SF_3IrF_6 (cubic[3], a = 5.58 Å) by way of the reaction expressed in Equation (4) as the IrF_6/aHF mixture melted, resulting in a colorless solution. Volatile compounds were evacuated and the solid product dried under dynamic vacuum for 3 h. The yield of SF_3IrF_6 was 65.4 mg (0.165 mmol), *i.e.* 50% of Ir in the $LiIrF_6$.

7.2.5. Interaction of $AgFIrF_6$ with BiF_5 in the Presence of F_2

$AgIrF_6$ (107 mg, 0.259 mmol) and BiF_5 (315 mg, 1.04 mmol) were loaded into one arm of a passivated FEP T-reactor. Approximately 2.1 mL aHF was condensed onto the solids at -196 °C, and then warmed to room temperature. No reaction was evident as a clear solution above orange solid resulted. Fluorine gas was introduced into the reactor, bringing the total internal pressure to 1500 torr. Continuous agitation was maintained for 4 h. During this time, the orange solid was slowly replaced by a mix of black and white solids (particles of each color were plainly visible) and a yellow solution. The yellow color in the HF was found to be vacuum transferable, and so was condensed, along with the HF, into a single-tube reactor. SF_4 was introduced into this reactor. As the yellow material warmed and the HF melted, interaction with the SF_4 resulted in a colorless solution {see Equation (4)}. Removal of all the volatile species left a grey solid mix in the T-reactor and light yellow SF_3IrF_6 (87 mg, 0.22 mmol, 85% yield) in the single-tube reactor. The XRPP of the grey solid mix showed no recognizable pattern.

7.2.6. Attempted Oxidation of PtF_6^-

$KPtF_6$ (119 mg, 0.342 mmol) and $AgFAsF_6$ (228 mg, 0.723 mmol) were loaded into separate arms of a standard FEP T-reactor. Approximately 1.5 mL aHF was condensed onto the $AgFAsF_6$ and then warmed to room temperature. AsF_5 was introduced into the reactor, providing for the complete dissolution of the $AgFAsF_6$ as a royal blue solution. This solution was poured onto the dry $KPtF_6$, and within seconds the solution turned green as a red-brown solid plated out on the walls of the reactor. A test for colored, volatile species was performed by condensing a small amount of HF into the other arm of the reactor. This test came up negative, so the reaction was left to agitate for 3 h. A second test for colored, volatile species also came up negative, so the HF was decanted and removed under vacuum, leaving behind a dark blue solid.

7.3. Results and Discussion

$AgFIrF_6$ is readily prepared in neutral aHF solution. However, acidification of this solution results in the liberation of IrF_6. As is commonly observed with AgF^+ salts, acidification of the solution with a very good fluoride ion acceptor is required to dissolve the silver compound. Presumably, such conditions break down the polymeric $(AgF)_n^{n+}$ chain cation by removing fluoride from the chain and providing an abundance of solution-phase complexing anions for the Ag(II). The resulting silver species may be represented as Ag^{II}_{solv} {this covers various possibilities including $[AgF(HF)_n]^+$ or $[Ag(HF)_n]^{2+}$}, and, since Ag^{II}_{solv} had already been shown[2] to oxidize O_2 to O_2^+, it was not

surprising to find that it oxidized IrF_6^- to IrF_6. The yield of IrF_6 {as measured gravimetrically after reaction with SF_4 to form SF_3IrF_6, expressed in Equation (4)} is only about 50%, the remainder of the IrF_6^- ending up in the Ag(I) salt $AgIrF_6$. The experimental findings indicate that Ag^+_{solv}, which is generated as Ag^{II}_{solv} oxidizes IrF_6^- to IrF_6, interacts with a second IrF_6^-, precipitating out as the extremely low solubility salt $AgIrF_6$, thus excluding half of the IrF_6^- from oxidation, as in Equation (5).

$$Ag^{II}_{(solv)} + 2\ IrF^-_{6\ (solv)} \rightarrow IrF_{6\ (g)} + AgIrF_{6\ (s)} \qquad (5)$$

Of course, half of the Ag(II) introduced as reagent remains unreduced and eventually ends up complexed with the anion of the fluoro-acid used in the reaction. However, as was experimentally shown, in the presence of fluorine, the Ag(I) in $AgIrF_6$ is oxidized back to Ag(II),

$$AgIrF_6 + \tfrac{1}{2}\,F_2 \xrightarrow{aHF} AgFIrF_6 \qquad (6)$$

reforming $AgFIrF_6$ which then dissolves in the acid solution, permitting more complete oxidation of the IrF_6^-. Therefore, the addition of F_2 to the reactor is seen to greatly increase the yield (to 85%). Because IrF_6 is not generated from the interaction of F_2 with an acidified solution of $KIrF_6$, the cationic silver is seen to behave as a catalyst in this electron oxidation of IrF_6^- by fluorine, the overall equation being:

$$IrF^-_{6\ (solv)} + \tfrac{1}{2}\,F_2 \xrightarrow[Ag^+]{aHF} IrF_6 + F^-_{(solv)} \qquad (7)$$

Presumably, the addition of a catalytic amount of Ag(I) to a reactor containing IrF_6^-, acidified aHF, and F_2 can ultimately generate a quantitative yield of IrF_6.

Since PtF_6 oxidizes oxygen to generate $O_2^+PtF_6^-$, but on sublimation dissociates to O_2 and PtF_6, it is evident that the oxidizing power of PtF_6 is not greatly different from that of Ag^{II}_{solv}. Indeed, the release of $MF_{6\,(g)}$ from aHF solution provides a favorable $T\Delta S$ term to aid the hypothetical oxidation of the kind expressed in Equation (8).

$$Ag^{II}_{(solv)} + PtF^-_{6\,(solv)} \xrightarrow[?]{aHF} Ag^+_{(solv)} + PtF_{6\,(g)} \qquad (8)$$

Nevertheless, this oxidation did not occur. It should also be noted that it was found subsequently (see Chapter 8) that PtF_6^- probably oxidizes Ag^I to Ag^{II} in making the pseudo-trifluoride $Ag^{II}Pt^{IV}F_6$. Certainly PtF_6 is a superior oxidizer to PtF_6^-. It is therefore clear that PtF_6 must be a superior oxidizer to Ag^{II}_{solv}. Thus, it is predicted that the reverse of the reaction expressed in Equation (8) would in fact occur:

$$Ag^+_{(solv)} + PtF_{6\,(g)} \xrightarrow{aHF} Ag^{II}_{(solv)} + PtF^-_{6\,(solv)} \qquad (9)$$

this being driven by three favorable enthalpy terms: (1) the electron affinity of PtF_6 (~184 kcal·mol^{-1}), (2) the enhanced solvation energy of Ag^{II}_{solv} relative to Ag^+_{solv} (because Ag^{II} has one half-filled *d* orbital of antibonding character whereas in Ag^+ that antibonding orbital is filled), and (3) the solvation energy of PtF_6^-. The ionization enthalpy of Ag^+ is, of course, the adverse energy term for the reverse reaction in Equation (8). Evidently, the electron affinity of Ag^{II}_{solv} (*i.e.* the ionization enthalpy of Ag^+_{solv} to give Ag^{II}_{solv}) is not sufficiently high to outweigh this combination.

7.4. Conclusions

Acidification of an aHF solution reproducibly generates a solution phase Ag^{II} species, Ag^{II}_{solv}, from AgF^{+} salts, this resulting species having a formidable electron affinity. Although $AgFIrF_6$ is preparable, a solution of Ag^{II}_{solv} has been experimentally shown to oxidize the IrF_6^- anion to the neutral IrF_6, thus confirming earlier findings that Ag^{II}_{solv} is a stronger oxidizer than the polymeric cation $(AgF)_n^{n+}$. In fact, while fluorine gas alone does not oxidize IrF_6^- in aHF, it does generate Ag^{II} from Ag^{+}, which, in acidic solution, then oxidizes the IrF_6^-. In this interaction, the cationic silver is seen to behave as a catalyst, permitting the electron oxidation of IrF_6^- by fluorine gas.

Consideration of the interaction of Ag^{II}_{solv} and O_2 gas, as well as that of PtF_6 and O_2 gas, suggests that the oxidizing potential of Ag^{II}_{solv} is close to that of PtF_6. Furthermore, entropy favors the generation of the gaseous PtF_6 from the solution phase PtF_6^-. However, in combination with the various unfavorable enthalpic terms associated with the oxidation of $PtF_{6\,(solv)}^-$, the electron affinity of Ag^{II}_{solv} is insufficient to affect this oxidation. Thus, PtF_6 is not generated from an aHF solution of Ag(II).

7.5. References

[1] B. Žemva, unpublished findings, (1993), U.C. Berkeley.

[2] W. J. Casteel, Jr., Ph. D. Thesis, (1992) Chapter 7, U.C. Berkeley, and C. Shen, Ph. D. Thesis, (1992) Chapter 8, U.C. Berkeley.

[3] N. K. Jha, Ph.D. Thesis, (1965) Chapter 2, U. British Columbia.

Chapter 8

$Ag^{I}M^{V}F_6$ *vs.* $Ag^{II}M^{IV}F_6$

8.1. Introduction

Many transition metals form silver(I) hexafluorometallate(V) salts, some of which are discussed in Chapter 5. However, it was reported by Müller and Hoppe[1] in 1972 that the silver hexafluorometallate salts of palladium and platinum (among others) are to be formulated as $Ag^{II}M^{IV}F_6$. This report provided no structural information on the two materials of interest, although magnetic susceptibility data for the palladium compound was provided. The only claim to a Pd(V) complex salt is that of Falconer and his coworkers,[2] who reported $O_2^+PdF_6^-$, but were unable to support this with any crystallographic data. The syntheses and subsequent X-ray analyses of the two $AgMF_6$ (M = Pd, Pt) compounds in this laboratory generated, in one instance for each, an XRPP containing only a faint rhombohedral pattern. Rhombohedral symmetry is exhibited[3] by the "trifluorides" of Pd and Pt, which are formulated as $M^{II}M^{IV}F_6$, as well as many of the true trifluorides, including[4] those of Ti, V, Cr, Fe, Co, Ni, Mo, Ru, Rh, and Ir. The

divalent metals in $Pd^{II}Pd^{IV}F_6$ and $Pt^{II}Pt^{IV}F_6$ lie in octahedral holes as a consequence of their high-spin d^8 electron configuration. That is, the $t_{2g}^6 e_g^2$ configuration favors no distortion from octahedral symmetry in order to avoid spin-pairing of the two e_g electrons. Divalent silver, however, is a d^9 species, and is predicted by Crystal Field Theory to distort to lower symmetry (Jahn-Teller distortion), thereby removing the degeneracy of the two e_g orbitals without requiring the input of electron spin-pairing energy. A distortion seemed much less likely in a compound formulated as $Ag^{I}M^{V}F_6$ (Crystal Field Theory predicts no distortion about a d^{10} Ag(I) center). Moreover, the possible existence of $O_2^+PdF_6^-$ and the proven ability of Ag^{II}_{solv} to oxidize O_2 to O_2^+ left open the possibility of $AgMF_6$ (M = Pd, Pt) being $Ag^+MF_6^-$ salts.

8.2. Experimental

8.2.1. Preparation of some A_2MF_6 salts from AF, metallic M, and F_2

Oxidation of Pd and Pt metals by fluorine to the +4 oxidation state was accomplished at room temperature in aHF which had been made basic with alkali fluoride. This represented a new and clean synthesis of such salts. The specific details of representative reactions are provided in Table 8.1. Because all MF_6^{2-} salts produced were very soluble in the aHF, preparations were usually performed with the metal reagent in slight excess so that pure product (identified by XRPP) could be obtained by merely decanting the supernatant solution.

Table 8.1. Preparation of A_2MF_6 from AF, metallic M, and F_2

Alkali Fluoride Reagent	Metal Reagent	Product and Yield	Unit Cell
KF 229 mg, 3.95 mmol	Pd 216 mg, 2.03 mmol	K_2PdF_6 529 mg, 90%	hexagonal[5], a_o = 5.717, c_o = 4.667 Å
CsF 297 mg, 1.96 mmol	Pd 108 mg, 1.02 mmol	Cs_2PdF_6 455 mg, 96%	hexagonal[6], a_o = 6.225, c_o = 5.018 Å
LiF 36 mg, 1.4 mmol	Pt 273 mg, 1.40 mmol	unknown, poorly crystalline	
KF 123 mg, 2.12 mmol	Pt 222 mg, 1.14 mmol	K_2PtF_6 409 mg, 100%	hexagonal[7], a_o = 5.778, c_o = 4.635 Å

8.2.2. Preparation of $AgPtF_6$

A passivated FEP T-reactor was loaded with $Ag(BiF_6)_2$ (524 mg, 0.695 mmol) in one tube and K_2PtF_6 (292 mg, 0.753 mmol) in the other tube. After evacuating the reactor, about 2.6 mL aHF was condensed onto the K_2PtF_6 at -196 °C. All of the K_2PtF_6 dissolved upon warming to room temperature, giving a yellow solution. This solution was cooled to -60 °C, and no solid was observed to precipitate. So the solid $Ag(BiF_6)_2$ was slowly shaken into the solution with agitation. A brown precipitate formed rapidly. Once all of the $Ag(BiF_6)_2$ had been shaken into the reaction tube, two small aliquots of aHF were successively condensed over into the other tube and used to rinse any residual $Ag(BiF_6)_2$ over. The reaction was warmed to room temperature and left to stand for 20 min. Four successive decantations were performed, followed by back-distillation of the HF, in order to separate the soluble reaction byproduct from the insoluble fraction.

Following this, the reactor was pressurized to 1400 torr with BF_3 and left for 15 min. A slight blue color became apparent in the aHF, so this was carefully decanted and the aHF/BF_3 removed under dynamic vacuum. The products were dried for 3 h. An X-ray powder photograph of the insoluble, brown precipitate gives a very faint rhombohedral XRPP (based on pure $AgPtF_6$, expected: 289 mg; found: 333 mg). The excessive mass is perhaps due to adsorbed $KBiF_6$ on the surface of the product, which was never exposed to liquid aHF after being brought completely to dryness and allowing the $KBiF_6$ to crystallize properly. No XRPP was taken of the brown byproduct (based on $KBiF_6$ product with excess K_2PtF_6, expected: 526 mg; found: 489 mg).

8.2.3. Preparation of $AgPdF_6$

$Ag(BiF_6)_2$ (752 mg, 0.998 mmol) and K_2PdF_6 (316 mg, 1.06 mmol) were placed into separate tubes of a passivated FEP T-reactor. About 2.3 mL aHF were condensed onto the K_2PdF_6 at -196 °C, then warmed to room temperature. All of the K_2PdF_6 dissolved to give a yellow-orange solution. This solution was then cooled to -60 °C, whereupon all of the material remained dissolved. The $Ag(BiF_6)_2$ was slowly added as a dry solid to the solution. Initially, a green solution resulted, but after just a few seconds a brown solid precipitated out and the green color faded to yellow. Once all the $Ag(BiF_6)_2$ had been added, the reactor was warmed to room temperature. The solution remained yellow, so the supernatant solution was decanted. Three washings of the brown solid were performed by back-distilling the HF then decanting it again. Then the reactor was

pressurized to 1500 torr with BF_3 and left for 15 min. There was no sign of reaction to form $AgFBF_4$ (as would have been expected had there been any AgF_2 present), as was evident from the continued lack of color in the aHF column above the brown solid. So this solution was decanted and then removed under vacuum. The products were dried for 3 h. The XRPP of the brown powder showed a material of poor crystallinity and rhombohedral pattern (like $Pd^{II}Pd^{IV}F_6$). SQUID magnetometry of this product revealed it to be a simple paramagnet with a magnetic moment of 1.80 B.M. (see Figure 8.1). This value is appreciably less than the 2.0 B.M. obtained by Müller and Hoppe[1] for their $AgPdF_6$. Based on the formula $AgPdF_6$, with the Ag(II) as the limiting component, the yield (expected: 328 mg; found: 357 mg) was too great to be pure (109%). The excessive mass is perhaps due to adsorbed $KBiF_6$ on the surface of the product, which was never exposed to liquid aHF after being brought completely to dryness and allowing the $KBiF_6$ to crystallize properly. However, the other arm of the reactor contained 98% of the expected byproduct mass (expected: 722 mg $KBiF_6$, 19 mg K_2PdF_6; observed: 724 mg), which indicates a net gain in overall reactor weight (perhaps due to FEP interaction with the HF).

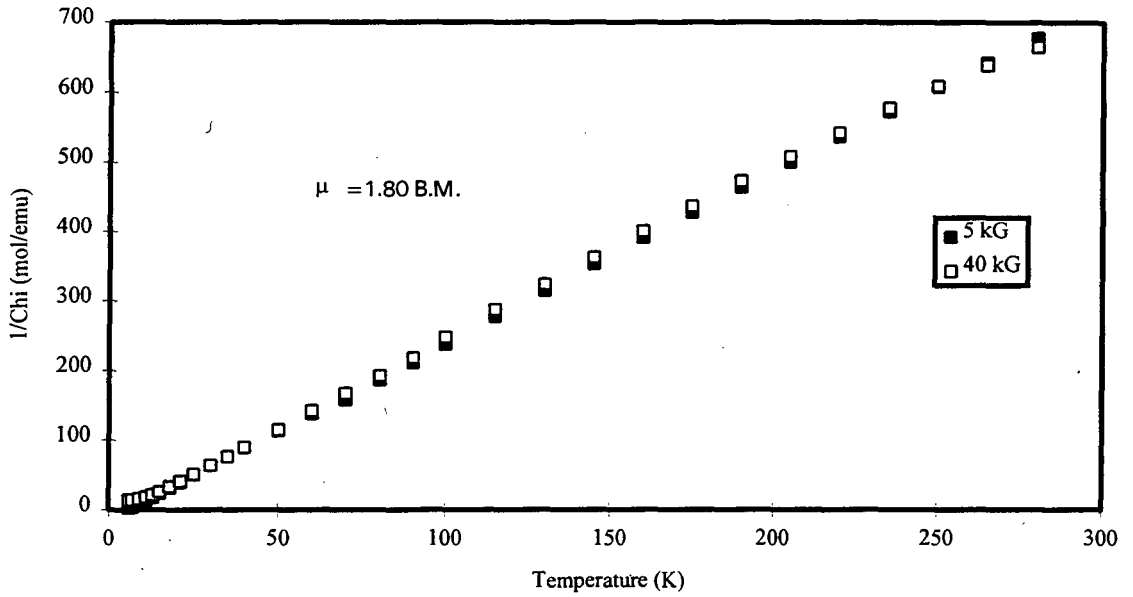

Figure 8.1. Magnetic data for $AgPdF_6$ indicating simple paramagnetic behavior.

8.2.4. Interaction of AgF with $KPtF_6$

A passivated FEP T-reactor was loaded with $KPtF_6$ (61 mg, 0.18 mmol) and AgF (43 mg, 0.34 mmol), each reagent in a separate tube. 1.5 mL aHF was condensed onto the AgF. Upon warming to room temperature, all the AgF dissolved to give a colorless solution. This was poured onto the $KPtF_6$, immediately forming a brown precipitate. The reactor was continuously agitated for 2 h before decanting the colorless HF. Two washings of the brown solid were accomplished by condensing the HF back over onto it and then decanting. The HF was removed under dynamic vacuum and the product dried for 3 h. An X-ray powder photograph of the product gives a very complicated XRPP.

The yield (79 mg brown solid) was excessive for production of pure $AgPtF_6$ (108% yield). And as in the previously described preparations, the excessive mass may be due to adsorbed $KBiF_6$ on the surface of the product, which was never exposed to liquid aHF after being brought completely to dryness and allowing the adsorbed K^+ and BiF_6^- to crystallize properly.

8.2.5. Interaction of F_2 with $AgPtF_6$ and $AgPdF_6$

Reactivity of $AgPtF_6$ with F_2 (~ 2 atm) in aHF was tested and resulted in no reaction. Similarly, the fluorination of $AgPdF_6$ was attempted at 150 °C under several atmospheres of F_2 (no aHF present) with no effect.

8.2.6. Interaction of O_2AsF_6 with PtF_6^{2-}

K_2PtF_6 (87 mg, 0.22 mmol) and O_2AsF_6 (53 mg, 0.24 mmol) were loaded into separate tubes of a passivated FEP T-reactor. Approximately 1.1 mL aHF was condensed onto each of the reagents at -196 °C. Upon warming the HF to room temperature, both solid reagents dissolved completely in their respective solutions. As the O_2AsF_6 solution was slowly poured onto the K_2PtF_6 solution, vigorous gas evolution was observed and the resulting solution became yellow-orange. After 10 min reaction time, all effervescence had ceased and no precipitate had formed. The solution was then cooled to -196 °C and the reactor opened to the pressure gauge. A pressure of 50 torr was measured in a total volume of approximately 85 mL. Using the ideal gas law, a yield of 0.23 mmol gas is calculated. The reactor was warmed to ~0 °C, whereupon a yellow precipitate remained

undissolved, so the solution was decanted. After removing the volatile species under dynamic vacuum, the products were dried for 2.5 h. An X-ray powder photograph of the decanted orange solid gives the XRPP associated[8, 9] with both $KPtF_6$ and $KAsF_6$, but with a rhombohedral unit cell size that lies between the two (product: a_o = 4.94 Å, α = 97.6 °, V = 117.1 Å^3; $KPtF_6$: a_o = 4.96 Å, α = 97.4 °, V = 118.7 Å^3; $KAsF_6$: a_o = 4.92 Å, α = 97.2 °, V =116.0 Å^3), indicating that a solid solution $KPtF_6/KAsF_6$ had been produced. The total mass expected ($KPtF_6/KAsF_6$ + remaining O_2AsF_6) was 132 mg; the total mass obtained (orange decantate: 29 mg, yellow precipitate: 100 mg) was 129 mg.

8.2.7. Interaction of O_2AsF_6 with PdF_6^{2-}

Similar reactivity and products were observed in reactions which used either K_2PdF_6 or Cs_2PdF_6 as the source of the palladium anion. In one of these experiments, a test for fluorine gas evolution was performed. This reaction began with O_2AsF_6 (142 mg, 0.643 mmol) in one tube of a passivated FEP T-reactor and K_2PdF_6 (193 mg, 0.648 mmol) in the other tube. Approximately 1.1 mL aHF was condensed onto each of the reagents at -196 °C. Upon warming to room temperature, all the K_2PdF_6 and some of the O_2AsF_6 went into solution. The O_2AsF_6 was then cooled to -25 °C while the K_2PdF_6 was cooled to 0 °C. The K_2PdF_6 solution was slowly added to the O_2AsF_6, resulting in immediate effervescence and a darkening of the orange color of the solution. A light orange solid precipitated out of solution. At this point, the reaction mixture was cooled to -78 °C and the reactor opened to the pressure gauge. A pressure of 50 torr (equating to

~0.2 mmol of ideal gas at STP, although a small portion of the system was being significantly cooled) was measured. Then this gas was removed (using a static vacuum) through a column packed with KF followed by KI. A small amount of discoloration of the colorless KI was observed, indicating the presence of F_2 in the gas. After closing the reactor valve and rewarming it to room temperature, there was no further sign of reaction, so the solution was decanted. At -196 °C, the HF was distilled back over but not decanted again. All volatile species were removed under dynamic vacuum and the solids dried for 2.5 h. An XRPP of the initial orange solid showed only the pattern of pure $KAsF_6$ (no solid solution); the solid retrieved from the highly soluble fraction gave no XRPP.

8.2.8. Interaction of K_2PdF_6 with PF_5

K_2PdF_6 (133 mg, 0.445 mmol) was placed into one tube of a passivated FEP T-reactor inside the DRILAB. After evacuating the reactor on the vacuum line, about 2.0 mL aHF was condensed onto the orange solid at -196 °C. Once the HF had melted and warmed to room temperature, all the K_2PdF_6 dissolved to give a light orange solution. Approximately 0.5 mmol PF_5 was metered into the reactor, immediately giving rise to a dark solid precipitate. The reaction was intermittently cooled and then rewarmed in an attempt to ensure good dissolution of the PF_5. Despite the orange color that remained in the solution, no further reaction was evident after 25 min. The solution was decanted, the volatile components removed under dynamic vacuum, and the remaining solids (dark

grey insoluble fraction: 68 mg; dirty yellow soluble fraction: 84 mg) dried overnight. Based upon the gain in total reactor weight, only 19 mg = 0.15 mmol PF_5 were taken up, suggesting that the reaction did not go to completion. An X-ray powder photograph of the dark grey solid gives the XRPP of KPF_6 (cubic[10], a_o = 7.71 Å) with some additional, unidentified lines.

8.2.9. Interaction of K_2PdF_6 with BiF_5

In an attempt to ensure complete reaction of a Lewis acid with the PdF_6^{2-} anion, a reaction similar to the previously described one was run, this time using a gravimetrically predetermined quantity of the strong fluoro-acid BiF_5. A passivated FEP T-reactor was loaded with K_2PdF_6 (76 mg, 0.25 mmol) in one tube and BiF_5 (77 mg, 0.25 mmol) in the other tube. After evacuation of the argon atmosphere in the reactor, ~1 mL aHF was condensed onto each of the reagents at -196 °C. At room temperature, all of the K_2PdF_6 dissolved to give a light orange solution, and most of the BiF_5 dissolved, with a tiny speck of white solid remaining. The BiF_5 solution was slowly added with agitation to the K_2PdF_6 solution. An orange precipitate formed immediately, and the reaction was intermittently agitated for 25 min. What remained was a light orange solution above an apparently orange solid. After decanting the solution, the aHF was back-distilled onto the precipitate and decanted twice more, with a faint color remaining in the solution on the last decantation. As the aHF was removed, a flaky yellow solid (123 mg) came out of solution; the products were vacuum dried for 3 h. As a dry solid, the reaction precipitate

(29 mg) had a yellow-orange appearance. An X-ray powder photograph of this material reveals a complex XRPP with moderate crystallinity.

8.3. Results and Discussion

The observation that PtF_6^{2-} quantitatively reduced O_2^+ to O_2 in the aHF to give a 1:1 solid solution of $K^+PtF_6^-$ and $K^+AsF_6^-$ shows that O_2^+ is unable to coexist with PtF_6^{2-}, no such salt as $K^+O_2^+PtF_6^{2-}$ is likely to exist. But, Ag^{2+} was shown by Casteel and Shen[11] to be approximately equivalent in oxidizing power to O_2^+ in aHF. They did so by establishing that $O_2^+AsF_6^-$ and $Ag^+AsF_6^-$ precipitate from aHF below -60 °C, the favoring of Ag^{II}_{solv} being almost complete at room temperatures:

$$Ag^{II}_{solv} + O_2 \underset{AsF_5}{\overset{aHF}{\rightleftharpoons}} O_2^+AsF_6^- + Ag^+AsF_6^- \qquad (1)$$

On the basis of these results, the formulation of $AgPtF_6$ as $Ag^+PtF_6^-$ seems more favorable than $Ag^{2+}PtF_6^{2-}$. However, for a formulation $A^{2+}X^{2-}$, there is a fourfold advantage to the lattice energy compared with A^+X^-, and this could prefer the former formulation in the crystal lattice. The lattice energy for a salt $A'^+A''^+X^{2-}$ is, for similarly sized cations, only about three-fourths[12] that for $A^{2+}X^{2-}$.

Unfortunately, the structural information provided by the experimental work on $AgPtF_6$ does not provide a definitive answer to the question is it $Ag^+Pt^VF_6^-$ or $Ag^{2+}Pt^{IV}F_6^{2-}$. In the experiments in which $AgPtF_6$ was precipitated from aHF by mixing $Ag^{2+}(BiF_6)_2$ with K_2PtF_6, the solid gave a weak X-ray powder pattern indicative of a rhombohedral

unit cell not very different from that of $Pd^{II}Pd^{IV}F_6$ or IrF_3. This is compatible with $Ag^{I}Pt^{V}F_6$, but not compelling for that formulation since $AgIrF_6$ is tetragonal[10] (a_o = 4.85, c_o = 9.70 Å) and the platinum analogue should be the same. In experiments where AgF (dissolved in aHF) and $KPtF_6$ (in aHF) were mixed to precipitate $AgPtF_6$, the X-ray powder patterns were reproducible from one preparation to another, but complex. These complex patterns were similar in some respects to those of AgF_3 and AuF_3, only more complicated than in these hexagonal trifluorides. The patterns showed no AgF_2 impurity nor any $AgIrF_6$-type pattern. It is plausible to associate this pattern with the lower symmetry to be expected as a consequence of the so-called Jahn-Teller distortion of a d^9 Ag(II) species.

Magnetic susceptibility data are not available for $AgPtF_6$, but, as in the case of $AgPdF_6$, such data are unlikely to be helpful in resolving the formulation since d^9 Ag(II) and d^5 Pt(V) each have one unpaired electron with no strong coupling between the magnetic centers.

A chemical point in favor of the formulation $Ag^{II}Pt^{IV}F_6$ is the failure to fluorinate the material in the manner of $AgIrF_6$ (see Chapter 5), generating $AgFIrF_6$ with F_2. It seems likely that $Ag^{+}PtF_6^{-}$ would have behaved similarly.

Like the $AgPtF_6$ precipitated from the mixing of $Ag^{2+}(BiF_6^{-})_2$ and K_2PtF_6, the $AgPdF_6$ obtained similarly using K_2PdF_6 was rhombohedral and the X-ray powder pattern similar to that of $Pd^{II}Pd^{IV}F_6$. The magnetic susceptibility is that of a simple

paramagnet and consistent with either $Ag^{I}Pd^{V}F_6$ or $Ag^{II}Pd^{IV}F_6$. Although the latter formulation should manifest a Jahn-Teller distortion, this could be frustrated as in the platinum counterpart by the presence of a regularly octahedral t_{2g}^6 configuration anion. It could be that slow crystallite formation in the $AgPtF_6$ preparation from AgF and $KPtF_6$ produced the lower symmetry material seen there. Since $KPdF_6$ is as yet unknown, the counterpart of the synthesis of $AgPtF_6$ from AgF and $KPtF_6$ could not be carried out.

The successful oxidation of PtF_6^{2-} by O_2^+ in aHF raised the possibility that a similar oxidation of PdF_6^{2-} could be carried out. Persuasive evidence for the existence of $O_2PdF_6^-$ was provided by Falconer *et al.*[2] in the form of Raman vibrational and magnetic susceptibility data. Although this report was not supported by crystallographic information, it did appear to be likely that the synthetic conditions were such as to favor the formation of O_2F (an excellent fluoro-base) and PdF_5, so begetting $O_2^+PdF_6^-$.

The interaction of O_2AsF_6 with K_2PdF_6 in aHF was also carried out in an attempt to generate $KPdF_6$. The products of this reaction were never fully characterized because of their amorphous nature. However, it was clear that the palladium ended up in two distinct phases: an insoluble orange powder, and a highly soluble red phase. The identity of the orange powder was never unambiguously determined. The XRPP of the colorless $KAsF_6$ salt (an obvious byproduct of the reaction) dominates the X-ray powder photograph (out to very high angle) so that no other lines are visible; and it is suspected that the color may arise from the presence of $KPdF_5$. PdF_5^- is perhaps a chain polymer in

which each PdF_6 is joined to two like neighbors by F bridges. If so, it could be difficult to obtain $KPdF_5$ as a crystalline phase. Reacting K_2PdF_6 with an equimolar quantity of BiF_5 was performed as a direct route to $KPdF_5$. No oxidation reaction was possible here since Bi(V) is surely far too weak to affect the oxidation of Pd(IV). Although the poorly crystalline, and very complex, XRPP obtained from the sparingly soluble product of this reaction revealed little about the material itself, the solid did have essentially the same color as the insoluble product observed in the interaction of O_2AsF_6 with K_2PdF_6. Furthermore, the presence of F_2 was detected in the evolved gas in the O_2^+ reaction, perhaps arising as a decomposition product of O_2F. Thus, it seems likely that this orange material is indeed $KPdF_5$, and that the reaction proceeded, at least in part, as follows:

$$O_2AsF_{6\,(solv)} + K_2PdF_{6\,(solv)} \xrightarrow{aHF} KAsF_{6\,(s)} + KPdF_{5\,(s)} + O_2F_{(g)} \qquad (2)$$

Due to the extreme solubility of the red product generated in the interaction of O_2AsF_6 and K_2PdF_6, it is most likely that this material does not contain the PdF_6^- anion. Such solubility is generally characteristic of doubly-negative ions. So it seems much more likely that the product is either the (bis)dioxygenyl salt $(O_2^+)_2PdF_6^{2-}$ or perhaps $K^+O_2^+$ PdF_6^{2-}. Either of these products would indicate that there exists a metathetical reaction in competition with the precipitation of $KPdF_5$. Perhaps the $O_{2\,(solv)}^+$ reacts to form O_2F, as in Equation (2), until the basicity of the solution becomes too low. At this point, the PdF_5^- and O_2^+ compete equally for available F^- ions and a stable solution containing O_2^+ and PdF_6^{2-} exists.

8.4. Conclusions

Preparations of $AgMF_6$ (M = Pd, Pt) have been investigated in an attempt to determine the oxidation states of the metal atoms in these salts. A definitive X-ray powder pattern has not been obtained in either case. The rhombohedral pattern obtained from the interaction of MF_6^{2-} with Ag(II) in aHF could be compatible with the formulation $Ag^{I}M^{V}F_6$ and is in agreement with expectations based upon the observed oxidation of PtF_6^{2-} by O_2^+. However, the favorable lattice energy of $Ag^{2+}MF_6^{2-}$ may result in the favoring by both $AgPtF_6$ and $AgPdF_6$ of the M(IV) and Ag(II) oxidation states.

8.5. References

[1] B. Müller and R. Hoppe, *Z. Anorg. Allg. Chem.*, **392** (1972), pp 37-41.

[2] W. E. Falconer, F. J. DiSalvo, A. J. Edwards, J. E. Griffiths, W. A. Sunder, and M. J. Vasile, *J. Inorg. Chem.*, **Supplement** (1976), p 59.

[3] A. Tressaud, M. Winterberger, N. Bartlett, and P. Hagenmuller, *C. R. Hebd. Seances Acad. Sci. Ser. C,* **282** (1976), p 1069; A. Tressaud, F. Pintchovski, L. Lozano, A. Wold, and P. Hagenmuller, *Mat. Res. Bull.,* **11** (1976), p 689.

[4] For Ti: E. O. Wollan, H. R. Child, W. C. Koehler, and M. K. Wilkinson, *Phys. Rev.,* **112** (1958), p 1132; K. Knox, *Acta Cryst.,* **13** (1960), p 507.

For V: P. Ehrlich and G. Pietska, *Z. Anorg. Allg. Chem.,* **275** (1954), p 121; S. Siegel, *Acta Cryst.,* **9** (1956), p 684.

For Cr: A. J. Jacobson, L. McBride, and B. E. F. Fender, *J. Phys. C,* **7** (1974), p 783.

For Fe, Co, Ru, Rh, Ir: M. A. Hepworth, K. H. Jack, R. D. Peacock, and G. J. Westland, *Acta Cryst.,* **10** (1957), p 63.

For Ni: B. Žemva, K. Lutar, L. Chacón, M. Fele-Beuermann, J. Allman, C. Shen, and N. Bartlett, *J. Am. Chem. Soc.,* submitted for review (1995).

For Mo: D. E. LaValle, R. M. Steele, M. K. Wilkinson, and H. L. Yakel, *J. Am. Chem. Soc.,* **82** (1960), p 2433.

[5] N. Bartlett and J. W. Quail, *J. Chem. Soc.*, (1961) p 3728.

---

[6] National Bureau of Standards (U.S.), Circ. 539, **6** (1956), p 27.

[7] National Bureau of Standards (U.S.), Circ. 539, **6** (1956), p 42.

[8] N. Bartlett and J. Lohmann, *J. Chem. Soc.*, (1964) p 619.

[9] National Bureau of Standards (U.S.) Monogr. **25** (1980), p 1757.

[10] R. D. W. Kemmitt, D. R. Russell, and D. W. A. Sharp, *J. Chem. Soc.*, **844** (1963), pp 4408-4413.

[11] W. J. Casteel, Jr., Ph. D. Thesis, (1992) Chapter 7, U.C. Berkeley, and C. Shen, Ph. D. Thesis, (1992) Chapter 8, U.C. Berkeley.

[12] A. F. Kapustinskii, Quarterly Reviews, **IX-X** (1955), London: The Chemical Society, p 283.

Appendix

Estimating the Second Electron Affinity of PtF_6

9.1. Discussion

By comparing the energies involved in the formation of $Ag^{I}Pt^{V}F_6$ with those involved in the formation of $Ag^{II}Pt^{IV}F_6$, a hypothetical estimate for the second electron affinity of PtF_6 may be derived. This calculation is only valid in the case that $AgPtF_6$ is indeed a Ag^{II} salt, as suggested by Müller and Hoppe[1], which has yet to be confirmed. First, consider the following Hess' Law (or pseudo-Born Haber) cycle:

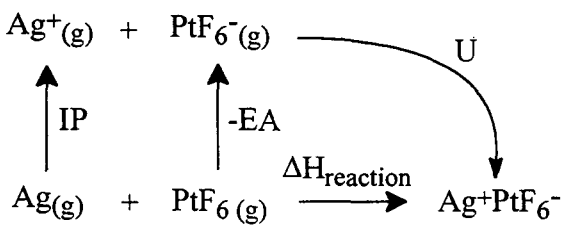

where IP is the first ionization potential of silver, EA is the first electron affinity of PtF_6, and U is the lattice energy of $Ag^{I}Pt^{V}F_6$. The heat of formation of $AgPtF_6$ is given in Equation (3).

$$\Delta H_{reaction} = IP - EA + U \quad (3)$$

Now consider the analogous Hess' Law cycle for the formation of the Ag(II) salt.

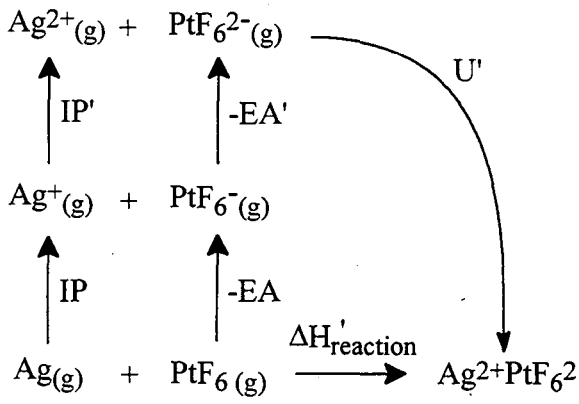

The heat of formation, in this case, is:

$$\Delta H'_{reaction} = IP + IP' - EA - EA' + U' \quad (4)$$

where IP' is the second ionization potential of silver, EA' is the second electron affinity of PtF_6, and U' is the lattice energy for the formation of $Ag^{II}Pt^{IV}F_6$. Since the entropy change is approximately the same for both reactions, ΔG scales with ΔH. $Ag^{2+}PtF_6^{2-}$ is the preferred form, so the energy change for its formation must be more negative than for $Ag^{+}PtF_6^{-}$ and therefore $\Delta H'_{reaction}$ more exothermic than for $\Delta H_{reaction}$. Thus, $\Delta H_f > \Delta H_f'$, as expressed in Equation (5).

$$IP - EA + U > IP + IP' - EA - EA' + U' \quad (5)$$

$$U > IP' - EA' + U'$$

Because the lattice energy, U, is proportional to the product of the charges q_+ and q_-, we have

$$U' \approx 4 \times U \quad (6)$$

which simplifies Equation (5) to

$$EA' > IP' + 3 \times U \qquad (7)$$

The second ionization potential of silver is known[1] to be 21.49 eV, or 496 kcal·mol^{-1}. And the lattice energy of an $Ag^{I}M^{V}F_6$ compound having the formula unit volume of $AgIrF_6$ may be estimated[2] to be -135 kcal·mol^{-1}. Therefore, the second electron affinity of PtF_6, or $EA(PtF_6^-)$, must be greater than approximately 94 kcal·mol^{-1}. (By analogy, the same lower bound may be placed on the electron affinity of PdF_6^-.) Although this value is in agreement with work performed by Jha[3], in which the *minimum* electron affinity for PtF_6^- was found to be 54 kcal·mol^{-1}, it represents an extraordinarily high electron affinity for an anion. Indeed, 94 kcal·mol^{-1} exceeds even the electron affinity[4] of atomic fluorine itself (78.4 kcal·mol^{-1}).

9.2. References

[1] C. E. Moore, *Natl. Ref. Data Ser., Natl. Bur. Stand.*, (1970) p 34.

[2] T. E. Mallouk, Ph.D. Thesis, (1983) Chapter 4, U.C. Berkeley.

[3] N. K. Jha, Ph.D. Thesis, (1965) Appendix IV, University of British Columbia.

[4] H. Hotop and W. C. Lineberger, *J. Phys. Chem. Ref. Data*, **4** (1975), p 539.

LAWRENCE BERKELEY LABORATORY
UNIVERSITY OF CALIFORNIA
TECHNICAL INFORMATION DEPARTMENT
BERKELEY, CALIFORNIA 94720